

# Degradable and Recyclable Polymers by Reversible Deactivation Radical Polymerization

Michael R. Martinez & Krzysztof Matyjaszewski\*

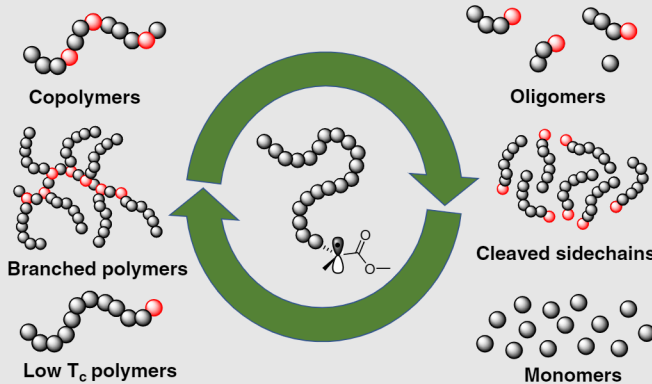
Department of Chemistry, Carnegie Mellon University, Pittsburgh, PA 15213

\*Corresponding author: [matyjaszewski@andrew.cmu.edu](mailto:matyjaszewski@andrew.cmu.edu)

Cite this: *CCS Chem.* **2022**, 4, 2176-2211

DOI: [10.31635/ccschem.022.202201987](https://doi.org/10.31635/ccschem.022.202201987)

Reversible deactivation radical polymerization (RDRP) provides unprecedented control over polymer composition, size, functionality, and topology. Various materials, such as linear polymers, star polymers, branched polymers, graft polymers, polymer networks, and hybrid materials, have been prepared by RDRP. The ability to control polymer topology also enabled precision synthesis of well-defined polymer topologies with degradable functional groups located at specific locations along a polymer chain. This review outlines progress in the synthesis of degradable polymers designed by RDRP, organized by topology and synthetic route. Recent progress in the depolymerization of polymers using RDRP mechanisms is highlighted and critically discussed.



**Keywords:** reversible deactivation radical polymerization, recycling, degradable, polymer, self-healing, depolymerization, atom transfer radical polymerization, radical addition-fragmentation transfer, nitroxide-mediated polymerization

## Introduction

Plastics have become an integral part of our world since their discovery more than 100 years ago. They are used in components of electronics, transportation, packaging, biomedical devices, infrastructure, textiles, and other diverse applications due to their low cost, light weight, and tunable mechanical properties. The ubiquitous nature of plastics is reflected in their history and projections of future growth. More than 360 million metric tons of synthetic plastic was produced in 2018.<sup>1</sup> The global plastic market size grew to

\$579.7 billion (U.S.) in 2020 and is expected to continue growing to \$750.1 billion (U.S.) by 2028.<sup>2</sup> The exponential growth of the plastics industry has, unfortunately, also led to environmental concerns through its reliance on fossil fuels as feedstocks and pollution into the environment. An estimated 6300 Mt of plastic waste was generated worldwide between 1950 and 2015, and the majority was discarded in landfills or the environment.<sup>3</sup> To this extent, we must critically assess recent and past progress in the synthesis of degradable and sustainable high-performance polymers to inform future work in this area.<sup>4-7</sup>

A significant fraction of commercial synthetic polymers are produced via conventional radical polymerization (RP) of vinyl monomers, such as various olefins, vinyl acetate, vinyl lactams, styrene, acrylates, and methacrylates (Figure 1).<sup>8,9</sup> The widespread use of RP is largely enabled by a broad functional group compatibility and tolerance to moisture and protic media. Polymers prepared by RP follow a standard chain growth mechanism consisting of initiation, propagation, transfer, and termination. Radicals are generated by slow decomposition of a radical initiator, followed by rapid propagation, and are terminated by biradical termination or transfer. Slow decomposition of initiator and lack of end-group retention in the absence of a chain transfer agent (CTA) provide minimal control over the molecular weight and end-group functionality of polymers produced by RP.

The invention of living ionic polymerizations led to advancements in polymer chemistry through optimization of polymerization kinetics. A living polymerization is a chain-growth polymerization which proceeds in the absence of chain-breaking events.<sup>10,11</sup> Polymers produced in a living process can have uniform chain length if the rate of initiation is higher than the rate of propagation. This enables the synthesis of low-dispersity polymers with chain-end functionality, as well as with complex topologies such as brushes, stars, and branched polymers.<sup>12,13</sup> However, application of living ionic polymerizations are limited by the sensitivity of the cationic and anionic propagating species to specific functional groups and moisture.

A compromise between the robust nature of radical polymerization and precision of a living polymerization was achieved through reversible deactivation radical polymerizations (RDRP). RDRP provides control over molecular structures in radical polymerizations through

reversible dissociation and combination with a thermally labile nitroxide adduct in a nitroxide-mediated polymerization (NMP) (Figure 2a), degenerative chain transfer with a CTA in radical addition-fragmentation transfer (RAFT) (Figure 2c), and by halogen atom transfer with a transition metal complex in an atom transfer radical polymerization (ATRP) (Figure 2b).<sup>14-18</sup> The fraction of terminated chains is significantly reduced in the presence of a large amount of dormant species. RDRP achieves uniform growth of polymer chains by maintaining a fast rate of initiation relative to propagation. These factors enable precise control over polymer chain length, dispersity, and chain-end functionality for monomers and reaction conditions suitable for radical polymerization. The use of multifunctional initiators enables the synthesis of branched polymer topologies, such as stars and molecular bottlebrushes, by tethering multiple initiators to a core or backbone.<sup>8,19-25</sup> Initiators can also be installed on the surface of various inorganic and organic scaffolds in the preparation of various hybrid composites.<sup>8,19,22,24,26,27</sup>

There has been significant progress in expanding the monomer scope, environmental impact, and cost efficiency of RDRP methods over the last two decades.<sup>4,9,28,29</sup> RDRP of styrene, acrylates, and methacrylates continue to be the state-of-the-art. However, progress has been made in the polymerization of challenging monomers, such as conjugated dienes<sup>30-32</sup> and vinyl chloride (Figure 1).<sup>33-36</sup> New methods of initiation by photoinduced electron/energy transfer RAFT and photoinduced ATRP enable polymerization under oxygen atmosphere upon exposure to low-intensity visible light.<sup>37-39</sup> Catalyst regeneration in the presence of external reducing agents or radical initiators enables well-controlled ATRP with a catalyst concentration as low as 10 ppm.<sup>40</sup> Polymers prepared by RDRP are used commercially as

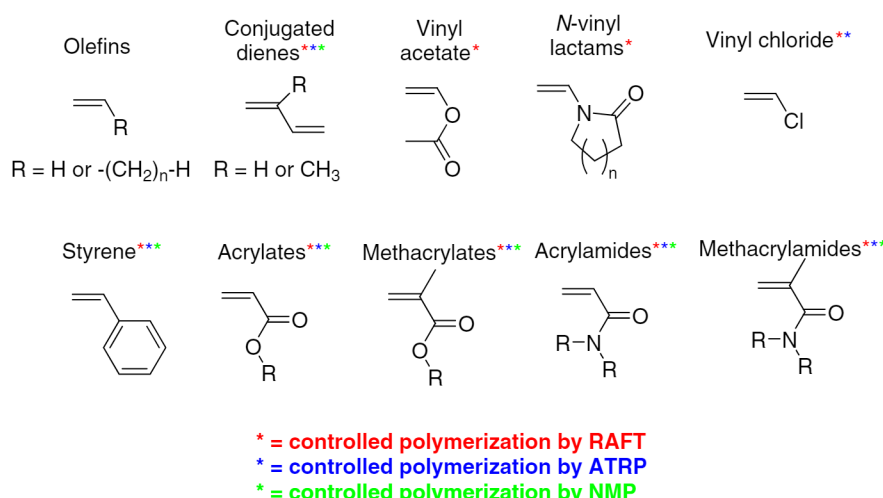


**Figure 1** | Polymerizable monomers by radical polymerization. The monomers denoted with a colored \* were reported to be polymerizable by the respective RDRP method.

DOI: 10.31635/ccschem.022.202201987

Citation: CCS Chem. 2022, 4, 2176-2211

Link to VoR: <https://doi.org/10.31635/ccschem.022.202201987>

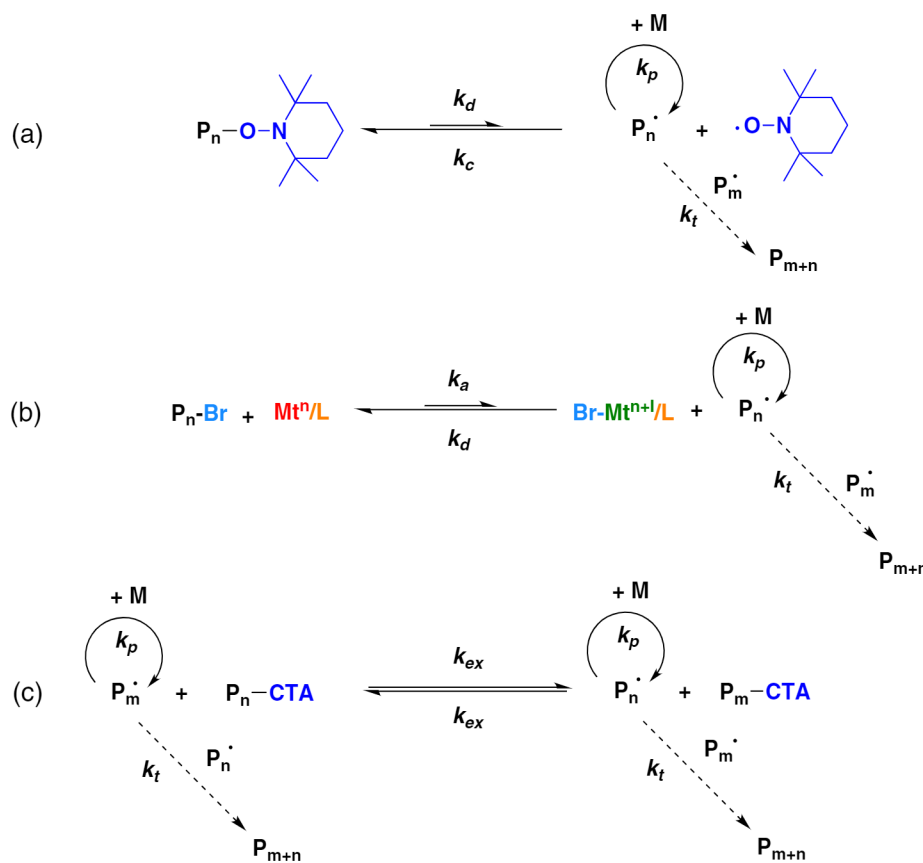


**Figure 2** | The general mechanism of RDRP mediated by (a) reversible decomposition and combination in a NMP; (b) reversible halogen atom transfer in an ATRP; (c) degenerative transfer with a CTA in a RAFT polymerization.

high-performance adhesives, sealants, rheology modifiers, surface modifiers, latex binders, chromatographic supports, solid polymer electrolytes, and smart (bio) materials.<sup>41–43</sup>

The ability to precisely incorporate degradable and reversible bonds into high-performance materials is an attractive opportunity for industry. Polyolefins are often cracked to lower molecular weight waxes and fuels under harsh conditions because they lack the degradable bonds necessary for selective bond scission under mild conditions.<sup>44,45</sup> Polyesters, such as poly(lactic acid) and poly(glycolic acid), have beneficial degradable properties, but applications have been limited by their high cost and poor mechanical properties.<sup>46,47</sup> There has been recent progress in improving the properties of polyesters which can match the properties of commodity plastics and in the upcycling of plastic waste.<sup>48–53</sup> All of these efforts continue to be difficult challenges for our field to overcome.<sup>50,54–58</sup>

This review focuses on the incorporation of degradable functional groups into high-performance polymers prepared by reversible deactivation radical polymerization. The first portion of this review provides an overview of linear polymers prepared by RDRP of degradable monomers.<sup>59</sup> Precise control over end-groups and topologies enables control over both polymer structure and

functionality at the junctions of branched polymers. The following sections are organized by polymer topology, starting from linear polymers and then (hyper)branched polymers, star polymers, molecular bottlebrushes, polymer networks, and composites. The final section of this review summarizes recent work on the depolymerization of polymers to monomers by depolymerizations mediated by RDRP mechanisms.

## Polymerizations and Copolymerizations of Degradable Monomers

Radical ring-opening polymerization (RROP) has emerged as a powerful method to install heteroatom-containing functional groups into a vinyl polymer backbone. The resulting copolymers have a statistical amount of (often) hydrolyzable functional groups along the backbone which enables polymer degradation to oligomers with low molecular weight (Scheme 1).

The amount and position of the degradable bonds along a copolymer backbone are dictated by the reactivity ratios of the monomers and the propensity of the monomer to polymerize via vinyl addition or RROP.

## Incorporation of esters by RROP

RROP of cyclic ketene acetals (CKAs) is the most common method used to statistically incorporate ester functionalities into a vinyl polymer backbone.<sup>59</sup> Incorporation of ester functional groups enables degradation by hydrolysis along the backbone, which is impossible for vinyl polymers with only C-C bonds in the backbone. The CKA functionality is typically less reactive than other vinyl comonomers, which leads to compositional drift during copolymerization which enriches vinyl repeat unit content at the beginning of the polymerization and ring-opened repeat units near the end of the reaction.<sup>60</sup> Thus, degradation of copolymers prepared by RROP of two monomers with poor compatibility yields ill-defined lower molecular weight oligomers,<sup>61</sup> which may influence their biodegradability.<sup>62</sup>

The 2-methylene-1,3-dioxepane (MDO) CKA was effectively copolymerized with monomers such as vinyl acetates, methacrylates, and pyrrolidones, via RAFT polymerization.<sup>63,64</sup> The reactivity of MDO is lower than the comonomers, which leads to slow and incomplete incorporation of MDO into the backbone at high loadings. The ester functional groups along the backbone are resistant to hydrolysis against potassium carbonate, which enabled selective hydrolysis of poly(vinyl chloroacetate)-co-poly(2-methylene-1,3-dioxepane) into poly(vinyl alcohol)-co-poly(2-methylene-1,3-dioxepane) without degrading the polymer backbone,<sup>65</sup> but are degradable in more basic solutions.

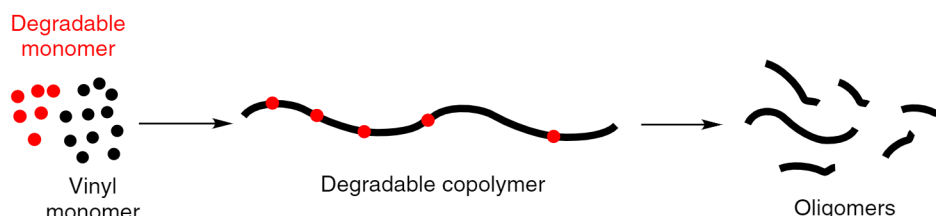
The addition of a phenyl functional group to the 7-member MDO CKA scaffold improved polymerization control due to better resonance stabilization of the opened radical. The RROP of 5,6-benzo-2-methylene-1,3-dioxepane (BMDO) was nearly quantitative to the ester, and yields a resonance-stabilized primary radical after ring opening (Schemes 2a and 2b). BMDO was successfully homopolymerized by ATRP, RAFT, and NMP to moderate chain lengths with decent control.<sup>66-68</sup> Similar to other CKAs, copolymerization of BMDO and most methacrylates have a large difference in reactivity ratios which favor homopolymerization of the methacrylates.<sup>69</sup> The copolymerization of pentafluorophenyl methacrylate (PFMA)

and BMDO is an exception due to the electron-withdrawing nature of the pentafluoro group in the side chain.<sup>70</sup> The large difference in electronics between electron-rich BMDO and electron-poor PFMA led to a near-alternating sequence.

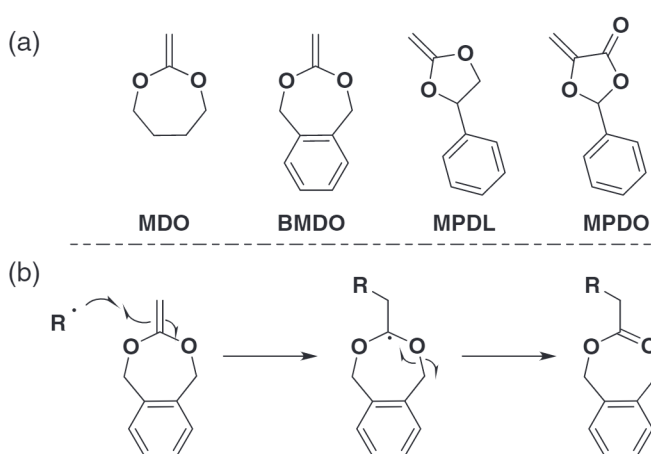
The ATRP and NMP of oligo(ethylene oxide) methacrylate (OEOMA) with a 2-methylene-4-phenyl-1,3-dioxolane (MPDL) CKA with a five-membered ring and a phenyl substituent had better living character than MDO and BMDO.<sup>71</sup> The reactivity of MPDL was still less favorable than polymerization of OEOMA. However, only a small fraction of degradable monomer might be necessary to induce a large change in polymer topology. P(OEOMA-co-MPDL) statistical copolymers with low mol fraction of MPDL ( $F_{MPDL}$ ) of 0.036 had a ~30% reduction in molecular weight ( $M_n$ ) after hydrolysis against 5% potassium hydroxide in 24 h.<sup>72</sup> Further increasing  $F_{MPDL}$  to 0.113 and 0.248 resulted in ~80% and ~95% reductions in  $M_n$ , respectively.<sup>73</sup> P(MPDL-co-OEOMA) copolymers had a similar degradation profile to hydrophobic poly(lactic acid) and poly(caprolactone) (PCL) polyesters over a one-year timeframe under physiological conditions.<sup>74</sup> Copolymerization of MPDL and ethyl maleimide (EMA) had an alternating sequence.<sup>75</sup> The preference for alternation was also attributed to electronics, where the MPDL was the electron-rich donor which had preference for addition to the electron-deficient EMA acceptor. Copolymerization of 5-Methylene-2-phenyl-1,3-dioxolan-4-one (MPDO) with methyl methacrylate (MMA) or styrene led to copolymers with a higher MPDO content than originally in the feed, due to its captodative structure. However, copolymerization of MPDO predominantly proceeded by 1,2-vinyl addition rather than ring opening.<sup>76</sup>

## Incorporation of thioesters via RROP

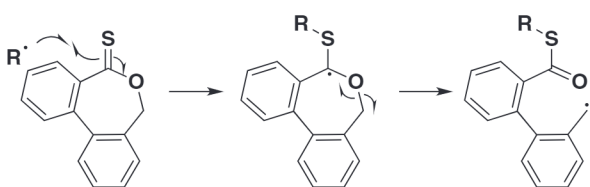
Thioester functional groups are an attractive alternative to polyesters due to their lower reactivity and possibility for enhanced degradability under mild conditions. Thioesters were installed by RROP RAFT of macrocyclic dibenzo[c,e]oxepane-5-thione (DOT) thionolactones with *n*-butyl acrylate (BA) and *t*-butyl methacrylate



**Scheme 1** | Degradable copolymer prepared by copolymerization of a vinyl monomer (black dot) with a degradable comonomer (red dot) can be cleaved into lower molecular weight oligomers after scission of the degradable bonds along the backbone.



**Scheme 2** | (a) CKAs polymerized by RDRP include MDO, BMDO, MPDL, and MPDO. (b) RROP of BMDO.



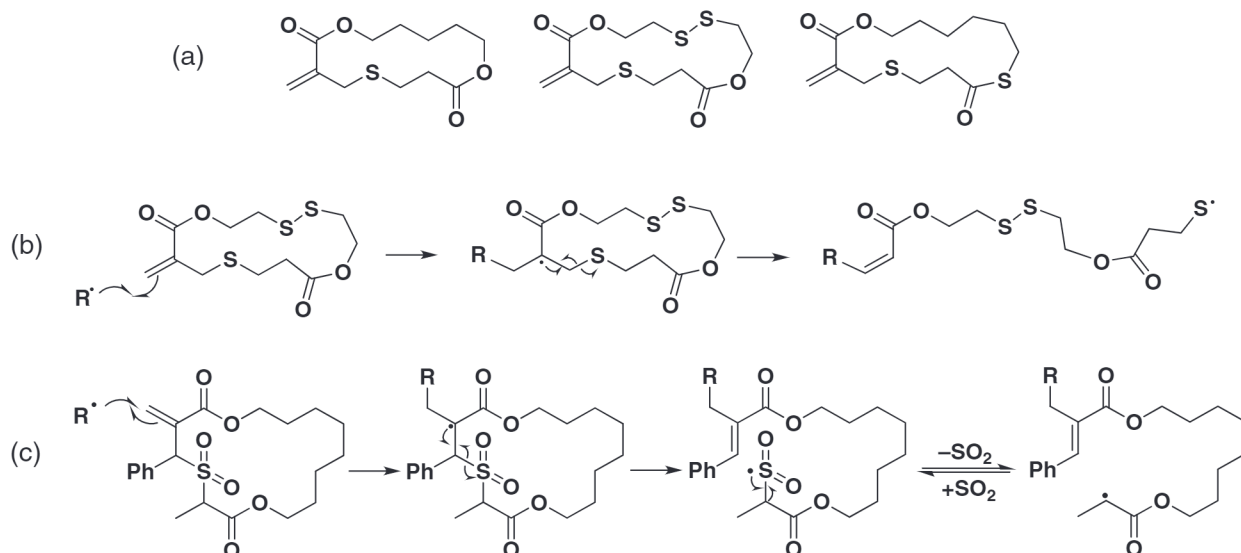
**Scheme 3** | Proposed mechanism for the RROP of DOT.<sup>255</sup>

(tBA) comonomers (Scheme 3).<sup>77</sup> Characterization of the purified polymers confirmed quantitative ring opening of the thionolactone. Copolymerization of BA with DOT

reached near quantitative consumption of thionolactone at loadings below 5 mol %. However, lower incorporation of DOT was observed in copolymerizations with high initial loadings of DOT. Alternating copolymers of thionolactone and maleimide were prepared by RAFT copolymerization with *N*-methylmaleimide, *N*-phenylmaleimide, and *N*-2,3,4,5,6-pentafluorophenylmaleimide.<sup>78</sup> Similar to the polyesters, thionolactone functional groups can be degraded by exposure to sodium methoxide and cysteine methyl ester.

### Radical ring opening polymerization of macrocycles

Macroyclic monomers with low ring strain were polymerized and copolymerized by RAFT radical ring-opening polymerization. Monomers with ester, disulfide, and thioester functional groups were reported in the literature (Scheme 4a).<sup>79</sup> Macroyclic monomers were designed such that propagation through the allylic sulfide would readily open the macrocycle through beta-scission to produce a new carbon–carbon double bond and thiyl radical capable of addition to other monomers (Scheme 4b).<sup>79,80</sup> The macrocycles were copolymerized with MMA, *N,N*-dimethylaminoethyl methacrylate (DMAEMA), 2-hydroxyethyl methacrylate (HEMA), and 2-hydroxypropyl methacrylate (HPMA).<sup>79,81</sup> The copolymers were degraded in solutions of sodium methoxide in tetrahydrofuran (THF),<sup>79</sup> and the disulfide-containing polymers were degraded by reduction upon exposure to a tris(2-carboxyethyl)phosphine reducing agent.<sup>81</sup>



**Scheme 4** | (a) Allylic sulfide macrocyclic monomers polymerized by RAFT copolymerization in the literature. (b) Mechanism of RROP of allylic sulfide macrocyclic monomers. (c) RROP by radical cascade ring opening polymerization of an allylic sulfone macrocyclic monomer.

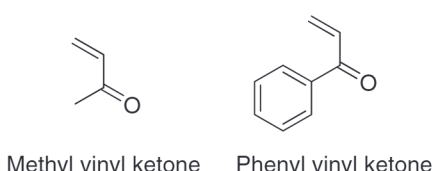


**Figure 3** | Structure of MVK and PVK.

The polymerization of macrocyclic allyl alkylsulfone monomers proceeded through a radical cascade process starting with  $\beta$ -elimination of alkylsulfone, followed by  $\alpha$ -scission and liberation of gaseous  $\text{SO}_2$ , providing a 2-propionate radical capable of propagation (Scheme 4c).<sup>82</sup> The macrocycles had nearly ideal reactivity with acrylic and acrylamide monomers due to the similar structure of the propagating radical after ring opening and loss of  $\text{SO}_2$ .<sup>83</sup> The ideal reactivity between these monomers and vinyl comonomers is a significant improvement over other RROP methods because the degradable bonds should be located roughly the same number of repeat units apart. This is anticipated to yield well-defined oligomers after degradation under the appropriate conditions.

## RDRP of degradable vinyl monomers

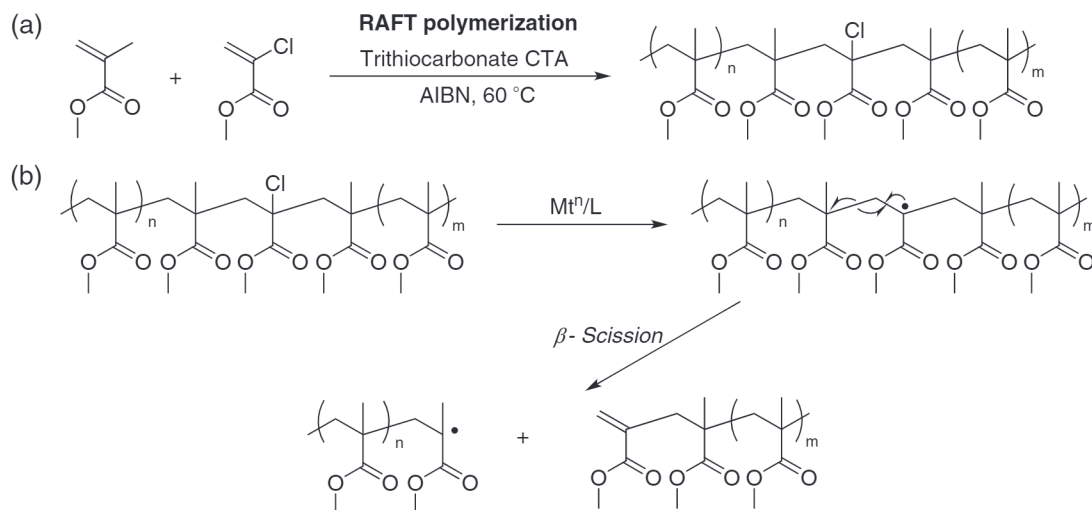
Some vinyl polymers can be degraded to lower molecular weight oligomers via photoinduced or catalyst-activated bond scission. Poly(vinyl ketone)s are a unique class of materials capable of degradation under ultraviolet (UV) irradiation through Norrish Type I and Norrish Type II reactions upon exposure to UV light, resulting in a degradation of polymer into shorter oligomers.<sup>84,85</sup> Methyl

vinyl ketone (MVK) and phenyl vinyl ketone (PVK) were polymerized by RAFT and subsequently degraded by photolysis (Figure 3).<sup>85,86</sup> Multiblock copolymers of poly(vinyl ketones) with nondegradable polymers provided materials with selectively etchable blocks. The morphology of polystyrene-*b*-poly(methyl vinyl ketone) thin films changed after etching the poly(methyl vinyl ketone) block by UV light exposure.<sup>86</sup> The modulus of triblock copolymers with a poly(*n*-butyl acrylate) middle block and PVK outer blocks decreased after selectively etching the PVK hard blocks.<sup>87</sup>

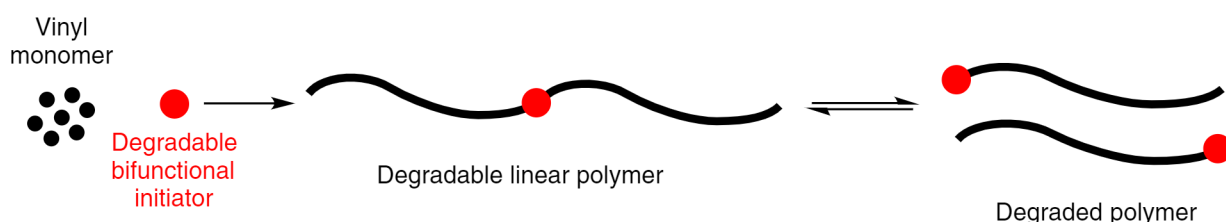
RAFT copolymerization of methyl  $\alpha$ -chloroacrylate (MCA) and MMA provided copolymers with chlorine functionalities along the backbone.<sup>88</sup> The chlorine functionality remained intact through the RAFT polymerization, and resembled a  $\alpha$ -chloroisobutyrate functionality along the backbone. Activation of the chlorines by ATRP catalysts generated acrylic midchain radicals, which were proposed to degrade through beta-scission and mid-chain cleavage of the copolymer along the backbone (Schemes 5a and 5b). The macroinitiator degraded from a starting  $M_p = 14,900$  ( $\bar{D} = 1.62$ ) to oligomers of  $M_p = 2000$  ( $\bar{D} = 1.32$ ) upon activation with  $\text{FeCl}_2$  and the tributylamine cocatalyst.

## Degradable Polymers from the Backbone via the Use of Bifunctional Initiators

Linear polymers with one degradable bond at the center of a linear polymer could be prepared by RDRP using bifunctional initiators.<sup>89</sup> The use of a bifunctional initiator enables growth of a polymer on both sides of the



**Scheme 5** | (a) RAFT polymerization of MMA and MCA. (b) Degradation of a P(MMA-co-MCA) copolymer by activation of chlorine bonds along the backbone with an ATRP catalyst, leading to beta scission into lower molecular weight oligomers.



**Scheme 6** | Scheme of an RDRP using a red bifunctional initiator installs the degradable bond at the middle of the polymer chain. Exposure to chemical or external stimuli cleaves the polymer into two polymers with half the molecular weight of the precursor. The degraded halves can reform the original polymer if the reaction is reversible.

degradable bond. Thus, degradation of the central linkage via chemical or external stimuli cleaves the high molecular weight polymer into two linear polymers with half the molecular weight of the precursor (Scheme 6). A diverse library of degradable bonds were installed in the middle of two ATRP initiators (Figure 4).

Redox degradable polyacrylates and PSs were prepared by ATRP with bifunctional 2-bromopropionic acid and 2-bromoisobutyrate diesters of bis(2hydroxyethyl) disulfide initiators.<sup>90,91</sup> The ATRP reaction can

be performed without reduction of the disulfide bond, providing high molecular weight polymers with one central disulfide bond. The disulfide linkage could be reversibly reduced by dithiothreitol (DTT) or tributylphosphine to yield linear polymers with half the molecular weight of the original material. The degraded mercapto-functional oligomers could be recoupled after oxidation in the presence of weak oxidizing agents, such as  $\text{FeCl}_3$  or iodine, to reform the high molecular weight polymer linked by the disulfide bonds.

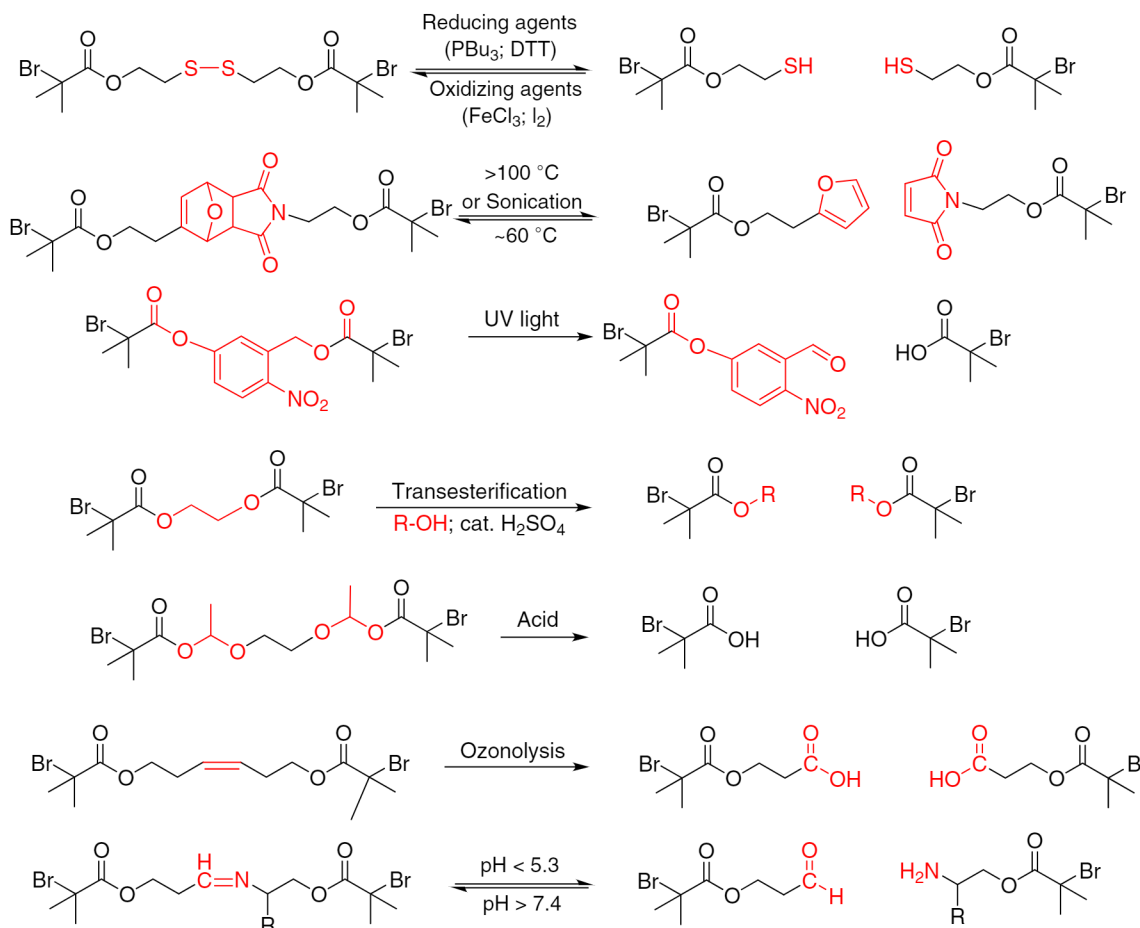


**Figure 4** | Bifunctional ATRP initiators with degraded products and conditions required to cleave the degradable bond.

The method of disulfide reduction and oxidation can affect the efficiency of the self-healing reaction. Reductive cleavage/nucleophilic substitution of a poly(methyl acrylate) (PMA) with a central disulfide bond and terminal bromine functionality with diethylamine base and DTT reduces the disulfide bond and installs an additional thiol at the chain-end by substitution of the bromine. Thus, oxidation of telechelic  $\alpha,\omega$ -bis(thiol)-functionalized PMA with  $I_2$  leads to step-growth polymerization by bridging disulfide bonds (Figures 5a and 5b).<sup>92</sup> Reduction of the disulfide bond over  $Bu_3SnH$  and Azobisisobutyronitrile (AIBN) saturates the bromine chain-end while reducing the disulfide bond, yielding two saturated chains with terminal thiol functionality. Oxidation of the polymer produced a new material with comparable molecular weight to the precursor.

Furfuryl-maleimide Diels-Alder (DA) functionalities enabled linear polymer degradation after thermal and mechanical treatment. Maleimide functionalized PMA was prepared by ATRP of methyl acrylate with a maleimide

functionalized  $\alpha$ -bromoisobutyrate initiator.<sup>93</sup> DA [4+2] cycloaddition between  $\omega$ -maleimide-PMA and a  $\omega$ -furan-poly(ethylene glycol) produced diblock copolymers with the furan-maleimide adduct at the center. The retro-Diels Alder reaction at 120 °C cleaved the adduct into the same  $\omega$ -furan-poly(ethylene glycol) and  $\omega$ -maleimide-PMA starting materials.<sup>93</sup> Ultrasonication of PMA with the same DA adduct led to mechanochemical retro-DA of the polymer into two PMA chains with half the molecular weight of the original polymer.<sup>94</sup>

## Multiblock Backbone Scission via RDRP then Step-Growth Polymerization

The chain-end functionality of polymers prepared by RDRP enables installation of various functional groups by substitution chemistries. Multiblock copolymers can be prepared by post-polymerization modification of

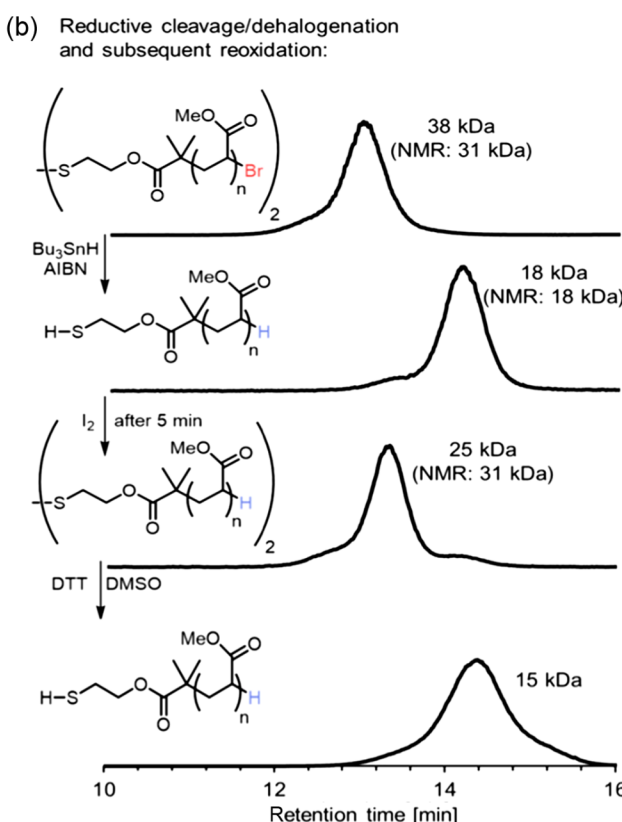
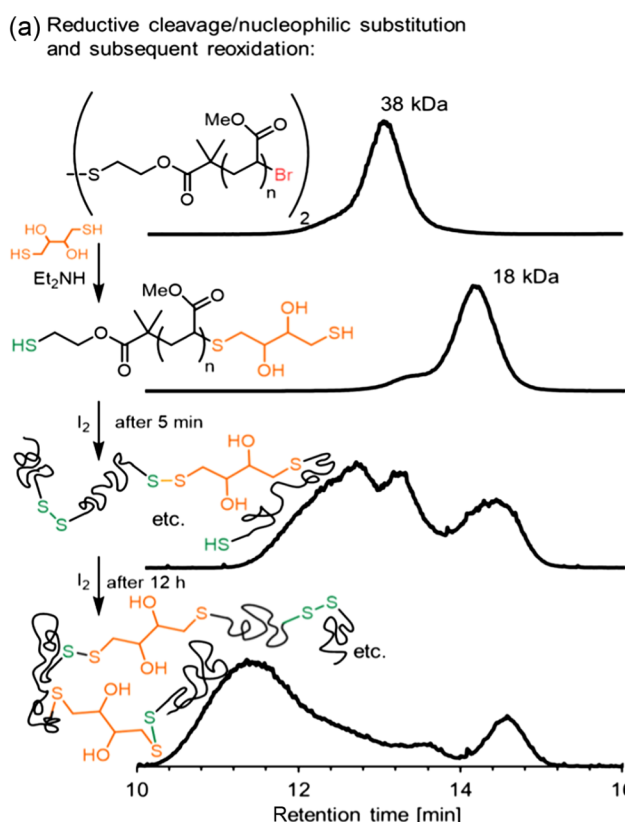
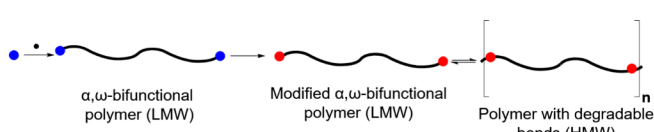


**Figure 5** | (a) Reaction scheme and gel permeation chromatography (GPC) traces illustrating the reduction of a polymer with a central disulfide bond with diethylamine as base and DTT as reducing agent, followed by oxidation to a higher molecular weight polymer containing multiple disulfide bonds. (b) Reaction scheme and GPC illustrating the reduction and hydrogenolysis of the same polymer by  $Bu_3SnH$ , followed by subsequent oxidation to disulfide polymer, then reduction with DTT in dimethyl sulfoxide. ( $M_n$  determined by GPC; values in parentheses determined by  $^1H$  NMR integration). Reproduced with permission from ref 92. Copyright 2018 Wiley-VCH Verlag GmbH & Co. KGaA, Weinheim.



**Scheme 7** | RDRP with a bifunctional initiator or CTA installs end-group functionality (blue) at both ends of the polymer. Modification of the end groups (red dots) can enable step-growth polymerization to high molecular weight, with degradable bonds placed between each macromer. Exposure to chemical or external stimuli can cleave the polymer into linear polymers with comparable molecular weight to the precursor.

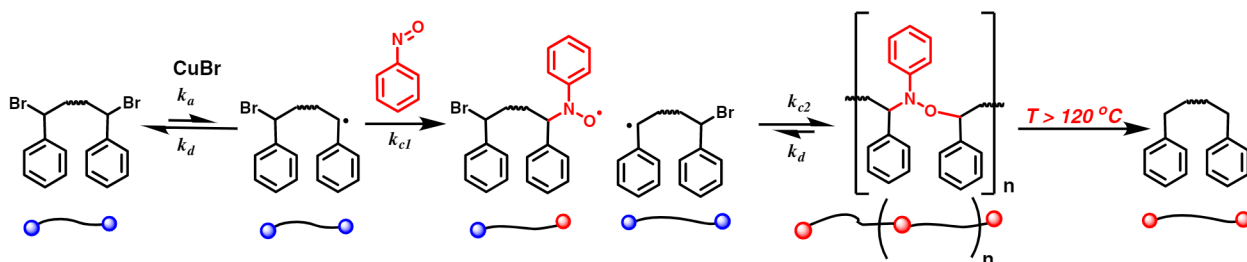
bifunctional polymers into macromonomers, followed by step-growth polymerization, to yield high molecular weight linear polymers (Scheme 7). The use of reversible, or degradable, bonds in the step-growth polymerization enables degradation from high to lower molecular weight upon exposure to the appropriate chemical or external stimuli.

Multisegment degradable polymers were prepared by radical trap-assisted atom transfer radical coupling (RTA-ATRC) of halogenated styrenic and (meth)acrylic polymers with nitroxide coupling agents.<sup>95</sup> ATRC is a method of coupling polymer chains by preference of crosstermination by combination.<sup>96,97</sup> Step-growth ATRC of  $\alpha,\omega$ -dihalogenated PS was performed in the presence of a bifunctional (2,2,6,6-Tetramethylpiperidin-1-yl)oxyl (TEMPO) adduct with, and without, a central disulfide bond.<sup>95,98</sup> PS prepared by ATRC was degraded thermally in the presence of excess TEMPO, due to exchange between the bifunctional crosslinker and the higher concentration of monofunctional TEMPO. High molecular weight polymers were also prepared by step-growth polymerization of a bifunctional 4-phenylene bis(2-bromoisobutyrate) ATRP initiator with a bifunctional TEMPO adduct by radical coupling between activated chain ends and TEMPO radical traps.<sup>99</sup> Thermogravimetric analysis of the poly(alkoxyamines) showed considerable mass loss below 200 °C, suggesting poor thermal stability caused by scission of the initiator-alkoxyamine bonds.

Nitroso radical traps were also used to install thermally cleavable alkoxyamine functionalities onto styrenic and acrylic polymers by ATRC.<sup>100</sup> The coupling of polymer chains with nitroso compounds proceeds in two steps (Scheme 8). In the first step, the polymeric chain-end radical reacts with the nitroso functional group to produce a polymer with nitroxide functionality. The chain-end nitroxide can trap a second polymeric radical to produce alkoxyamine-linked polymer topologies. Thermolysis of the alkoxyamine cleaves the bond and produces two polymer chains with similar  $M_n$  and  $D$  as the starting material. This approach was first outlined in the RTA-ATRC of a monobrominated PMMA-Br precursor with a nitrosobenzene radical trap.<sup>100</sup> Brominated PS and PMA were also coupled by RTA-ATRC using nitrosobenzene radical traps, and later work applied the concept to multiblock copolymers.<sup>101</sup> Under dilute conditions, the coupling reaction produces cyclic polymers which can be degraded back to linear polymers by thermolysis.<sup>102</sup>

Nucleophilic substitution of halogen chain-end functionality (CEF) can install thiol linkages on telechelic  $\alpha,\omega$ -dibromo vinyl polymers.<sup>90,103</sup> Telechelic polymers with thiol functionalities could also be prepared by aminolysis of trithiocarbonate (TTC; Scheme 9)<sup>104</sup> or xanthate RAFT CTAs.<sup>105</sup> Oxidative coupling of linear  $\alpha,\omega$ -dithiol polymers produces high molecular weight linear polymers connected by disulfide bonds, which can be reversibly degraded to the low molecular weight telechelic  $\alpha,\omega$ -dithiol pre-polymer after reduction.

Oxidative step-growth polymerization of  $\alpha,\omega$ -bis(thiol) polymers enabled the synthesis of degradable random multiblock copolymers. Multiblock telechelic copolymers were prepared by oxidative coupling of  $\alpha,\omega$ -bis(thiol)-poly(styrene)-*b*-poly(*n*-butyl acrylate)-*b*-poly(*tert*-butyl acrylate).<sup>105</sup> Oxidative coupling of  $\alpha,\omega$ -bis(thiol) poly(*N*-isopropyl acrylamide) (PNIPAM) ( $M_n = 7860$ ,  $D = 1.24$ ) and  $\alpha,\omega$ -bis(thiol) poly(2-(dimethylamino)ethyl methacrylate) (PDMAEMA) ( $M_n = 7780$ ,  $D = 1.18$ ) at a 1:1 weight ratio produced a high molecular weight ( $M_n = 180,000$  and  $D = 5.1$ ) temperature and pH-responsive multiblock copolymer.<sup>106</sup> The multiblock copolymers were degraded to lower molecular weight by reduction with DTT.

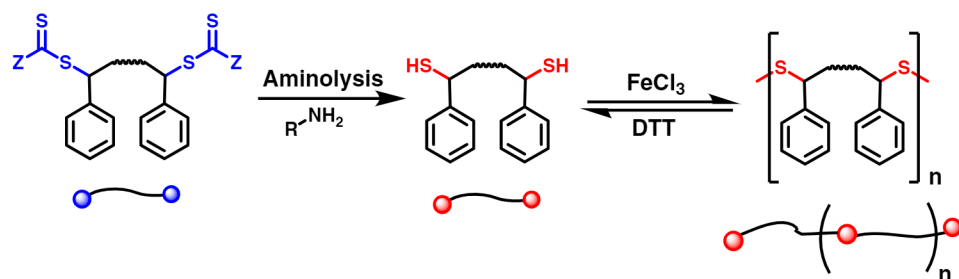


**Scheme 8** | ATRC of bifunctional PS with nitrosobenzene

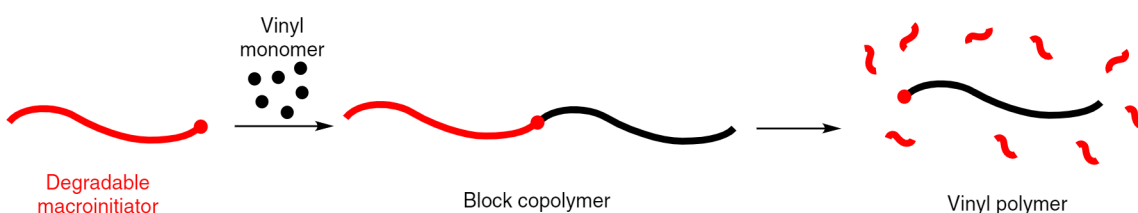
DOI: 10.31635/ccschem.022.202201987

Citation: CCS Chem. 2022, 4, 2176-2211

Link to VoR: <https://doi.org/10.31635/ccschem.022.202201987>



**Scheme 9** | Aminolysis of RAFT chain ends enables the synthesis of bifunctional PS with thiol chain ends. Two thiols can couple after oxidation to disulfide bonds to yield high molecular weight PS. The polymer could be degraded back to low molecular weight after reduction of the disulfide bonds.



**Scheme 10** | Use of a degradable macroinitiator (red) enabled the synthesis of a block copolymer with one degradable block (red) and one nondegradable vinyl polymer block (black). The degradable block can be selectively etched to yield the nondegradable vinyl polymer.

## Block Copolymers

Degradable functionalities can also be installed using a degradable macroinitiator. This has often involved the use of polymer macroinitiators prepared by ROP, such as poly(lactic acid), polycaprolactone, polypeptides, or polyphosphates as the degradable block (Scheme 10).<sup>107–109</sup>

Multifunctional initiators can be used to initiate ring-opening polymerization and controlled radical polymerization.<sup>110,111</sup> Block copolymers of vinyl polymers and polyesters were prepared in one pot using a hydroxyl-functionalized TTC CTA as a dual RAFT and ROP initiator.<sup>112</sup> Block copolymers of epoxides and acrylamides were prepared by a photoiniferter/organocatalyst dual catalysis approach using a hydroxyl-functionalized TTC as the ROP/RAFT initiator.<sup>113</sup>

## Degradable Hyperbranched Polymers

Hyperbranched polymers are polymers with irregular branched topologies.<sup>114–117</sup> Branching reduces the hydrodynamic size and entanglement between molecules in solution and the melt, resulting in reduced viscosity and a higher local concentration of functional groups relative to a linear polymer. These materials are commonly used in industrial coatings, resins, and adhesives as well as

high performance applications like drug delivery and therapeutics.

## Synthesis of hyperbranched polymers by self-condensing vinyl polymerization

Hyperbranched polymers can be prepared by polymerization, and copolymerization, of vinyl “inimers” with initiator and monomer functional groups in a self-condensing vinyl polymerization (SCVP). The degree of branching in a SCVP by ATRP is partially determined by the difference in the activation-rate constant for the inimer ( $k_{a,s}$ ) and backbone ( $k_{a,b}$ ) dormant species (Figure 6).<sup>118</sup> Predominantly linear polymers are produced if the activity of the dormant backbone is larger than the activity of the inimer ( $k_{a,s} << k_{a,b}$ ), or vice versa in the opposite case ( $k_{a,s} >> k_{a,b}$ ). Comparable activity between inimer and backbone initiators can provide densely branched copolymers.

Thus, the size of a degraded hyperbranched polymer prepared by ATRP of a degradable inimer should be tunable by the reactivity of the inimer and backbone, respectively (Figure 6).<sup>118</sup> Degradation of a hyperbranched polymer prepared by polymerization of a degradable inimer with a higher activity backbone and low activity initiator ( $k_{a,s} << k_{a,b}$ ) yields a polymer with the majority of degradable bonds in the side chains and will not degrade to a significantly lower molecular weight.

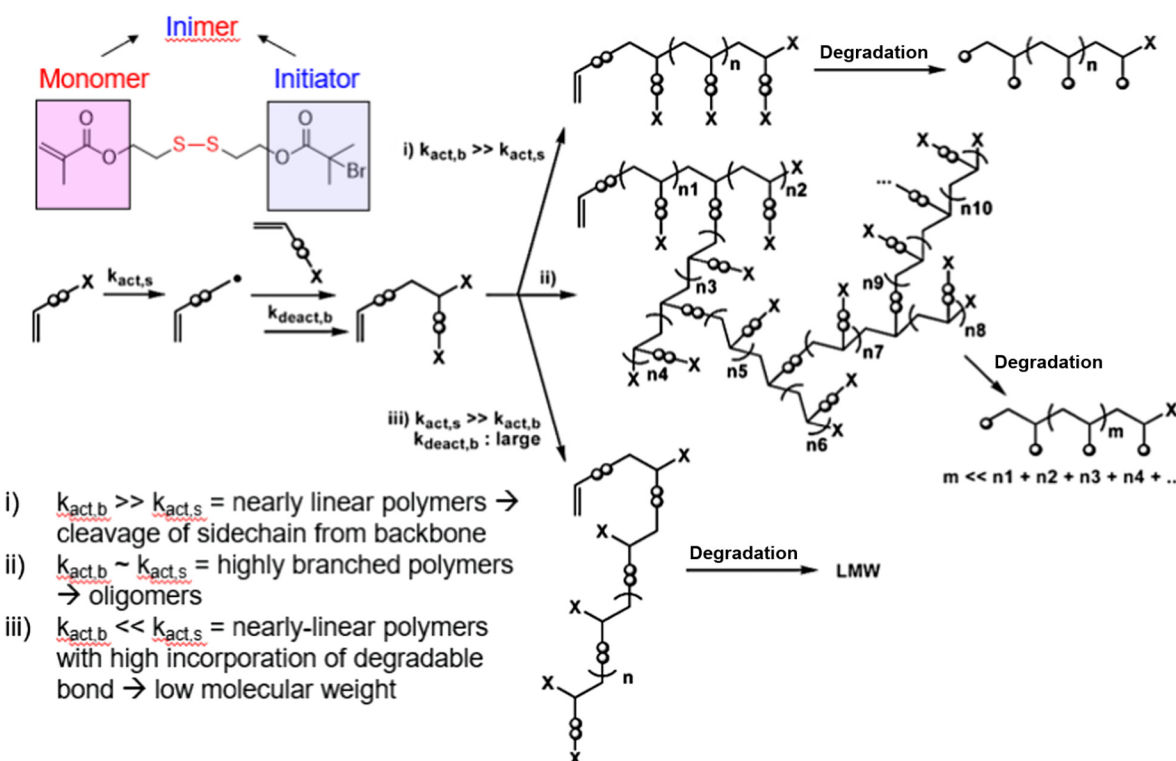


**Figure 6** | Possible structures of polymers derived from an inimer with a degradable functionality and products of their complete degradation. Figure adapted with permission from ref 118. Copyright 2009 Wiley-VCH Verlag GmbH & Co. KGaA, Weinheim.

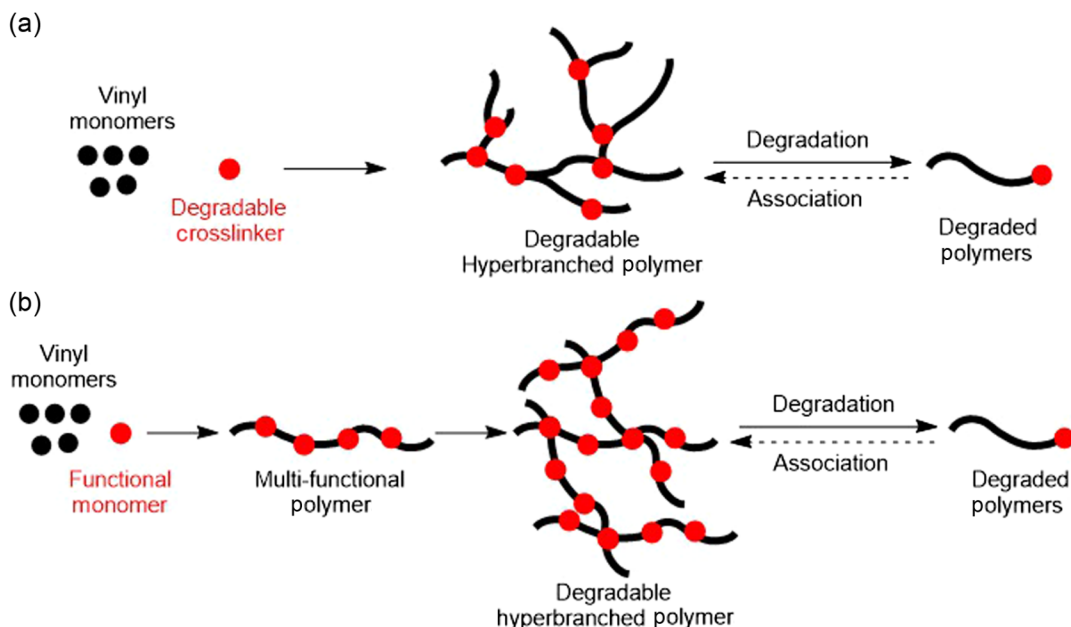
A degradable hyperbranched polymer prepared from inimers with comparable backbone and initiator reactivity will yield a highly branched polymer that can be degraded to lower molecular weight linear polymers ( $k_{a,s} \sim k_{a,b}$ ). Finally, polymerization of a degradable inimer with high initiator reactivity and low backbone reactivity produces mostly linear polymers with degradable bonds along the backbone. Degradation of this polymer produces low molecular weight fragments, analogous to the polymerization and degradation of vinyl chloropropionates by atom transfer radical addition.<sup>119</sup>

Highly branched degradable polymers were prepared by polymerization of inimers with redox-active disulfide and acid-sensitive acetal functionalities.<sup>118,120</sup> Copolymerization of 2-(2-bromopropionyloxy)ethyl acrylate with styrene provided densely hyperbranched copolymers due to the large difference in activation between the initiator and backbone dormant species (i.e.,  $k_{a,s} >> k_{a,b}$ ). A disulfide-containing methacrylic inimer copolymerized with MMA provided well-defined branched copolymers with a lower degree of branching due to similar reactivities between the backbone and side chain (i.e.,  $k_{a,s} \sim k_{a,b}$ ).<sup>118</sup> The topology of the branches was confirmed by degradation of the inimer and analysis of the low molecular weight polymer by GPC.

A segmented hyperbranched poly(methyl methacrylate) (PMMA) copolymer with a furan-maleimide branch junctions was synthesized by SCVP by ATRP of MMA with a DA inimer.<sup>121</sup> The retro-DA reaction at 120 °C cleaved polymer arms into linear PMMA segments with statistical distributions of furan in the side chains and maleimide chain ends. The PMMA segments could be grafted to single-chain nanoparticles by DA cycloaddition between the dissociated furan and maleimide macroinitiators.

### Synthesis of hyperbranched polymers by (co) polymerization of a degradable crosslinker

Degradable branched polymers and single chain nanoparticles can also be prepared by copolymerization of monofunctional vinyl monomers with degradable crosslinkers (Schemes 11a and 11b). The topology of the material and location of the degradable bonds is dictated by the polymerization recipe. The copolymerization of MMA and HPMA with a disulfide-based dimethacrylate (DSDMA) via RAFT-produced high molecular weight hyperbranched polymers bridged by disulfide bonds between branch points.<sup>122-124</sup> Reduction of the disulfide bonds degraded the high molecular weight branched polymer to short oligomers.



**Scheme 11** | Degradable hyperbranched polymers can be prepared by RDRP through (a) copolymerization of a degradable crosslinker (red) with a spacer monomer (black), or (b) coupling of multifunctional linear arms into randomly crosslinked/branched nanoparticles with degradable bonds. The highly branched polymers have degradable bonds located at the junctions of the branches. Thus, degradation of the branches provides linear polymers of lower molecular weight. Branched polymers can be reformed in some cases.

Segregation of the polymerization into an immiscible phase, via RDRP in an emulsion or miniemulsion can yield densely branched nanoparticles. OEOMA was polymerized by activators regenerated by electron transfer ATRP in the presence of a disulfide crosslinker using the inverse miniemulsion technique, then chain-extended with styrene.<sup>125,126</sup> The block copolymer nanoparticles were degraded to linear PS-*b*-P(OEOMA)

block copolymers which self-assembled into micelles with a PS core and POEOMA corona in water. Degradable OEOMA nanogels had promising biomedical properties due to an affinity to biotin and a fast drug release profile in the presence of glutathione.<sup>127</sup>

The rate of branched polymer degradation varies by the crosslinker structure. Hyperbranched polyacrylates with imine crosslinks hydrolyzed faster when less stable

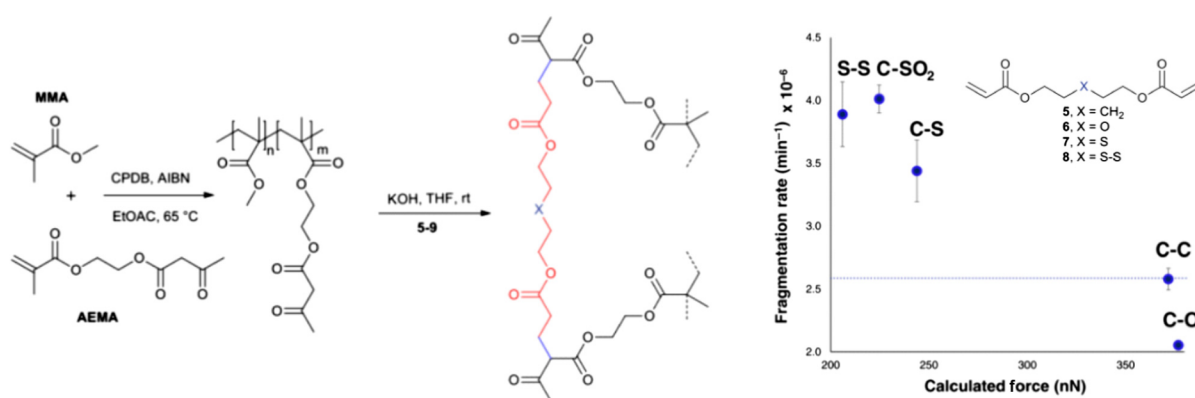


**Figure 7** | Mechanochemical degradation of single chain nanoparticles prepared by RAFT copolymerization of MMA with 2-(methacryloyloxy)ethyl acetoacetate ( $M_n \sim 100,000$ ) followed by postpolymerization Michael addition of pendant 1,3-diketones with divinyl crosslinkers. The fragmentation rate scaled with the calculated force to break the crosslinker where weaker disulfide and sulfone bonds broke faster than the stronger ether and carbon-carbon bonds. Reproduced with permission from ref 129. Copyright 2020 Wiley-VCH Verlag GmbH & Co. KGaA, Weinheim.

hydrazone functional groups were installed in the branches, compared to more stable oxime functional groups.<sup>128</sup> Mechanochemical scission of hyperbranched polymethacrylate arms with weaker disulfide and sulfonyl functionalities at the junctions was ~2 times faster than mechanochemical scission of hyperbranched polymers with alkyl and ether crosslinks (Figure 7).<sup>129</sup>

## Star Polymers

Polymer stars are branched polymers with a defined length and number of arms extending from a central core.<sup>130–132</sup> Similar to other branched polymers, star polymers have a reduced molecular size which leads to less entanglement and lower viscosity in the melt and in solution.<sup>133</sup> Star polymers are generally more well defined than hyperbranched polymers and could be used for similar applications in biomedicine, energy, and nanotechnology. Star polymers can be prepared by the “core-first” and “arm-first” approaches.<sup>130–132</sup>

### Star polymers by the “core-first” approach

The core-first approach involves the synthesis of a multifunctional polymer core as the macroinitiator, followed by polymerization of monomers from the core (Scheme 12). The core-first approach enables the synthesis of polymer stars with a precise number and length of polymer arms. However, core-first synthesis by RDRP can lead to coupling and eventual macroscopic gelation if a significant portion of stars terminate via biradical combination. Polymer stars can be degraded to linear polymers if the multifunctional core contains degradable functional groups.

Biobased  $\alpha$ -D-glucose and  $\beta$ -cyclodextrin were used to prepare multifunctional star cores by base catalyzed esterification with 2-bromoisobutyryl bromide.<sup>134,135</sup> A similar approach installed ATRP initiators onto PCL which was used as a star core in the synthesis of degradable core-shell polymers.<sup>136</sup> Star polymer arms can be grafted from the cores via ATRP and cleaved from the

core by transesterification of the ester with a strong acid catalyst. Star polymer arms grafted from tannic acid cores can be degraded in a mild methanol/bicarbonate solution due to the poorer stability of the phenyl ester bond tethering the arms to the core.<sup>137</sup>

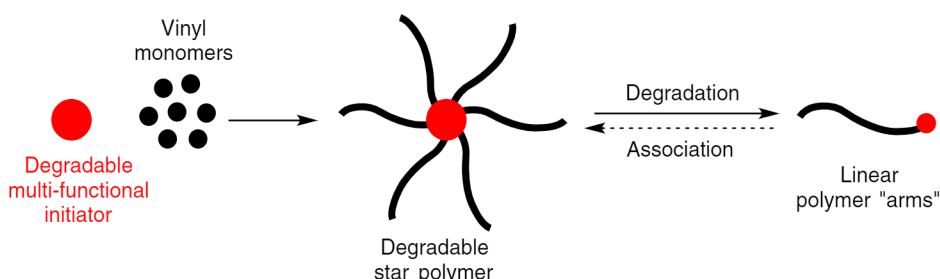
Multifunctional CTAs with disulfide links were used to prepare redox degradable polymer stars via the core-first RAFT approach (Figure 8).<sup>139,140</sup> The cores were prepared such that the disulfide bonds and “R” groups of the CTA were inside of the core, and the radical stabilizing Z-groups were on the outside. This enabled polymerization from the core without dissociation of the arms. The linear arms were cleaved from the star core after reduction of the disulfide bonds.

### Degradable star polymers by the “arm-first” approach

The arm-first approach involves the synthesis of a (block) copolymer arm (Scheme 13a), followed by chain extension with a divinyl crosslinker (Scheme 13b). This approach provides precise control over the length of polymer arms and is less likely to reach macroscopic gelation than the core-first approach. However, the method provides less control over the number of arms in the final product. Miktoarm polymer stars can be prepared by chain-extension from the polymer core via an “in-out” approach.

The use of a degradable crosslinker enables the synthesis of polymer stars with degradable cores via the arm-first approach. Degradable divinyl crosslinkers with acetal, imine, DA, and disulfide functional groups were reported in the literature (Figure 9). The arm-first method could also involve coupling of a functionalized-nonfunctionalized diblock copolymer via other chemistry. Degradation of the polymer core liberates the linear polymer arms (Scheme 13c). In some cases, the cleaved polymer arms could reassociate back to form the original polymer star (Scheme 13d).

Redox-degradable star polymers were prepared by chain-extension of PMMA and PS-co-PMMA block



**Scheme 12** | Core-first synthesis of a star polymer. The use of a multifunctional degradable polymer core enables cleavage of the polymer arms from the core. Some functional groups enable association of degraded star arms to reform polymer star upon exposure to external stimuli or via postdegradation modification.

DOI: 10.31635/ccschem.022.202201987

Citation: CCS Chem. 2022, 4, 2176–2211

Link to VoR: <https://doi.org/10.31635/ccschem.022.202201987>

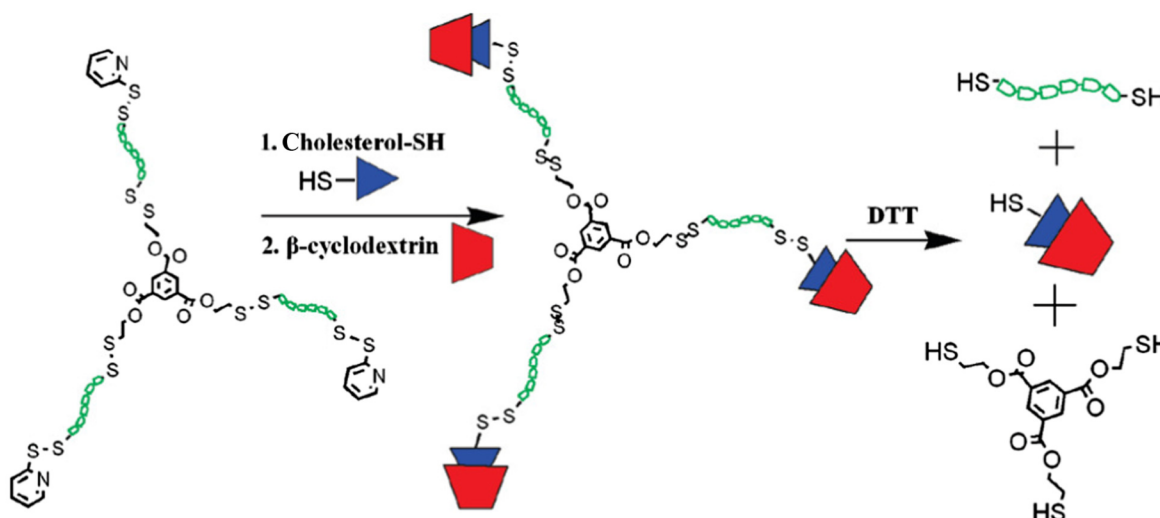
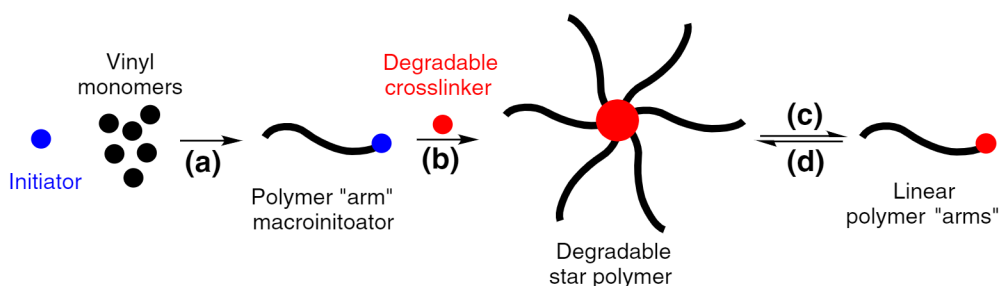


**Figure 8** | A multifunctional RAFT agent was used to prepare polymer stars with degradable cores by the transfer-from core-first approach. The RAFT CEF was reduced, then functionalized with  $\beta$ -cyclodextrin at the arms. Reproduced with permission from ref 138. Copyright 2009 American Chemical Society.



**Scheme 13** | Degradable polymer stars can be synthesized via the arm-first approach by chain extension with a degradable crosslinker. The degradable bonds at the core enable a change in topology back to low molecular weight linear arms after scission. The cleaved arms can be reconnected in some cases.

copolymers with a redox-degradable disulfide crosslinker via ATRP.<sup>141</sup> Redox-degradable star polymers are promising for biomedical applications. Stars with oligo (ethylene oxide) arms and cationic cores complexed with negatively charged siRNA, which allowed for cellular internalization of siRNA using the polymer scaffold as a biocompatible delivery vehicle (Figure 10).<sup>142</sup> Cationic nanogels crosslinked with disulfide crosslinks were also effective at nucleic acid delivery.<sup>143</sup> Star polymers with POEOMA-*b*-PBMA arms self-assembled into nanocapsules with a diameter of 140~195 nm after crosslinking with a bis(2-methacryloyloxyethyl)disulfide (DSDMA) crosslinker.<sup>144</sup>

Copolymerization of two macroinitiators with a crosslinker yields mikto-arm polymer stars. ATRP and ROP were used to prepare a library of hydrolytically degradable star polymers by the arm-first approach.<sup>145</sup> Copolymers were prepared by ROP of caprolactone from a

2-hydroxyethyl  $\alpha$ -bromoisobutyrate initiator, followed by arm-first crosslinking by ATRP with divinyl benzene (DVB). Conversely, PMMA or PS arms could be prepared first by ATRP, then crosslinked by ROP with a bifunctional lactone, to yield star polymers with degradable cores. This approach was later expanded to the synthesis of core-shell block copolymers with PCL-*b*-PMMA arms.<sup>146</sup> Block copolymer stars with PCL blocks on the outside were crosslinked by ATRP with ethylene glycol dimethacrylate (EDGMA) and could be degraded back to PMMA polymer stars via hydrolysis. Conversely, crosslinking the PCL blocks by ROP with a bifunctional lactone-produced star polymers with PCL cores.

Thermally degradable polymer stars were prepared by chain-extension of a polymer macroinitiator with a thermally unstable crosslinker. Polymer stars with 4,4'-azobis (4-cyanovaleric acid) crosslinks in the core irreversibly degraded upon exposure to high temperature and

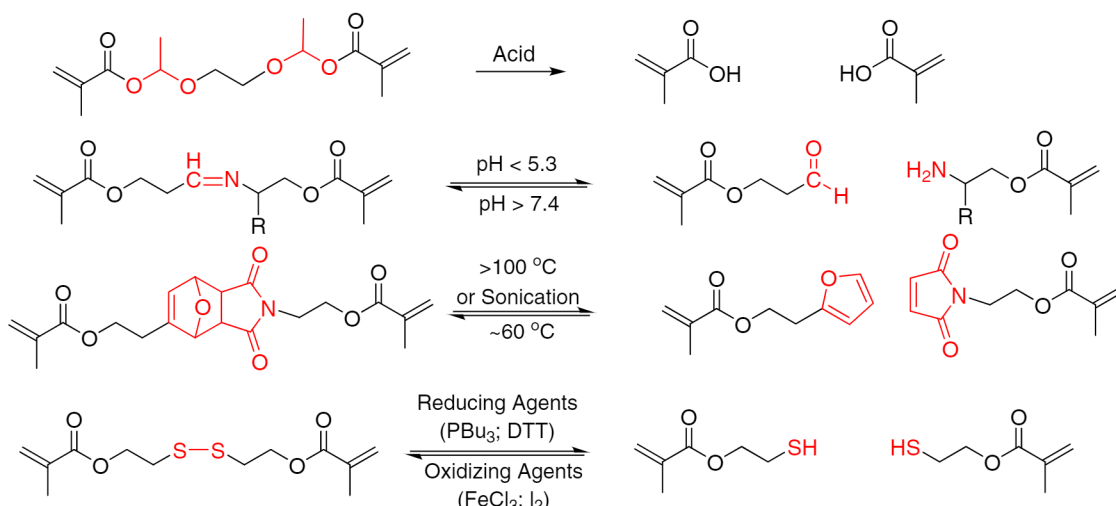


**Figure 9** | Common degradable crosslinkers reported in the literature.

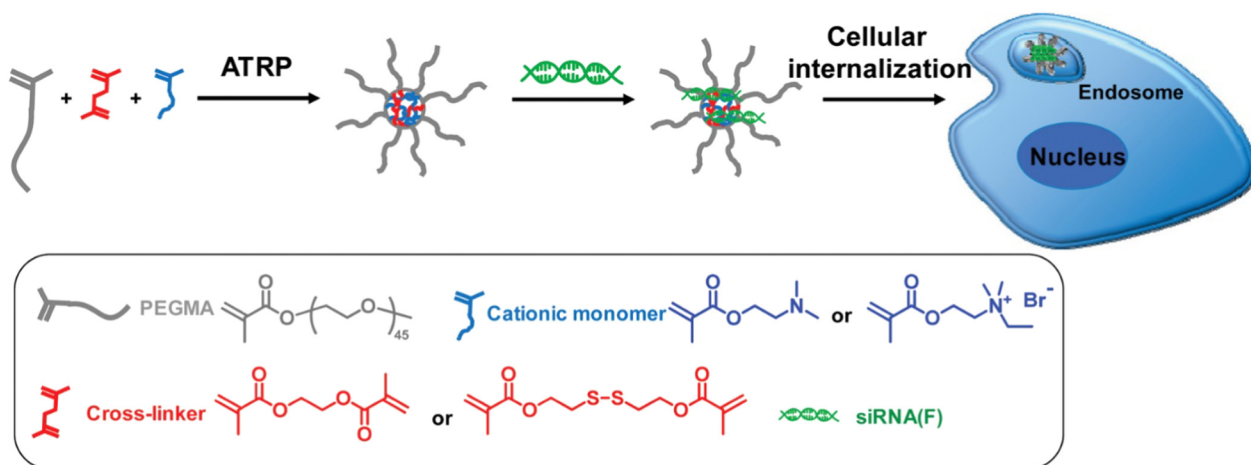


**Figure 10** | Synthesis of star copolymers with PEG arms and a degradable cationic core by ATRP through the arm-first approach. The star polymers complexed with siRNA. Reproduced with permission from ref 142. Copyright 2011 American Chemical Society.

light.<sup>147</sup> Temperature-responsive arms crosslinked by DA bonds reversibly aggregated into 18 nm aggregates and dissociated to 6 nm unimers by DA and retro-DA exchange.<sup>148</sup>

Reversible detachment of polymer arms from a star was also accomplished with alkoxyamine exchange chemistry. The arm-first synthesis of polymer stars using PMMA-TEMPO macromonomers via NMP with DVB was reported.<sup>149</sup> The PMMA arms were designed such that the TEMPO adduct remained attached to PMMA after decomposition. Thus, heating the star polymer at 100 °C with a stoichiometric excess of alkoxyamines cleaved PMMA arms from the core by dynamic-covalent exchange. PS polymer stars were also crosslinked by dynamic-covalent exchange of alkoxyamine units in the side chain.<sup>150,151</sup> Reflux of two complementary block

copolymers liberated the nitroxide radical from one polymer backbone and produced nonfunctional PS radical in the other backbone. Trapping of the functional PS radicals in the side chain enabled reversible dynamic-covalent assembly of polymer stars at 100 °C. Mikto-arm star polymers were also prepared by heating the polymer stars in the presence of another alkoxyamine functionalized polymer.

## Bottlebrushes

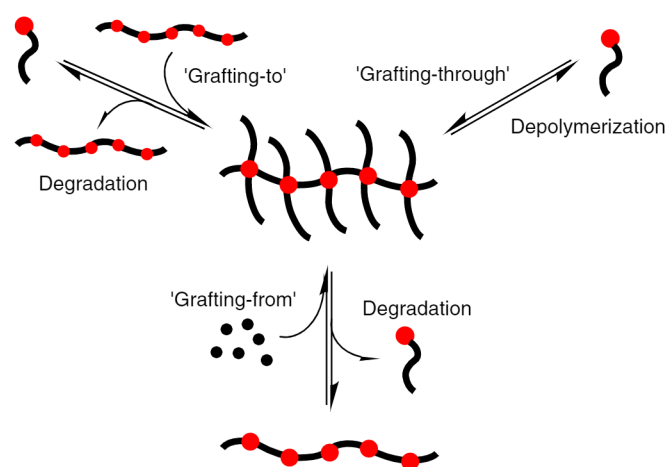
Molecular bottlebrushes are densely grafted molecules which consist of side chains attached to a polymer backbone. The steric repulsion between the side chains elongates the polymeric backbone and side chains, such that densely grafted molecular bottlebrushes with a high

aspect ratio exist in rod-like conformations. Bottlebrushes have reduced viscosity and suppressed chain entanglement, which make them useful for potential applications in lubrication, soft materials, and biomedicine.<sup>21,152,153</sup>

The intrinsic tension of a densely grafted bottlebrush with side chains attached to every repeat unit in the backbone was on the order of  $f_0 N^\alpha$ , where  $N$  is the side chain length and  $\alpha = 3/8$  in good solvents,  $1/3$  in theta solvents, and  $f_0$  in poor solvents and melts.<sup>154</sup> The tension of a fully extended molecular bottlebrush in the melt is on the order of 1 pN. Tension increases when the polymer adsorbs to an attractive substrate, as the monomeric units try to maximize interaction with the surface despite the steric congestion and tension already present in the backbone and side chains.<sup>155,156</sup> The attractive forces amplify the tension of the bottlebrushes up to the  $nN$  range.<sup>155</sup>

Scission of carbon–carbon bonds was observed when molecular bottlebrushes were adsorbed onto attractive liquid and solid substrates (Figure 11).<sup>157</sup> Atomic force microscopy (AFM) of poly(*n*-butyl acrylate) (PBA) bottlebrushes on a water/isopropanol surface showed a reduction in contour length with time spent on the surface.<sup>157</sup> The rate of backbone C–C bond scission was dependent on the substrate surface energy. The rate of bond scission was six times faster when the surface energy of the substrate was increased from 69.2 to 71.2 mN/m.<sup>158,159</sup> Bond scission in PBA bottlebrushes had anti-Arrhenius behavior due to the decrease in surface energy of the substrate upon heating, which resulted in an overall decrease in tension of the adsorbed macromolecules.<sup>160,161</sup>

The selectivity of molecular bottlebrush bond scission after adsorption on a surface was improved by installation of a weaker disulfide bond in the middle of the backbone.<sup>162</sup> Similarly, spoked-wheel molecular



**Scheme 14** | The three synthetic strategies used to prepare molecular bottlebrushes are the grafting-through, grafting-to, and grafting-from approaches.

bottlebrush star polymers showed preferential scission of the ester-linked arms before the scission of carbon–carbon covalent bonds in the bottlebrush backbone.<sup>163</sup>

Outside of the intrinsic tension in molecular bottlebrushes, degradable bonds can be installed in the backbone and side chains, analogous to polymer stars. Molecular bottlebrushes can be prepared by the grafting-through, grafting-from, and grafting-to approaches (Scheme 14).

### Degradable bottlebrushes by the “grafting-through” approach

The grafting-through approach involves the polymerization of “macromonomers,” which are oligomers with one

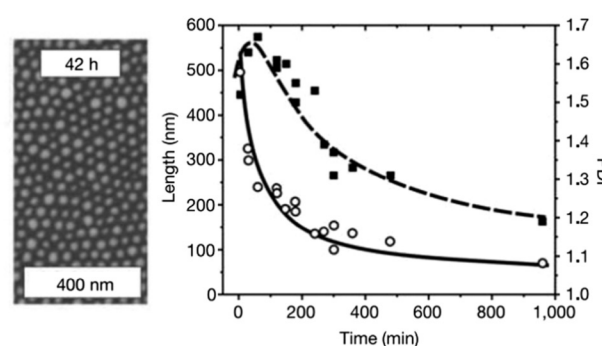
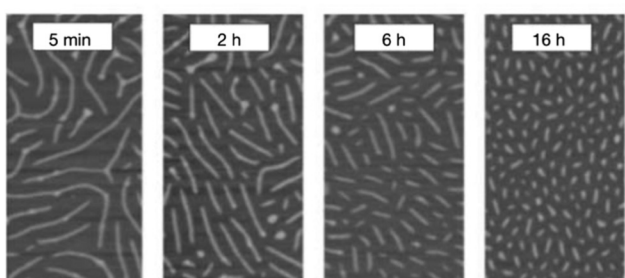


**Figure 11** | (left) Height AFM micrographs of molecular bottlebrushes with long side chains measured at different exposure times after adsorption on a water/propanol (99.8/0.2 w/w%) substrate. (right) The number average contour length decreases with increasing exposure time (white circles); the solid line is a fit to the experimental data assuming bond scission as a first-order reaction. The experimentally determined dispersity (PDI) initially increases and then decays and is also in agreement with the computer simulations (dashed line). Reproduced with permission from ref 157. Copyright 2006 Springer Nature Limited.

polymerizable functional group.<sup>164–166</sup> The grafting-through synthesis of bottlebrushes by RDRP is often limited by the dilute repeat unit concentration and high viscosity of the macromonomers. This lowers the bulk repeat unit concentration, leading to poorer kinetic control due to the low concentration of CTA and catalyst required to mediate polymerization and a lower ceiling temperature ( $T_c$ ).<sup>25</sup> The low  $T_c$  of methacrylic poly(monomer)s enables depolymerization of methacrylic molecular bottlebrushes back to macromonomers at elevated temperatures by RDRP mechanisms.<sup>167–169</sup> The depolymerization of polymers by RDRP will be discussed in detail at the end of this review.

### Degradable bottlebrushes by the “grafting-from” approach

The grafting-from approach involves the polymerization of small molecule monomers from a multifunctional backbone macroinitiator.<sup>170–172</sup> The grafting-from approach enables the synthesis of molecular bottlebrushes with long backbones and high graft densities. However, grafting-from by RDRP may lead to coupling and macroscopic gelation if bimolecular combination is not adequately suppressed.<sup>171,172</sup> Bottlebrush arms can be removed from the backbone by degradation of the backbone or by postpolymerization modification if they are attached by a degradable functional group. Degradable polymer backbones can enable a transition from bottlebrush to linear topology, with the molecular weight of the degraded product closely matching the separated side chains and backbone.

Side chains grafted from N-carboxy anhydride and cellulose backbones can be released by hydrolysis along the polymer backbone.<sup>173,174</sup> Poly(*n*-butyl acrylate) side chains grafted from poly(2-bromoisobutyryl ethyl methacrylate) macroinitiator backbones are commonly etched from the backbone by transesterification with butanol to calculate initiation efficiency (Scheme 15).<sup>172,174–176</sup> Weaker silanol

moieties installed along the backbone enabled hydrolysis of zwitterionic poly(2-methacryloyloxyethyl phosphorylcholine) side chains from bottlebrush backbones under milder conditions.<sup>177</sup>

### Degradable bottlebrushes by the “grafting-to” approach

The grafting-to approach involves a complementary reaction between a multifunctional backbone and polymeric side chains with one pendant functionality.<sup>178,179</sup> An analogous approach to bottlebrush degradation can be accomplished if the grafting-to method relies on dynamic covalent, or degradable, functional groups to attach the arms to the backbone.

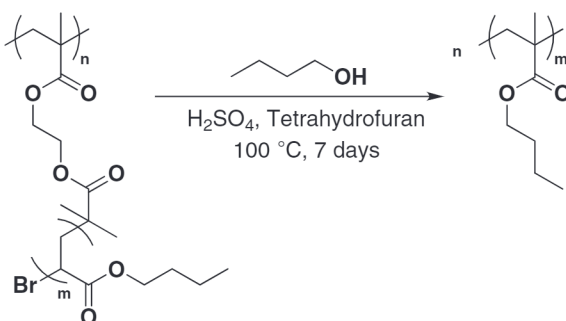
PS bottlebrushes with UV-cleavable side chains were prepared by grafting linear PS with terminal nitrobenzylloxycarbonyl and alkyne functionality onto a poly(3-azido-2-hydroxypropyl methacrylate) backbone by CuAAC.<sup>180</sup> The side chains were cleaved from the polymer backbone after ten minutes of UV light exposure, which led to a decrease in the intrinsic viscosity ( $[\eta]$ ), from a starting  $[\eta] = 12$  mL/g to a final  $[\eta] = 7.39$  mL/g.

ATRP of an alkoxyamine functional methacrylate and MMA at low temperature was used to prepare a polymer backbone with dormant alkoxyamine functionalities.<sup>181</sup> PS side chains were grafted onto the backbone via an alkoxyamine exchange reaction between the alkoxyamines on the backbone and a stoichiometric excess of alkoxyamine-capped PS (Figures 12a–12c). The side chains were removed from the backbone by heating them at 100 °C with an excess of small molecule alkoxyamine.

### Networks

Degradable polymer networks can be designed to contain degradable bonds placed at the junctions or in the middle of the mesh. The controlled radical copolymerization of vinyl monomers with a degradable crosslinker installs the degradable functional group only at the junctions of a network. Thus, degradation of the network yields mostly linear polymers because all branching points should contain the degradable bond. Multifunctional initiators containing degradable bonds could install degradable bonds at the center of a mesh if the initiator is bifunctional or at the junction if polymer stars are linked via irreversible coupling chemistry.

Redox degradable polymer networks were prepared by copolymerization of acrylic monomers with a bis(2-methacryloyloxyethyl) disulfide (DSDMA) crosslinker.<sup>91</sup> Similar to other redox degradable materials, reduction of the disulfide bonds led to dissolution of polymer gels into soluble linear polymers which can be characterized by gel permeation chromatography (Figures 13a–13c).<sup>182</sup> The degraded thiol-functionalized polymers can be



**Scheme 15** | Removal of side chains from a poly(2-bromoisobutyryl oxyethyl methacrylate-graft-*n*-butyl acrylate) bottlebrush by acid-catalyzed transesterification with butanol.

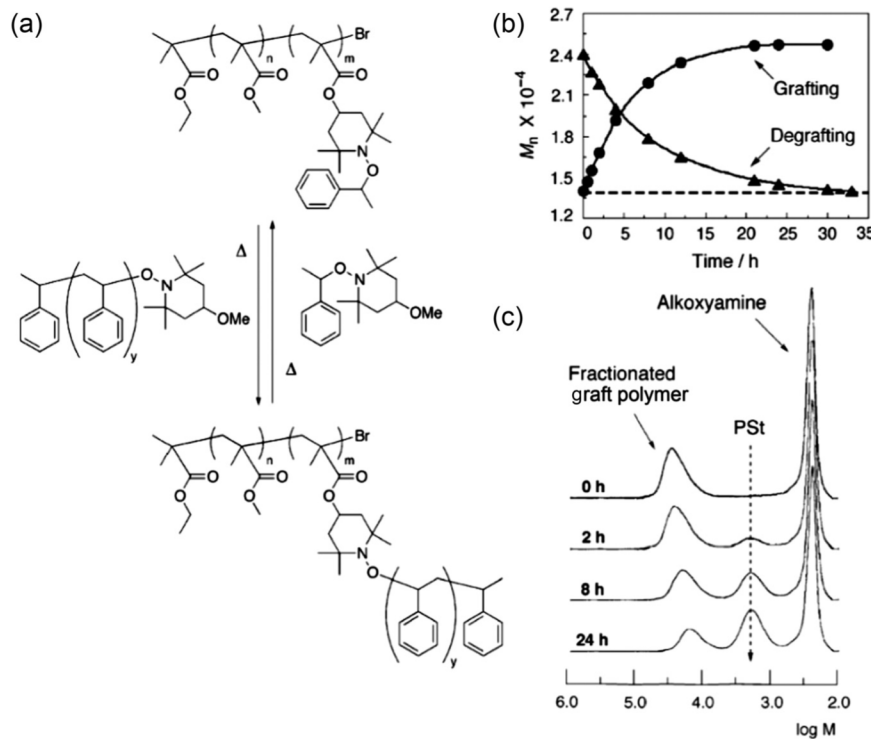


**Figure 12** | (a) Scheme of reversible synthesis of PMMA-g-PS bottlebrushes by the grafting-to alkoxyamine exchange method, and side chain removal at 100 °C. (b) Dependence of  $M_n$  on reaction time for (circle) polymer reaction of the backbone ( $M_n = 11,800$ ,  $D = 1.18$ , 92 mg) with the TEMPO-capped PS ( $M_n = 1700$ ,  $D = 1.15$ , 918 mg, 5.0 equiv/alkoxyamine units) in anisole (1 wt % polymer solution) at 100 °C. Triangles correspond to side chain removal of the fractionated bottlebrush ( $M_n = 24,000$ ,  $D = 1.16$ , 50.2 mg) with an excess of small molecule alkoxyamine (73 mg, 8.3 equiv/alkoxyamine units) in anisole (1 wt % polymer solution) at 100 °C. (c) GPC traces for the removal of PS side chains by heating in the presence of a stoichiometric excess of alkoxyamine. Reproduced with permission from ref 181. Copyright 2004 American Chemical Society.

cured into polymer networks by reformation of disulfide bonds.<sup>183</sup> Segregation of the disulfide crosslinkers in an immiscible phase enabled the synthesis of redox-degradable latex nanoparticles and high internal phase emulsion polymers.<sup>184-186</sup>

Degradable model networks were synthesized by ATRP and click chemistry using two distinct approaches. The first approach (Figure 14a) involved polymerization from a bifunctional ATRP initiator, followed by azide substitution of the halogen chain ends, to yield a bifunctional azide functionalized macromonomer with a photocleavable moiety at its center.<sup>188</sup> Copper-catalyzed azide-alkyne click chemistry (CuAAC) with a tetrafunctional alkyne provided model networks with pore sizes defined by the initial size of the macromonomer and four-arm star polymer crosslinker. Degradation of the model network under UV irradiation provided a mixture of star polymer and macromonomer. The second approach (Figure 14b) involves crosslinking of a tetrafunctional polymer star with photocleavable groups within

the core, followed by crosslinking via CuAAC.<sup>187,189</sup> Degradation of this network produced linear polymers with half the molecular weight of the star polymer (i.e., twice the size of the star arms).

Dynamic covalent exchange of functional groups enables self-healing under select conditions. The degenerative transfer mechanism of the RAFT process was used to introduce self-healing behavior in crosslinked polymer gels by reshuffling of TTGs at the junctions under UV irradiation. Multiple rounds of self-healing and degradation of polymer networks was accomplished by the photo-iniferter exchange mechanism (Figures 15a-15c).<sup>190-193</sup> This approach was recently applied to 3D printed networks. Application of a crosslinker during the self-healing reaction led to an increase in tensile strength after self-healing due to the increase in crosslinking density.<sup>194</sup>

Copolymerization of a TEMPO-methacrylate, styrene, and a butadiene crosslinker with pendant vinyl functionalities provided polymer networks with dynamic-covalent character through alkoxyamine exchange.<sup>195</sup>

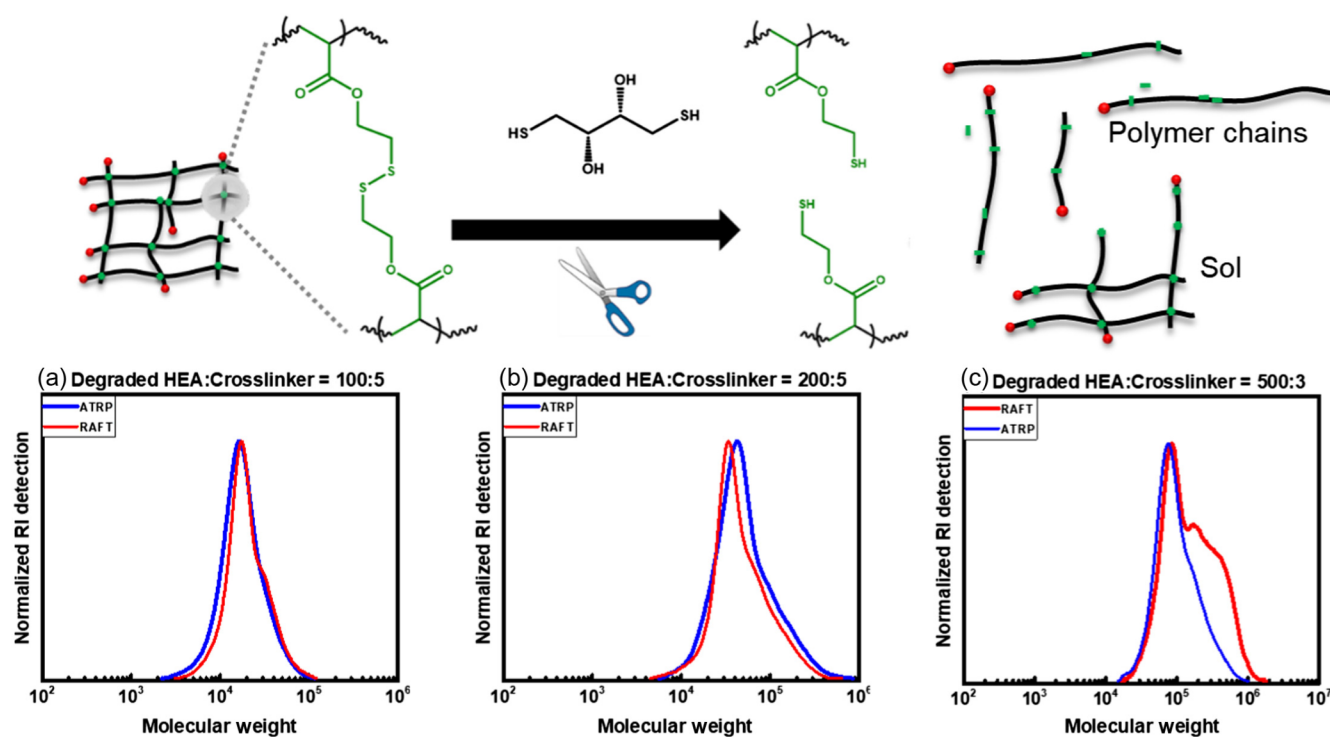


**Figure 13** | Poly(hydroxyethyl acrylate) polymer networks were prepared by RAFT and ATRP copolymerization with a bifunctional 2,2'-dithiodiethanol diacrylate (DSDA) crosslinker. The crosslinks were reduced by DDT to liberate and dissolve linear chains within the mesh. The dissolved polymers were comparable for RAFT and ATRP with (a) DP = 100 and (b) DP = 200 mesh, but RAFT networks had a higher dispersity at a (c) DP = 500. GPC of the sol showed comparable internal structure of polymer networks with primary chain lengths of DP = 100 and 200. However, the cleaved polymers from the ATRP network at a higher primary chain length of 500 had lower  $D$  than the RAFT counterpart. The difference between the primary chain lengths was observed as a higher swelling ratio and lower moduli in the DP = 500 mesh size ATRP networks. Reproduced with permission from ref 182. Copyright 2021 American Chemical Society.

The high activation energy of the alkoxyamine degradation provides negligible creep at 80 °C but fast exchange at high temperature when dissociation of the alkoxyamine bond becomes favorable. Alkoxyamine exchange enabled reprocessing of materials.<sup>196</sup> Model networks cured by RTA-ATRC of polymer stars with nitrosobenzene were degraded into soluble components resembling the original polymer star after decomposition of the alkoxyamines.<sup>197</sup>

Self-healing character was also introduced into methacrylic polymers via the Diels-Alder reaction. Furan functional groups in the backbone were used to crosslink networks by DA cycloaddition with a bis-maleimide crosslinker at ~50 °C.<sup>93,198</sup> The crosslinks could be reversibly cleaved via retro-DA of the DA adducts above 130 °C.

PMMA vitrimers were prepared by curing of P(MMA-co-AEMA) copolymers with tris(2-aminoethyl) amine via condensation at room temperature.<sup>199</sup> The vitrimers had a tensile moduli of 1800 MPa, and exhibited temperature-dependent stress relaxation at elevated temperature, with an activation energy ( $E_a$ ) of crosslink exchange of  $102 \pm 8$  kJ/mol. The vitrimers

retained comparable mechanical properties to the virgin material after five cycles of breaking, followed by reprocessing via compression molding. Segregation of the dynamic-covalent adduct into a separate immiscible block led to reduced macroscopic flow and suppressed creep behavior at longer time scales and larger deformations.<sup>200</sup>

## Biopolymer-Synthetic Polymer Hybrids

Polymers can be grafted from natural products, including cellulose derivatives and biological macromolecules. Wood-derived natural products are an important class of renewable materials which are not derived from fossil fuel feedstocks. These materials are commonly used as polymer backbones in the synthesis of composite materials by surface-initiated RAFT or ATRP, analogous to the grafting-from approach in the synthesis of molecular bottlebrushes or inorganic nanoparticles.

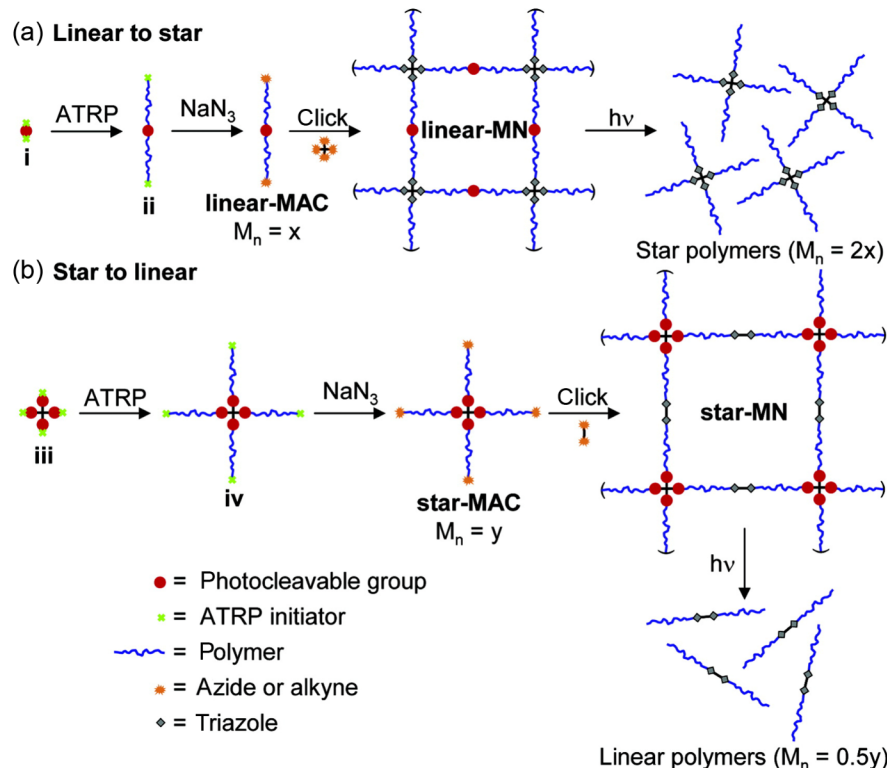
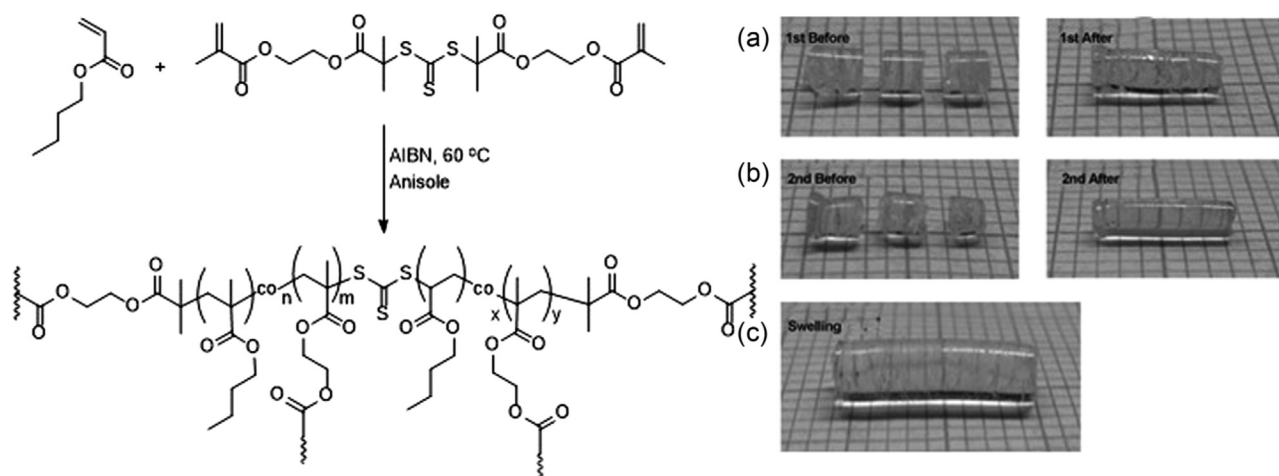
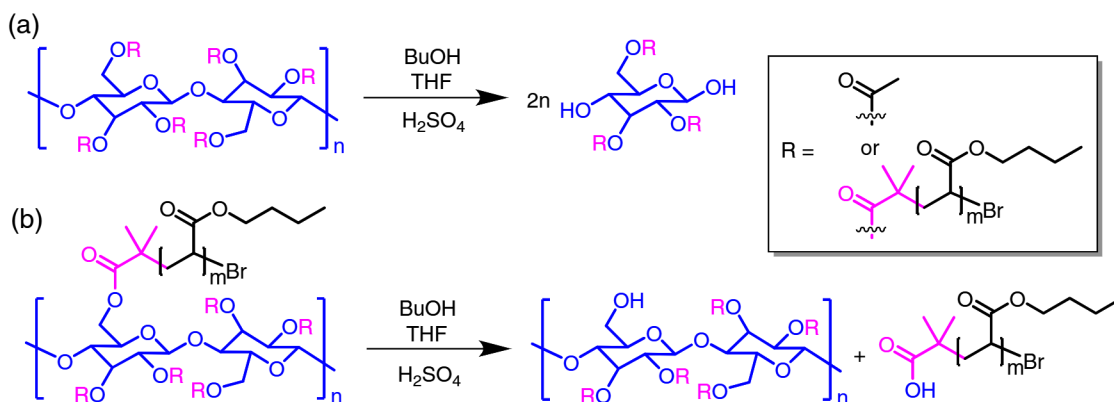


**Figure 14** | Design strategies used to prepare photodegradable model networks. Reproduced with permission from ref 187. Copyright 2007 American Chemical Society.



The synthesis of wood-polymer composites by RDRP was recently reviewed and will not be discussed in extensive detail in this article.<sup>201-204</sup> Grafting nondegradable polymers from wood-derived materials endowed the bio-based materials with properties unique to polymers from

petroleum-based feedstocks but with additional structural integrity and degradability. Hybrid composites were prepared by SI-ATRP from diverse substrates such as filter paper,<sup>205</sup> starch,<sup>206</sup> chitin,<sup>207</sup> and hyaluronic acid.<sup>208</sup>



**Scheme 16** | Degradation of poly(*n*-butyl acrylate) bottlebrushes grafted from a cellulose backbone were observed to degrade by hydrolysis along the backbone, or cleavage of the side chains from the backbone. High graft density cellulose bottlebrushes preferentially favored scission of the side chains from the backbone while low graft density bottlebrushes degraded more readily along the backbone. Reproduced with permission from ref 174. Copyright 2019 Wiley-VCH Verlag GmbH & Co. KGaA, Weinheim.

Molecular poly(*n*-butyl acrylate) bottlebrushes grafted from a cellulose backbone had degradation rates which depended on the graft density. Bottlebrushes with low grafting density degraded to lower molecular weight by scission of the  $\beta$ -1,4-glycosidic bonds along the backbone while bottlebrushes with high graft density primarily degraded by scission of the side chains due to steric protection of the backbone by the side chains (Schemes 16a and 16b).<sup>174</sup>

Biomolecule-polymer conjugates are typically employed to improve the stability, solubility, and half-lives of therapeutics for biomedical applications.<sup>209</sup> Many conjugates are prepared by PEGylation with chain-end functionalized PEG in a grafting-to approach. However, biomolecule-polymer conjugates prepared by RDRP provide greater control over the topology, functionality, and degradability of the grafted polymer chains.<sup>210-212</sup> The grafting-from RDRP approach can be used to prepare protein-polymer conjugates with the polymer side chains extending from a specific location on a protein backbone (Figures 16a-16f). RDRP was used to graft from biomacromolecules such as proteins, DNA and RNA, and exosomes.<sup>214-221</sup> Biomolecules could be functionalized with pH-responsive, thermoresponsive, or even multiblock or graft copolymer shells with degradable bonds installed at specific sites along the polymeric ligands.<sup>218,222,223</sup> The initiation efficiency of a grafting-from RDRP from biomacromolecule initiators was calculated by selective etching of the degradable backbones in solutions of strong acid or base (Figure 17).<sup>217,218,220,222,224-227</sup>

The addition of a degradable bond between the polymeric ligand and the biomacromolecule can provide targeted deshielding of the biomolecule upon cleavage of the ligands and enhanced stability or stealth behavior

when the ligand remains bound to the biopolymer. Polymeric ligands bound to proteins and siRNA by disulfide bonds were released by reduction to thiols, leaving both unattached linear polymer and intact biopolymers.<sup>216,219,228-231</sup> Multiconjugate polymers containing siRNA and folate targeting moieties were prepared for delivery of siRNA to cancer cells overexpressing folate receptors.<sup>232</sup> A portion of the poly[N-(2-hydroxypropyl)methacrylamide-*r*-(*N*-(3-aminopropyl)methacrylamide)] copolymer side chains were functionalized with folate reactive functional groups and thiol-functionalized si-RNA. The RNA side chains were cleaved from the backbone after reduction with glutathione.

Exosome polymer hybrids were prepared by grafting cholesterol functionalized DNA-polymer hybrids, or 5'- $\alpha$ -bromoisobutyrate DNA macroinitiators, onto the surface of the membrane (Figures 18a and 18b).<sup>221</sup> The DNA-polymer conjugates significantly improved the stability of the exosome cargo at ambient temperatures and improved the resilience of the particles against proteolytic enzymes. Inclusion of a nitrophenyl group between the cholesterol and DNA segments enabled selective cleavage of the DNA-polymer conjugates from the surface of the exosome membrane without compromising the exosome or conjugate structure.

An arm-first approach was used to prepare OEOMA star polymers with terminal azido-functionalities. The star polymers were complexed with alkyne-functionalized DNA by CuAAC. The star polymers were annealed in the presence of complementary strands, which led to reversible complexation between complementary biopolymers-polymer conjugates into higher-order structures up to 75 nm in size.<sup>233</sup>

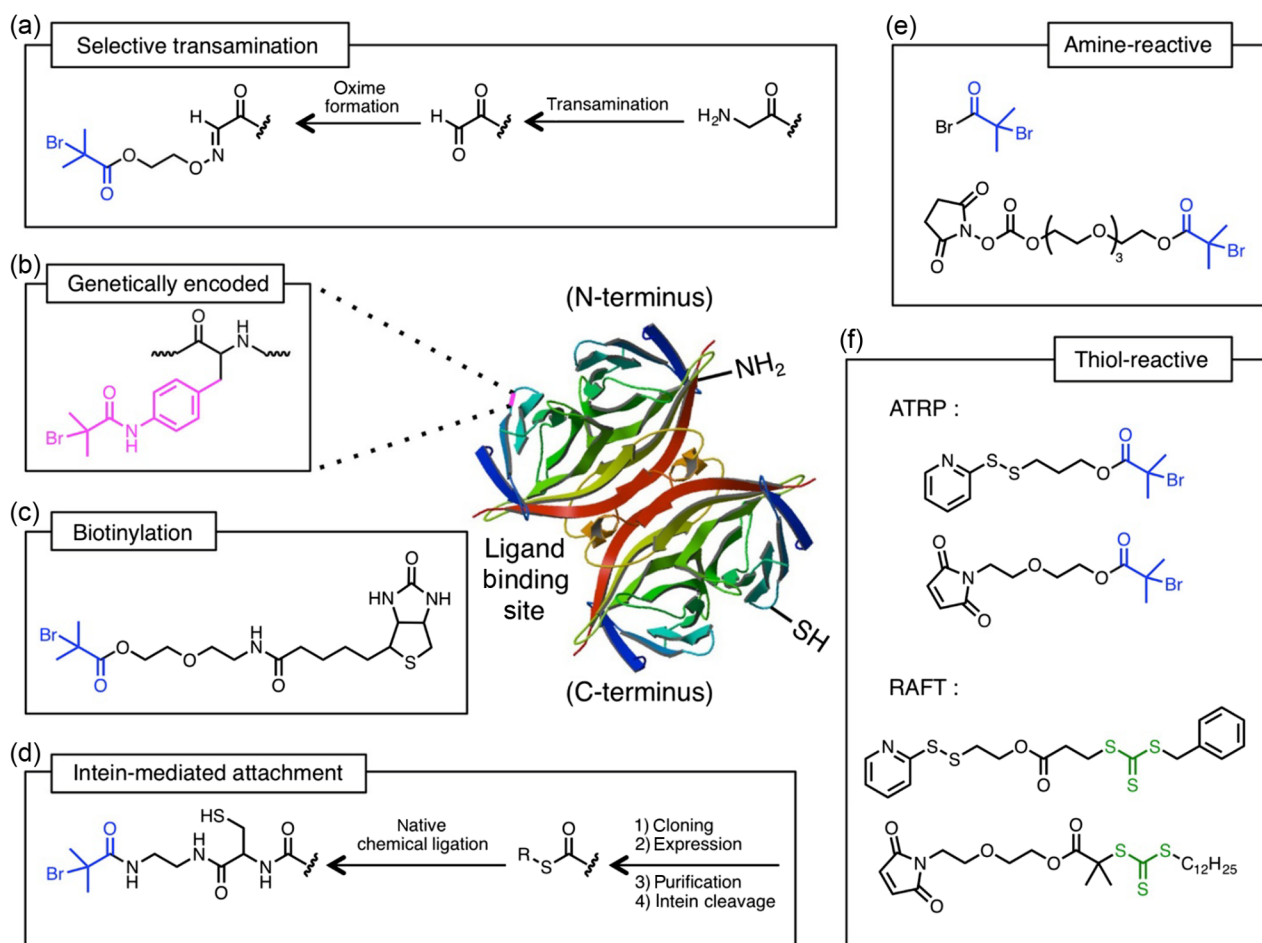


**Figure 16** | Schematic representation of possible methods used to functionalize a streptavidin protein with initiators or CTA for subsequent grafting-from synthesis of protein-polymer hybrids. Initiators could be installed (a) at the N-terminus by transamination of the primary amine at the N-terminus to an oxoamide, followed by oxime formation with the initiator; (b) at any location along the backbone by genetically incorporating a 4-(2'-bromoisobutyramido) phenylalanine ATRP initiator onto a peptide backbone; (c) at sites along a Streptavidin backbone with strong binding affinity to biotin functional groups; (d) intein-mediated protein ligation of the C-terminus into a thioester which could be ligated with an amino-functionalized ATRP initiator; (e) at all amines along a backbone by amination with an activated ester or acyl halide functionalized initiator; and (f) at cysteine functional groups by thiole click chemistry with maleimide functional initiators, or oxidative coupling of deprotected thiol-functional initiators. Reproduced with permission from ref 213. Copyright 2014 American Chemical Society.

## Inorganic Hybrid Materials

Inorganic nanoparticles are often prepared by the grafting-from or grafting-to approach by RDRP (Scheme 17).<sup>8,19,22,24,26,27</sup> In the grafting-from approach, initiators are functionalized on the surface of a nanoparticle using complementary chemistry. The initiators are then used to grow small-molecule monomer from the surface to yield a densely grafted nanoparticle or surface. The grafting-to approach involves grafting premade polymer chains onto a substrate through complementary chemistry. However, this approach typically yields sparsely grafted nanoparticles due to blocking of neighboring

functional groups. Cleavage of arms from the surface can be accomplished by dissolution of the nanoparticle or by selective removal through cleavage of a functional group. Indeed, the polymer fraction was selectively etched from inorganic  $\text{SiO}_2$  particle brushes by dissolving the inorganic fraction in hydrofluoric acid to assess the structure of polymers grafted from the particle.<sup>234-236</sup>

The grafting-to approach can install degradable functional groups anywhere along a polymeric ligand arm. Degradation of polymeric ligand arms altered the dispersibility of the nanoparticles within a matrix, resulting in a change in macroscopic properties. Cleavage of Diels-Alder adducts installed in the center of PS-*b*-PEG

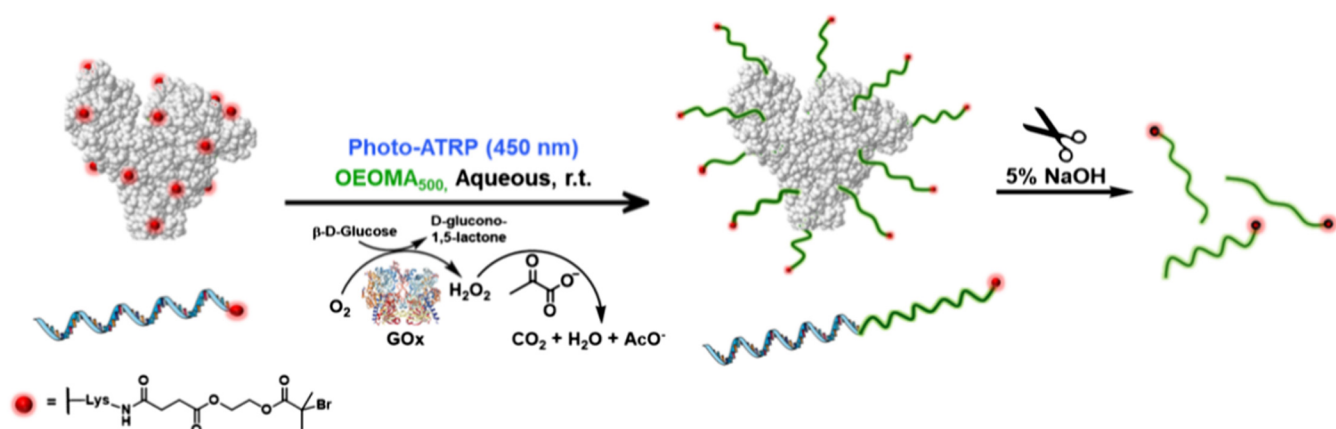


**Figure 17** | Grafting-from ATRP of OEOMA from initiator-modified Bovine serum albumin protein (BSA) and DNA macroinitiators by photo-ATRP under 450 nm irradiation. The biomacromolecule-polymer conjugates were degraded in 5% NaOH. Reproduced with permission from ref 217. Copyright 2018 American Chemical Society.

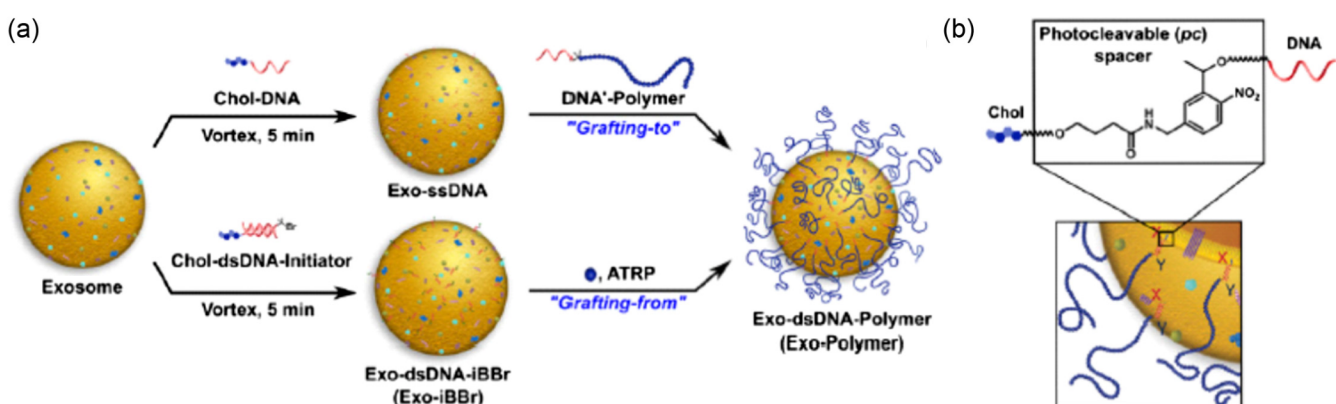


**Figure 18** | (a) Exosome-polymer hybrids were prepared by the grafting-to and grafting-from approach. The grafting-to approach involved grafting DNA-cholesterol hybrids onto the exosome, followed by grafting DNA-P (OEOMA) hybrids onto the DNA segments on the surface of the exosome. The grafting-from approach was achieved by grafting a cholesterol-DNA macroinitiator with a 5'- $\alpha$ -bromoisobutyrate group onto the surface of the exosome, then grafting polymers from the surface by photoinduced ATRP. (b) Incorporation of a degradable nitrophenyl group between the cholesterol and DNA segments enable selective release of DNA or DNA-polymer functionalities from the surface by cleavage under UV light.<sup>221</sup> Copyright 2021 National Academy of Sciences.

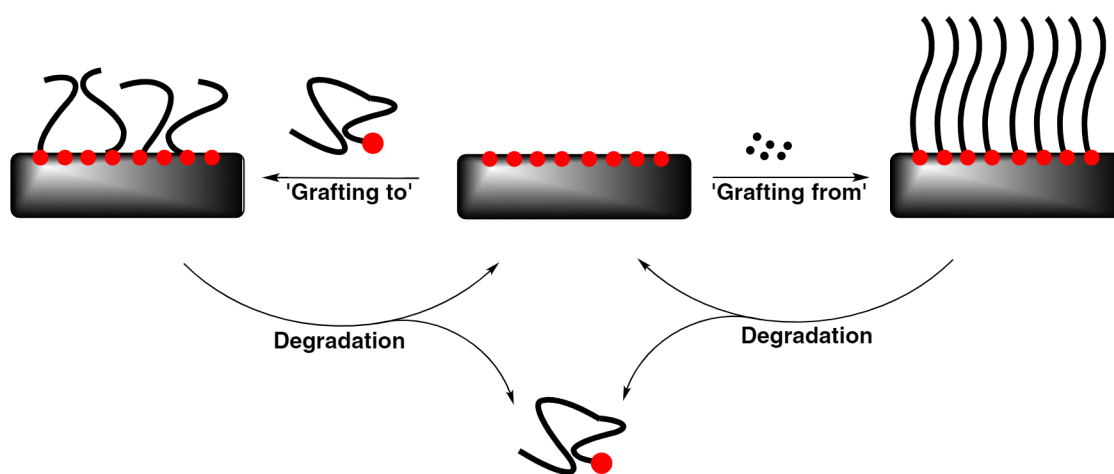
block copolymer ligands led to aggregation of gold nanoparticles within a PMMA-*b*-PS block polymer matrix.<sup>237</sup> A combination of grafting-from ATRP and grafting-to alkoxyamine exchange was utilized to prepare dispersible comb-on-nanoparticle brushes with cleavable functional arms.<sup>238</sup> A PMMA polymer brush with statistical incorporation of dormant alkoxyamine side chains was grown from a 100 nm SiO<sub>2</sub> nanoparticle via a surface ATRP with an alkoxyamine inimer at low temperature. Alkoxyamine-terminated poly(4-vinyl pyridine) was grafted onto the particle and improved stability of the nanoparticles in water and methanol. The comb topology was reverted back to a linear brush topology by alkoxyamine exchange with other nitroxides. An

analogous method was applied to reversibly tune the surface chemistry of a surface-grafted brush grown from a silicon wafer.<sup>239</sup>

Silicon oxide surfaces were modified with anthracene functional groups on the surface.<sup>240</sup> Oligomeric PS or PBA were grafted onto the surface of the substrate via anthracene dimerization under visible light. The surface-grafted brushes could be selectively etched by exposure to low-intensity UV light in order to pattern the surface.

## Depolymerization to Monomer

Recent work has mediated the depolymerization of vinyl polymers back to monomers via a self-immolative



**Scheme 17** | Synthesis of inorganic hybrid materials with cleavable arms via the grafting-from or grafting-to approaches.

approach.<sup>241,242</sup> In this approach, polymer macroinitiators were prepared by RDRP with retained chain-end functionality at low temperature. Activation of the polymer chain-end at elevated temperature yields the chain-end radical which can either propagate, depropagate, terminate, or be deactivated by the respective RDRP mechanism. The thermodynamics of the reaction dictate the RDRP's tendency towards propagation or depropagation. Polymerizations of vinyl monomers are exothermic ( $\Delta H_p < 0$ ), exoentropic ( $\Delta S_p < 0$ ), and favorable at low temperatures typical for radical polymerization.<sup>243</sup> The contribution of depropagation is generally negligible at lower temperature, unless polymerizations are conducted

under dilute conditions or at high temperature, when the initial monomer concentration ( $[M]_0$ ) is close to the equilibrium monomer concentration ( $[M]_{eq}$ ) (Figure 19). Reported depolymerizations of vinyl polymers by an RDRP mechanism relied on elevated temperature to increase the contribution of the entropic component ( $-T\Delta S_p$ ), leading to a higher free energy of polymerization ( $\Delta G_p$ ) and tendency towards depropagation.

The polymerization of 1,1-disubstituted vinyl monomers is generally less exothermic than mono-substituted acrylic and styrenic monomers. Methacrylates have an enthalpy of polymerization low enough ( $\Delta H_p < 60$  kJ/mol) for depropagation to become significant at temperatures

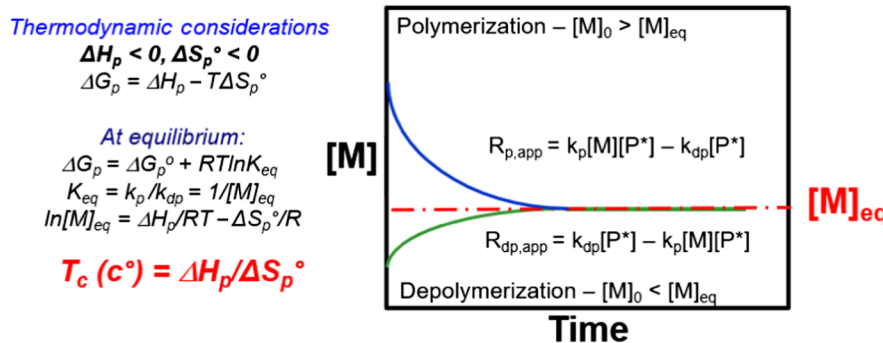


**Figure 19** | Thermodynamic considerations for ideal living polymerizations with an initial monomer concentration close to the equilibrium monomer concentration, and for depolymerization reactions in absence of monomer in an ideal living process. Polymerizations proceed at an apparent rate equal to the difference between the rate of propagation and rate of depropagation until the rate of propagation equals the rate of depropagation at the  $[M]_{eq}$ . The depolymerization of polymers proceeds at an apparent rate equal to the difference between the rate of depropagation and rate of propagation until equilibrium is established at the same  $[M]_{eq}$ . A polymerization and depolymerization by RDRP will be affected by loss of chain-end functionalities, which may lead to a dead-end scenario where radical concentration approaches zero and stops the reaction before it could reach equilibrium.

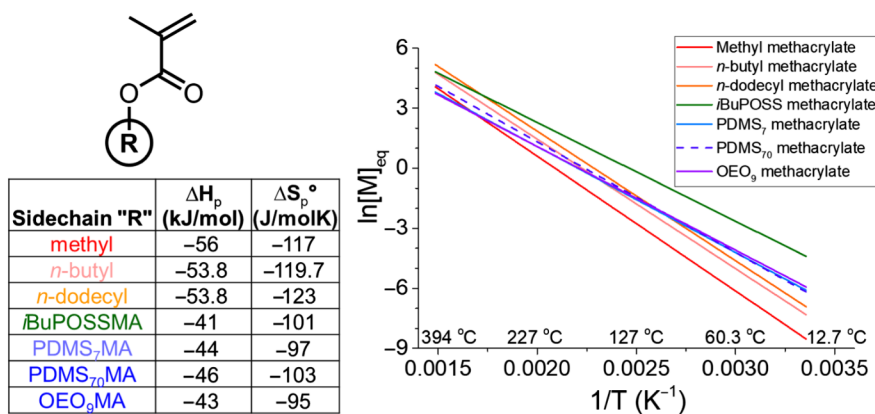


**Figure 20** | The equilibrium monomer concentration of MMA, *n*-butyl methacrylate, *n*-dodecyl methacrylate, POSSMA, PDMSMA, and OEOMA calculated between 25–300 °C using the scaling relationship  $\ln[M]_{eq} = \Delta H/RT - \Delta S^\circ/R$ . The thermodynamic parameters were gathered from references.<sup>167,168,244,245</sup>

above 120 °C. Methacrylic monomers with bulkier side chains typically have less favorable thermodynamics which lead to higher equilibrium monomer concentrations than smaller monomers (Figure 20). Additionally, the larger side chain of bulkier methacrylic monomers lowers the repeat unit concentration such that the bulk monomer concentration is not significantly higher than the  $[M]_{eq}$ . These effects increase the impact of depropagation during both the polymerization and depolymerization of bulky methacrylic macromonomers. In fact, the first reports of polymethacrylate depolymerizations mediated by RDRP were part of kinetic studies investigating the thermodynamic contribution of depropagation during the grafting-through RDRP of macromonomers.

Depolymerization of poly[polyhedral oligomeric silsesquioxane methacrylate] (P(POSSMA)) was observed after an ATRP reached thermodynamic equilibrium at ~80% conversion at 60 °C was transferred to an oil bath at 90 °C.<sup>167</sup> Depolymerization occurred until equilibrium was reestablished at ~60% monomer conversion, in agreement with what would be observed in a depolymerization caused by an increase in  $[M]_{eq}$  with temperature in a living polymerization.

Poly(dimethylsiloxane) methacrylate (P(PDMSMA)) and poly(oligoethylene oxide) methacrylate (P(OEOMA)) bottlebrushes were depolymerized from an initial repeat unit concentration ( $[P]_0$ ) of 100 mM to the  $[M]_{eq} \sim 30$  mM by a RAFT-mediated process induced by decomposition of the CTA.<sup>168</sup> The polymerizations conducted at a  $[M]_0 = 100$  mM stopped at a comparable  $[M]_{eq}$  as the depolymerizations, which confirmed the reactions plateaued at the same equilibrium in both the forward and reverse directions.

A similar approach was optimized for the depolymerization of polymethacrylates by thermal decomposition

of the terminal dithiobenzoate CTA.<sup>246</sup> Depolymerizations of macroinitiators at a  $[P]_0 = 5$  mM (c.a. 0.05 wt % solid content) at 120 °C reached up to 92% conversion of polymer to monomer over 8 h. The reactions were conducted at a  $[P]_0$  far below the  $[M]_{eq}$  of typical methacrylates at 120 °C, which highlights the use of dilution as a way to overcome thermodynamic constraints necessary to achieve high depolymerization yields at lower temperature. The high yield also suggests thermolysis of dithiobenzoates was not significant using this experimental set-up.<sup>247,248</sup>

Depolymerization of poly(methyl methacrylate) mediated by ATRP with a ruthenium (II) chloride catalyst reached a modest monomer recovery of 8% after 7 h of stirring at 120 °C, at a  $[P]_0 \sim 500$  mM.<sup>249</sup> The yield of this depolymerization agrees with the reaction stopping close to the  $[M]_{eq} \sim 50$  mM for PMMA at this temperature. Up to 13.8% monomer recovery occurred after four rounds of reiterative depolymerizations at 100 °C for 10 h.

Degradation of halogen CEF was observed in depolymerizations of poly(*n*-butyl methacrylate) by ATRP with a copper(II) chloride/tris(2-pyridylmethyl) amine catalyst at 170 °C.<sup>250</sup> The depolymerizations reached up to 67% monomer recovery at a  $[P]_0 = 750$  mM (8 wt %) within 10 min. However, the reactions stopped below the theoretical  $[M]_{eq}$ . The plateau in conversion was attributed to loss of chlorine CEF by termination and lactonization, which accumulated kinetically trapped chains which were unavailable for depolymerization. Indeed, the importance of CEF preservation in depolymerizations by ATRP was also emphasized in polymerization/depolymerization cycling experiments with P(PDMS<sub>11</sub>MA) (Figures 21a and 21b).<sup>169</sup> The first round of the cycle depolymerized 81% of the bottlebrush in 15 min. Subsequent cycles of repolymerization and depolymerization

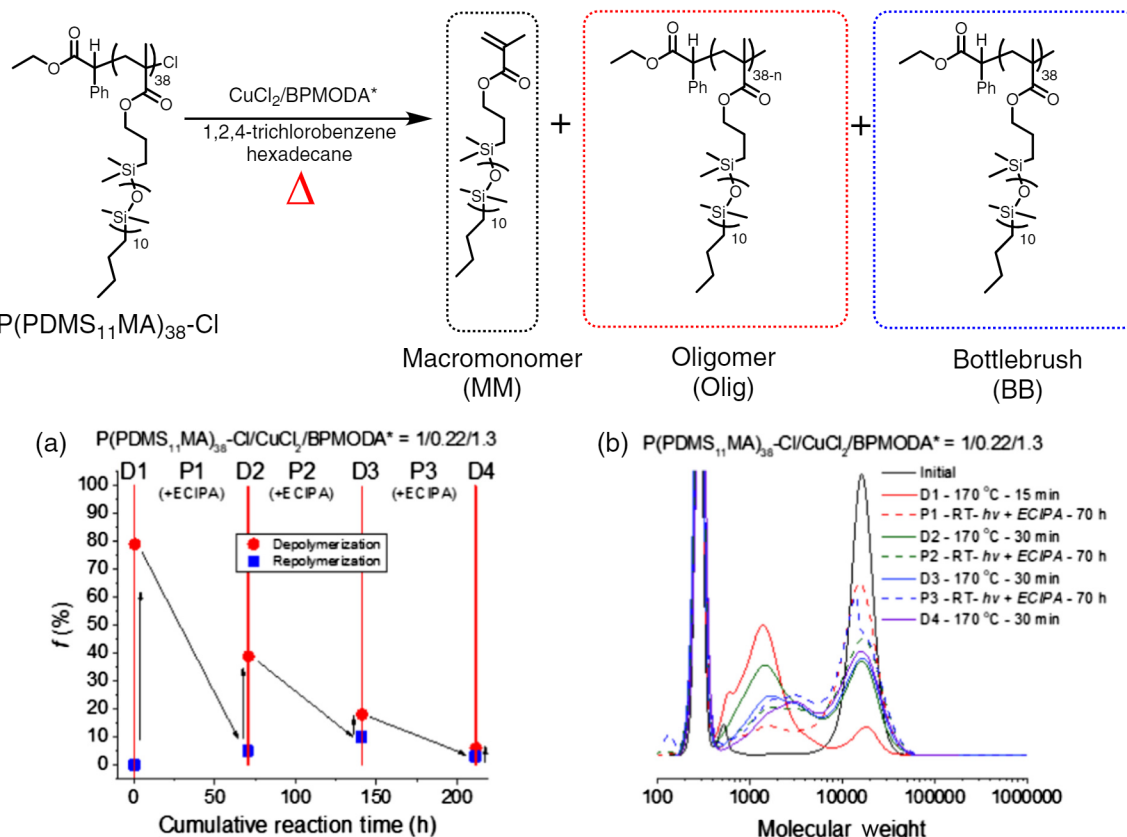


**Figure 21** | Depolymerization/repolymerization cycling of  $\text{PDMS}_{11}\text{MA}$  by ATRP, starting from a depolymerization of  $\text{P}(\text{PDMS}_{11}\text{MA})\text{-Cl}$  macroinitiator. (a) Kinetic plot of the mol fraction of macromonomer measured after each cycle. The red lines are markers for the beginning and end of a cycle. The black arrows are guides for the eye. (b) Crude GPC traces of depolymerization/repolymerization cycling experiments at each timepoint were taken relative to linear PMMA standards in THF. The traces are normalized to the hexadecane peak and cut off at the initial height of the macroinitiator. First depolymerization (D1) conditions:  $[\text{P}(\text{PDMS}_{11}\text{MA})\text{-Cl}]_0/[\text{CuCl}_2]_0/[\text{BPMODA}^*]_0 = 1/0.22/1.3$  at a  $[\text{P}]_0 = 275 \text{ mM}$ , Solvent = 1,2,4-trichlorobenzene and 11.7 vol % hexadecane  $T = 170 \text{ }^\circ\text{C}$ . Repolymerization reactions were conducted under UV light with 0.36 equiv ECIPA initiator (relative to the initial alkyl halide concentration) as an additive without prior purification. All other rounds of depolymerization were accomplished by moving the flask to the oil bath preheated to  $170 \text{ }^\circ\text{C}$  without prior purification. Reproduced with permission from ref 169. Copyright 2021 American Chemical Society.

isolated approximately half the amount of monomer as the preceding cycle, leading to an accumulation of kinetically inactive chains lacking halogen CEF. The chains lacking the relevant RDRP CEF cannot be activated in a depolymerization or polymerization, emphasizing the importance of CEF retention both during macroinitiator synthesis and in the depolymerization reaction.

## Conclusion and Perspectives

This review summarized recent progress in synthetic strategies towards the topological transformation of vinyl polymers to polymers of lower molecular weight, or different topology, organized by topology of the polymer

precursor and route of degradation. RDRP provides unparalleled control over polymer topology, composition, and functionalities. The ability to tether initiators to functionalized substrates, comprising biomolecules, inorganic surfaces, and to other polymers such as grafts and side chains, enabled the preparation of materials with complex topologies with embedded functional groups at the junctions. The use of (multi)functional macroinitiators with initiators tethered by dynamic covalent bonds enabled the synthesis of polymers with cleavable, and/or reversible, topologies. This included polymers which can shift from high to low molecular weight, branched polymers that could disconnect and reconnect side chains, and surfaces that can be reversibly etched or functionalized.

Future work should investigate the properties of polymeric materials before and after degradation to evaluate whether the technology could be feasibly adapted to a circular polymer economy for applications outside of academic laboratories. For example, the transformation of high molecular weight polymers to lower molecular weight oligomers, or the selective cleavage of polymer arms from a high molecular weight graft polymer to low molecular weight arms/branches, may reduce the viscosity of polymer and can have beneficial properties for processing (and reprocessing). Self-healing materials, and materials with dynamic-covalent bonds, may have applications as recyclable thermosets.

Polymer depolymerizations by RDRP highlight two general strategies to reach appreciable monomer recovery. The first method involves depolymerization at high dilution and low enough temperature to ensure that CEF remains intact. Dilution is required because the  $[M]_{eq}$  of the reaction is low and the contribution of propagation needs to be mitigated for the reaction to reach completion. High monomer recovery can be achieved. However, separation of monomer from solvent and scalability may be challenging. The other strategy operates at higher concentration and higher temperature to raise  $[M]_{eq}$ . The high temperature comes at a cost to livingness. CEF commonly used to regulate RDRP are prone to thermal degradation to inactive species which kinetically traps chain ends and diminishes depolymerization yields. Polymethacrylates with chlorine and bromine CEF were reported to degrade via lactonization above 150 °C.<sup>250,251</sup> Dithiocarbonates and TTCS were also reported to decompose between 120–180 °C.<sup>247,248,252</sup> NMPs of methacrylic polymers remain challenging to control. However, the rate of bond dissociation for an alkoxyamine increases with temperature.<sup>253</sup> Thus, future work in this area should account for both the thermodynamic and kinetic favorability of RDRP reactions at elevated temperatures and high dilution. The use of midchain triggers, such as  $\alpha$ -halo-acrylate or *N*-(acyloxy)phthalimide comonomers, may enable depolymerization through a combination of midchain scission and radical unzipping.<sup>88,254</sup>

The majority of plastics, including high-performance materials, are not recycled.<sup>3</sup> This warrants a continued focus on incorporation of degradable bonds which are durable enough to last for the duration of a material's usable lifetime but may be dissolved into low-toxicity oligomers if the materials are disposed of in a landfill or leech into the environment. These materials may be prepared by copolymerization of vinyl monomers and a cyclic monomer by RROP or through the use of degradable bonds installed at specific junctions on a polymeric backbone/side chain which can degrade under the appropriate conditions. Future work in RROP should aim to simplify

synthetic preparation of (macro)cyclic monomers, and to improve reactivity ratios between vinyl monomers and cyclic monomers. There should also be more emphasis on the characterization of degradation under ambient (i.e., nonaccelerated) conditions to evaluate whether the degradable bonds installed on polymeric materials are faster than state-of-the-art biopolymers and polyesters. The toxicity of degraded products should also be a priority in future work, particularly for materials with potential biomedical applications.

## Conflict of Interest

There is no conflict of interest to report.

## Acknowledgments

Financial support from NSF DMR 1921858 and NSF DMR 2202747 is acknowledged. MM acknowledges support from the Harrison Fellowship (CMU Department of Chemistry).

## References

1. Plastics Europe. Plastics—the Facts 2019: An Analysis of European Plastics Production, Demand and Waste Data. <https://plasticeurope.org/knowledge-hub/plastics-the-facts-2019/> (accessed March 2022).
2. Grand View Research. (2021). Market size of plastics worldwide from 2016 to 2028 (in billion U.S. dollars). Statista Inc. (accessed March 1, 2022).
3. Geyer, R.; Jambeck, J. R.; Law, K. L. Production, Use, and Fate of All Plastics Ever Made. *Sci. Adv.* **2017**, 3, e1700782.
4. Dworakowska, S.; Lorandi, F.; Gorczyński, A.; Matyjaszewski, K. Toward Green Atom Transfer Radical Polymerization: Current Status and Future Challenges. *Adv. Sci.* **2022**, 2106076.
5. Fortman, D. J.; Brutman, J. P.; De Hoe, G. X.; Snyder, R. L.; Dichtel, W. R.; Hillmyer, M. A. Approaches to Sustainable and Continually Recyclable Cross-Linked Polymers. *ACS Sustain. Chem. Eng.* **2018**, 6, 11145–11159.
6. Schneiderman, D. K.; Hillmyer, M. A. 50th Anniversary Perspective: There Is a Great Future in Sustainable Polymers. *Macromolecules* **2017**, 50, 3733–3749.
7. Shieh, P.; Hill, M. R.; Zhang, W.; Kristufek, S. L.; Johnson, J. A. Clip Chemistry: Diverse (Bio)(macro)molecular and Material Function through Breaking Covalent Bonds. *Chem. Rev.* **2021**, 121, 7059–7121.
8. Braunecker, W. A.; Matyjaszewski, K. Controlled/Living Radical Polymerization: Features, Developments, and Perspectives. *Prog. Polym. Sci.* **2007**, 32, 93–146.
9. Corrigan, N.; Jung, K.; Moad, G.; Hawker, C. J.; Matyjaszewski, K.; Boyer, C. Reversible-Deactivation Radical Polymerization (Controlled/Living Radical Polymerization): From Discovery to Materials Design and Applications. *Prog. Polym. Sci.* **2020**, 111, 101311.

10. Matyjaszewski, K.; Müller, A. H. *Controlled and Living Polymerizations: From Mechanisms to Applications*; John Wiley & Sons: Hoboken, NJ, **2009**.

11. Szwarc, M.; Van Beylen, M. *Ionic Polymerization and Living Polymers*; Springer: Dordrecht, The Netherlands, **1993**.

12. Hadjichristidis, N.; Pitsikalis, M.; Pispas, S.; Iatrou, H. Polymers with Complex Architecture by Living Anionic Polymerization. *Chem. Rev.* **2001**, *101*, 3747–3792.

13. Matyjaszewski, K.; Gnanou, Y.; Leibler, L. *Macromolecular Engineering: Precise Synthesis, Materials Properties, Applications*; Wiley-VCH: Weinheim, Germany, **2011**.

14. Matyjaszewski, K.; Xia, J. Atom Transfer Radical Polymerization. *Chem. Rev.* **2001**, *101*, 2921–2990.

15. Wang, J.-S.; Matyjaszewski, K. Controlled/“Living” Radical Polymerization. Atom Transfer Radical Polymerization in the Presence of Transition-Metal Complexes. *J. Am. Chem. Soc.* **1995**, *117*, 5614–5615.

16. Moad, G.; Rizzardo, E.; Thang, S. H. Living Radical Polymerization by the RAFT Process. *Aust. J. Chem.* **2005**, *58*, 379–410.

17. Nicolas, J.; Guillaneuf, Y.; Lefay, C.; Bertin, D.; Gigmes, D.; Charleux, B. Nitroxide-Mediated Polymerization. *Prog. Polym. Sci.* **2013**, *38*, 63–235.

18. Hawker, C. J.; Bosman, A. W.; Harth, E. New Polymer Synthesis by Nitroxide Mediated Living Radical Polymerizations. *Chem. Rev.* **2001**, *101*, 3661–3688.

19. Matyjaszewski, K. Atom Transfer Radical Polymerization (ATRP): Current Status and Future Perspectives. *Macromolecules* **2012**, *45*, 4015–4039.

20. Oh, J. K.; Drumright, R.; Siegwart, D. J.; Matyjaszewski, K. The Development of Microgels/Nanogels for Drug Delivery Applications. *Prog. Polym. Sci.* **2008**, *33*, 448–477.

21. Sheiko, S. S.; Sumerlin, B. S.; Matyjaszewski, K. Cylindrical Molecular Brushes: Synthesis, Characterization, and Properties. *Prog. Polym. Sci.* **2008**, *33*, 759–785.

22. Matyjaszewski, K.; Tsarevsky, N. V. Macromolecular Engineering by Atom Transfer Radical Polymerization. *J. Am. Chem. Soc.* **2014**, *136*, 6513–6533.

23. Chong, Y.; Le, T. P.; Moad, G.; Rizzardo, E.; Thang, S. H. A More Versatile Route to Block Copolymers and Other Polymers of Complex Architecture by Living Radical Polymerization: The RAFT Process. *Macromolecules* **1999**, *32*, 2071–2074.

24. Brinks, M. K.; Studer, A. Polymer Brushes by Nitroxide-Mediated Polymerization. *Macromol. Rapid Commun.* **2009**, *30*, 1043–1057.

25. Floyd, T. G.; Häkkinen, S.; Hartlieb, M.; Kerr, A.; Perrier, S. Complex Polymeric Architectures Synthesized through RAFT Polymerization. In *RAFT Polymerization: Methods, Synthesis and Applications*; Moad, G., Rizzardo, E., Eds.; Wiley-VCH: Weinheim, Germany, **2022**; Vol. 2; pp 933–981.

26. Pyun, J.; Kowalewski, T.; Matyjaszewski, K. Synthesis of Polymer Brushes Using Atom Transfer Radical Polymerization. *Macromol. Rapid Commun.* **2003**, *24*, 1043–1059.

27. Yan, J.; Bockstaller, M. R.; Matyjaszewski, K. Brush-Modified Materials: Control of Molecular Architecture, Assembly Behavior, Properties and Applications. *Prog. Polym. Sci.* **2020**, *100*, 101180.

28. Scholten, P. B. V.; Moatsou, D.; Detrembleur, C.; Meier, M. A. R. Progress toward Sustainable Reversible Deactivation Radical Polymerization. *Macromol. Rapid Commun.* **2020**, *41*, 2000266.

29. Parkatzidis, K.; Wang, H. S.; Truong, N. P.; Anastasaki, A. Recent Developments and Future Challenges in Controlled Radical Polymerization: A 2020 Update. *Chem.* **2020**, *6*, 1575–1588.

30. Moad, G. Reversible Addition-Fragmentation Chain Transfer (Co)polymerization of Conjugated Diene Monomers: Butadiene, Isoprene, and Chloroprene. *Polym. Int.* **2017**, *66*, 26–41.

31. Lauterbach, F.; Rubens, M.; Abetz, V.; Junkers, T. Ultra-fast PhotoRAFT Block Copolymerization of Isoprene and Styrene Facilitated through Continuous-Flow Operation. *Angew. Chem. Int. Ed.* **2018**, *57*, 14260–14264.

32. Benoit, D.; Harth, E.; Fox, P.; Waymouth, R. M.; Hawker, C. J. Accurate Structural Control and Block Formation in the Living Polymerization of 1,3-Dienes by Nitroxide-Mediated Procedures. *Macromolecules* **2000**, *33*, 363–370.

33. De Bon, F.; Ribeiro, D. C.; Abreu, C. M.; Rebelo, R. A.; Isse, A. A.; Serra, A. C.; Gennaro, A.; Matyjaszewski, K.; Coelho, J. F. Under Pressure: Electrochemically-Mediated Atom Transfer Radical Polymerization of Vinyl Chloride. *Polym. Chem.* **2020**, *11*, 6745–6762.

34. Mendes, J. P.; Branco, F.; Abreu, C. M.; Mendonça, P. V.; Serra, A. n. C.; Popov, A. V.; Guliashvili, T.; Coelho, J. F. Sulfolane: An Efficient and Universal Solvent for Copper-Mediated Atom Transfer Radical (Co)polymerization of Acrylates, Methacrylates, Styrene, and Vinyl Chloride. *ACS Macro Lett.* **2014**, *3*, 858–861.

35. Abreu, C. M. R.; Mendonça, P. V.; Serra, A. C.; Coelho, J. F. J.; Popov, A. V.; Gryn'ova, G.; Coote, M. L.; Guliashvili, T. Reversible Addition-Fragmentation Chain Transfer Polymerization of Vinyl Chloride. *Macromolecules* **2012**, *45*, 2200–2208.

36. Sun, Z.; Mi, X.; Yu, Y.; Shi, W.; Feng, A.; Moad, G.; Thang, S. H. “All-PVC” Flexible Poly(Vinyl Chloride): Nonmigratory Star-Poly(Vinyl Chloride) as Plasticizers for PVC by RAFT Polymerization. *Macromolecules* **2021**, *54*, 5022–5032.

37. Szczepaniak, G.; Fu, L.; Jafari, H.; Kapil, K.; Matyjaszewski, K. Making ATRP More Practical: Oxygen Tolerance. *Acc. Chem. Res.* **2021**, *54*, 1779–1790.

38. Chen, M.; Zhong, M.; Johnson, J. A. Light-Controlled Radical Polymerization: Mechanisms, Methods, and Applications. *Chem. Rev.* **2016**, *116*, 10167–10211.

39. Lee, Y.; Boyer, C.; Kwon, M. S. Visible-Light-Driven Polymerization towards the Green Synthesis of Plastics. *Nat. Rev. Mater.* **2022**, *7*, 74–75.

40. Ribelli, T. G.; Fantin, M.; Daran, J.-C.; Augustine, K. F.; Poli, R.; Matyjaszewski, K. Synthesis and Characterization of the Most Active Copper ATRP Catalyst Based on Tris[(4-dimethylaminopyridyl)methyl]amine. *J. Am. Chem. Soc.* **2018**, *140*, 1525–1534.

41. Moad, G. An Industrial History of RAFT Polymerization. In *RAFT Polymerization: Methods, Synthesis and Applications*; Moad, G., Rizzardo, E., Eds.; Wiley-VCH: Weinheim, Germany, **2022**; Vol. 2; pp 1077–1169.

42. Destarac, M. Controlled Radical Polymerization: Industrial Stakes, Obstacles and Achievements. *Macromol. React. Eng.* **2010**, *4*, 165–179.

43. Destarac, M. Industrial Development of Reversible-Deactivation Radical Polymerization: Is the Induction Period Over? *Polym. Chem.* **2018**, *9*, 4947–4967.

44. Serrano, D. P.; Aguado, J.; Escola, J. M. Developing Advanced Catalysts for the Conversion of Polyolefinic Waste Plastics into Fuels and Chemicals. *ACS Catal.* **2012**, *2*, 1924–1941.

45. Chu, M.; Liu, Y.; Lou, X.; Zhang, Q.; Chen, J. Rational Design of Chemical Catalysis for Plastic Recycling. *ACS Catal.* **2022**, *12*, 4659–4679.

46. Castro-Aguirre, E.; Iñiguez-Franco, F.; Samsudin, H.; Fang, X.; Auras, R. Poly(lactic acid)—Mass Production, Processing, Industrial Applications, and End of Life. *Adv. Drug Deliv. Rev.* **2016**, *107*, 333–366.

47. Jem, K. J.; Tan, B. The Development and Challenges of Poly(Lactic Acid) and Poly (Glycolic Acid). *Adv. Ind. Eng. Polym. Res.* **2020**, *3*, 60–70.

48. Häußler, M.; Eck, M.; Rothauer, D.; Mecking, S. Closed-Loop Recycling of Polyethylene-Like Materials. *Nature* **2021**, *590*, 423–427.

49. De Hoe, G. X.; Zumstein, M. T.; Tiegs, B. J.; Brutman, J. P.; McNeill, K.; Sander, M.; Coates, G. W.; Hillmyer, M. A. Sustainable Polyester Elastomers from Lactones: Synthesis, Properties, and Enzymatic Hydrolyzability. *J. Am. Chem. Soc.* **2018**, *140*, 963–973.

50. Cywar, R. M.; Rorrer, N. A.; Hoyt, C. B.; Beckham, G. T.; Chen, E. Y. X. Bio-Based Polymers with Performance-Advantaged Properties. *Nat. Rev. Mater.* **2022**, *7*, 83–103.

51. Jehanno, C.; Alty, J. W.; Roosen, M.; De Meester, S.; Dove, A. P.; Chen, E. Y. X.; Leibfarth, F. A.; Sardon, H. Critical Advances and Future Opportunities in Upcycling Commodity Polymers. *Nature* **2022**, *603*, 803–814.

52. Cywar, R. M.; Rorrer, N. A.; Mayes, H. B.; Maurya, A. K.; Tassone, C. J.; Beckham, G. T.; Chen, E. Y. X. Redesigned Hybrid Nylons with Optical Clarity and Chemical Recyclability. *J. Am. Chem. Soc.* **2022**, *144*, 5366–5376.

53. Abel, B. A.; Snyder, R. L.; Coates, G. W. Chemically Recyclable Thermoplastics from Reversible-Deactivation Polymerization of Cyclic Acetals. *Science* **2021**, *373*, 783–789.

54. Shi, C.; Reilly, L. T.; Kumar, V. S. P.; Coile, M. W.; Nicholson, S. R.; Broadbelt, L. J.; Beckham, G. T.; Chen, E. Y.-X. Design Principles for Intrinsically Circular Polymers with Tunable Properties. *Chem* **2021**, *7*, 2896–2912.

55. Vogt, B. D.; Stokes, K. K.; Kumar, S. K. Why Is Recycling of Postconsumer Plastics so Challenging? *ACS Appl. Polym. Mater.* **2021**, *3*, 4325–4346.

56. Coates, G. W.; Getzler, Y. D. Chemical Recycling to Monomer for an Ideal, Circular Polymer Economy. *Nat. Rev. Mater.* **2020**, *5*, 501–516.

57. Rahimi, A.; García, J. M. Chemical Recycling of Waste Plastics for New Materials Production. *Nat. Rev. Chem.* **2017**, *1*, 1–11.

58. Hong, M.; Chen, E. Y. X. Future Directions for Sustainable Polymers. *Trends Chem.* **2019**, *1*, 148–151.

59. Tardy, A.; Nicolas, J.; Gigmes, D.; Lefay, C.; Guillaneuf, Y. Radical Ring-Opening Polymerization: Scope, Limitations, and Application to (Bio) Degradable Materials. *Chem. Rev.* **2017**, *117*, 1319–1406.

60. Gigmes, D.; Van Steenberge, P. H.; Siri, D.; D'hooge, D. R.; Guillaneuf, Y.; Lefay, C. Simulation of the Degradation of Cyclic Ketene Acetal and Vinyl-Based Copolymers Synthesized via a Radical Process: Influence of the Reactivity Ratios on the Degradability Properties. *Macromol. Rapid Commun.* **2018**, *39*, 1800193.

61. De Smit, K.; Marien, Y. W.; Van Geem, K. M.; Van Steenberge, P. H.; D'hooge, D. R. Connecting Polymer Synthesis and Chemical Recycling on a Chain-by-Chain Basis: A Unified Matrix-Based Kinetic Monte Carlo Strategy. *React. Chem. Eng.* **2020**, *5*, 1909–1928.

62. Barbon, S. M.; Carter, M. C. D.; Yin, L.; Whaley, C. M.; Albright III, V. C.; Tecklenburg, R. E. Synthesis and Biodegradation Studies of Low-Dispersity Poly(acrylic Acid). *Macromol. Rapid Commun.* **2022**, *2100773*.

63. Hedin, G. G.; Bell, C. A.; Leong, N. S.; Chapman, E.; Collins, I. R.; O'Reilly, R. K.; Dove, A. P. Functional Degradable Polymers by Xanthate-Mediated Polymerization. *Macromolecules* **2014**, *47*, 2847–2852.

64. Hedin, G. G.; Bell, C. A.; O'Reilly, R. K.; Dove, A. P. Functional Degradable Polymers by Radical Ring-Opening Copolymerization of MDO and Vinyl Bromobutanoate: Synthesis, Degradability and Post-Polymerization Modification. *Biomacromolecules* **2015**, *16*, 2049–2058.

65. Hedin, G.; Stubbs, C.; Aston, P.; Dove, A. P.; Gibson, M. I. Synthesis of Degradable Poly(Vinyl Alcohol) by Radical Ring-Opening Copolymerization and Ice Recrystallization Inhibition Activity. *ACS Macro Lett.* **2017**, *6*, 1404–1408.

66. He, T.; Zou, Y.-F.; Pan, C.-Y. Controlled/“Living” Radical Ring-Opening Polymerization of 5,6-Benzo-2-Methylene-1,3-Dioxepane Based on Reversible Addition-Fragmentation Chain Transfer Mechanism. *Polym. J.* **2002**, *34*, 138–143.

67. Yuan, J.-Y.; Pan, C.-Y.; Tang, B. Z. “Living” Free Radical Ring-Opening Polymerization of 5,6-Benzo-2-methylene-1,3-dioxepane Using the Atom Transfer Radical Polymerization Method. *Macromolecules* **2001**, *34*, 211–214.

68. Tardy, A.; Delplace, V.; Siri, D.; Lefay, C.; Harrisson, S.; de Fatima Albergaria Pereira, B.; Charles, L.; Gigmes, D.; Nicolas, J.; Guillaneuf, Y. Scope and Limitations of the Nitroxide-Mediated Radical Ring-Opening Polymerization of Cyclic Ketene Acetals. *Polym. Chem.* **2013**, *4*, 4776.

69. Decker, C. G.; Maynard, H. D. Degradable PEGylated Protein Conjugates Utilizing RAFT Polymerization. *Eur. Polym. J.* **2015**, *65*, 305–312.

70. Lai, H.; Ouchi, M. Backbone-Degradable Polymers via Radical Copolymerizations of Pentafluorophenyl Methacrylate with Cyclic Ketene Acetal: Pendant Modification and Efficient Degradation by Alternating-Rich Sequence. *ACS Macro Lett.* **2021**, *10*, 1223–1228.

71. Delplace, V.; Tardy, A.; Harrisson, S.; Mura, S.; Gigmes, D.; Guillaneuf, Y.; Nicolas, J. Degradable and Comb-Like PEG-Based Copolymers by Nitroxide-Mediated Radical

Ring-Opening Polymerization. *Biomacromolecules* **2013**, *14*, 3769–3779.

72. Delplace, V.; Guegain, E.; Harrisson, S.; Gigmes, D.; Guillaneuf, Y.; Nicolas, J. A Ring to Rule Them All: A Cyclic Ketene Acetal Comonomer Controls the Nitroxide-Mediated Polymerization of Methacrylates and Confers Tunable Degradability. *Chem. Commun. (Camb.)* **2015**, *51*, 12847–12850.

73. Tran, J.; Guégain, E.; Ibrahim, N.; Harrisson, S.; Nicolas, J. Efficient Synthesis of 2-Methylene-4-phenyl-1,3-dioxolane, a Cyclic Ketene Acetal for Controlling the NMP of Methyl Methacrylate and Conferring Tunable Degradability. *Polym. Chem.* **2016**, *7*, 4427–4435.

74. Guégain, E.; Michel, J.-P.; Boissenot, T.; Nicolas, J. Tunable Degradation of Copolymers Prepared by Nitroxide-Mediated Radical Ring-Opening Polymerization and Point-by-Point Comparison with Traditional Polyesters. *Macromolecules* **2018**, *51*, 724–736.

75. Hill, M. R.; Guégain, E.; Tran, J.; Figg, C. A.; Turner, A. C.; Nicolas, J.; Sumerlin, B. S. Radical Ring-Opening Copolymerization of Cyclic Ketene Acetals and Maleimides Affords Homogeneous Incorporation of Degradable Units. *ACS Macro Lett.* **2017**, *6*, 1071–1077.

76. Smith, Q.; Huang, J.; Matyjaszewski, K.; Loo, Y.-L. Controlled Radical Polymerization and Copolymerization of 5-Methylene-2-phenyl-1,3-dioxolan-4-one by ATRP. *Macromolecules* **2005**, *38*, 5581–5586.

77. Smith, R. A.; Fu, G.; McAteer, O.; Xu, M.; Gutekunst, W. R. Radical Approach to Thioester-Containing Polymers. *J. Am. Chem. Soc.* **2019**, *141*, 1446–1451.

78. Spick, M. P.; Bingham, N. M.; Li, Y.; de Jesus, J.; Costa, C.; Bailey, M. J.; Roth, P. J. Fully Degradable Thioester-Functional Homo- and Alternating Copolymers Prepared through Thiocarbonyl Addition-Ring-Opening RAFT Radical Polymerization. *Macromolecules* **2020**, *53*, 539–547.

79. Paulusse, J. M. J.; Amir, R. J.; Evans, R. A.; Hawker, C. J. Free Radical Polymers with Tunable and Selective Bio- and Chemical Degradability. *J. Am. Chem. Soc.* **2009**, *131*, 9805–9812.

80. Evans, R. A.; Moad, G.; Rizzardo, E.; Thang, S. H. New Free-Radical Ring-Opening Acrylate Monomers. *Macromolecules* **1994**, *27*, 7935–7937.

81. Ratcliffe, L. P. D.; Couchon, C.; Armes, S. P.; Paulusse, J. M. J. Inducing an Order-Order Morphological Transition via Chemical Degradation of Amphiphilic Diblock Copolymer Nano-Objects. *Biomacromolecules* **2016**, *17*, 2277–2283.

82. Huang, H.; Sun, B.; Huang, Y.; Niu, J. Radical Cascade-Triggered Controlled Ring-Opening Polymerization of Macroyclic Monomers. *J. Am. Chem. Soc.* **2018**, *140*, 10402–10406.

83. Wang, W.; Zhou, Z.; Sathe, D.; Tang, X.; Moran, S.; Jin, J.; Haeffner, F.; Wang, J.; Niu, J. Degradable Vinyl Random Copolymers via Photocontrolled Radical Ring-Opening Cascade Copolymerization. *Angew. Chem. Int. Ed.* **2022**, *61*, e202113302.

84. Reeves, J. A.; De Alwis Watuthantrige, N.; Boyer, C.; Konkolewicz, D. Intrinsic and Catalyzed Photochemistry of Phenylvinylketone for Wavelength-Sensitive Controlled Polymerization. *ChemPhotoChem* **2019**, *3*, 1171–1179.

85. Nwoko, T.; Watuthantrige, N. D. A.; Parnitzke, B.; Yehl, K.; Konkolewicz, D. Tuning Molecular Weight Distributions of Vinylketone-based Polymers using RAFT Photopolymerization and UV Photodegradation. *Polym. Chem.* **2021**, *12*, 6761–6770.

86. Cheng, C.; Sun, G.; Khoshdel, E.; Wooley, K. L. Well-Defined Vinyl Ketone-Based Polymers by Reversible Addition–Fragmentation Chain Transfer Polymerization. *J. Am. Chem. Soc.* **2007**, *129*, 10086–10087.

87. De Alwis Watuthantrige, N.; Reeves, J. A.; Dolan, M. T.; Valloppilly, S.; Zanjani, M. B.; Ye, Z.; Konkolewicz, D. Wavelength-Controlled Synthesis and Degradation of Thermoplastic Elastomers Based on Intrinsically Photoresponsive Phenyl Vinyl Ketone. *Macromolecules* **2020**, *53*, 5199–5207.

88. Kimura, T.; Kuroda, K.; Kubota, H.; Ouchi, M. Metal-Catalyzed Switching Degradation of Vinyl Polymers via Introduction of an “In-Chain” Carbon–Halogen Bond as the Trigger. *ACS Macro Lett.* **2021**, *10*, 1535–1539.

89. Rikkou, M. D.; Patrickios, C. S. Polymers Prepared Using Cleavable Initiators: Synthesis, Characterization and Degradation. *Prog. Polym. Sci.* **2011**, *36*, 1079–1097.

90. Tsarevsky, N. V.; Matyjaszewski, K. Reversible Redox Cleavage/Coupling of Polystyrene with Disulfide or Thiol Groups Prepared by Atom Transfer Radical Polymerization. *Macromolecules* **2002**, *35*, 9009–9014.

91. Tsarevsky, N. V.; Matyjaszewski, K. Combining Atom Transfer Radical Polymerization and Disulfide/Thiol Redox Chemistry: A Route to Well-Defined (Bio)degradable Polymeric Materials. *Macromolecules* **2005**, *38*, 3087–3092.

92. Fritze, U. F.; Craig, S. L.; von Delius, M. Disulfide-Centered Poly(Methyl Acrylates): Four Different Stimuli to Cleave a Polymer. *J. Polym. Sci. A: Polym. Chem.* **2018**, *56*, 1404–1411.

93. Sun, H.; Kabb, C. P.; Dai, Y.; Hill, M. R.; Ghiviriga, I.; Bapat, A. P.; Sumerlin, B. S. Macromolecular Metamorphosis via Stimulus-Induced Transformations of Polymer Architecture. *Nat. Chem.* **2017**, *9*, 817–823.

94. Duan, H.-Y.; Wang, Y.-X.; Wang, L.-J.; Min, Y.-Q.; Zhang, X.-H.; Du, B.-Y. An Investigation of the Selective Chain Scission at Centered Diels–Alder Mechanophore under Ultrasound. *Macromolecules* **2017**, *50*, 1353–1361.

95. Nicolay, R.; Marx, L.; Hemery, P.; Matyjaszewski, K. Synthesis of Multisegmented Degradable Polymers by Atom Transfer Radical Cross-Coupling. *Macromolecules* **2007**, *40*, 9217–9223.

96. Wang, G.; Huang, J. Versatility of Radical Coupling in Construction of Topological Polymers. *Polym. Chem.* **2014**, *5*, 277–308.

97. Sarbu, T.; Lin, K.-Y.; Ell, J.; Siegwart, D. J.; Spanswick, J.; Matyjaszewski, K. Polystyrene with Designed Molecular Weight Distribution by Atom Transfer Radical Coupling. *Macromolecules* **2004**, *37*, 3120–3127.

98. Nicolay, R.; Matyjaszewski, K. Synthesis of Cyclic (Co) polymers by Atom Transfer Radical Cross-Coupling and

Ring Expansion by Nitroxide-Mediated Polymerization. *Macromolecules* **2011**, *44*, 240–247.

99. Wang, X.; Huang, J.; Chen, L.; Liu, Y.; Wang, G. Synthesis of Thermal Degradable Poly(alkoxyamine) through a Novel Nitroxide Radical Coupling Step Growth Polymerization Mechanism. *Macromolecules* **2014**, *47*, 7812–7822.

100. Valente, C. J.; Schellenberger, A. M.; Tillman, E. S. Dimerization of Poly(methyl methacrylate) Chains Using Radical Trap-Assisted Atom Transfer Radical Coupling. *Macromolecules* **2014**, *47*, 2226–2232.

101. Butcher, W. E.; Radzinski, S. C.; Tillman, E. S. Selective Formation of Diblock Copolymers Using Radical Trap-Assisted Atom Transfer Radical Coupling. *J. Polym. Sci. A: Polym. Chem.* **2013**, *51*, 3619–3626.

102. Voter, A. F.; Tillman, E. S.; Findeis, P. M.; Radzinski, S. C. Synthesis of Macroyclic Polymers Formed via Intramolecular Radical Trap-Assisted Atom Transfer Radical Coupling. *ACS Macro Lett.* **2012**, *1*, 1066–1070.

103. Whittaker, M. R.; Goh, Y.-K.; Gemici, H.; Legge, T. M.; Perrier, S.; Monteiro, M. J. Synthesis of Monocyclic and Linear Polystyrene Using the Reversible Coupling/Cleavage of Thiol/Disulfide Groups. *Macromolecules* **2006**, *39*, 9028–9034.

104. You, Y.-Z.; Manickam, D. S.; Zhou, Q.; Oupicky, D. A Versatile Approach to Reducible Vinyl Polymers via Oxidation of Telechelic Polymers Prepared by Reversible Addition Fragmentation Chain Transfer Polymerization. *Biomacromolecules* **2007**, *8*, 2038–2044.

105. Hakobyan, K.; McErlean, C. S. P.; Müllner, M. RAFT Without an “R-Group”: From Asymmetric Homo-Telechelics to Multiblock Step-Growth and Cyclic Block Copolymers. *Macromolecules* **2021**, *54*, 7732–7742.

106. You, Y.-Z.; Zhou, Q.-H.; Manickam, D. S.; Wan, L.; Mao, G.; Oupicky, D. Dually Responsive Multiblock Copolymers via Reversible Addition-Fragmentation Chain Transfer Polymerization: Synthesis of Temperature- and Redox-Responsive Copolymers of Poly(N-isopropylacrylamide) and Poly(2-(dimethylamino)ethyl methacrylate). *Biomacromolecules* **2007**, *40*, 8617–8624.

107. Ko, N. R.; Yao, K.; Tang, C.; Oh, J. K. Synthesis and Thiol-Responsive Degradation of Polylactide-Based Block Copolymers Having Disulfide Junctions Using ATRP and ROP. *J. Polym. Sci. A: Polym. Chem.* **2013**, *51*, 3071–3080.

108. Cunningham, A.; Oh, J. K. New Design of Thiol-Responsive Degradable Polylactide-Based Block Copolymer Micelles. *Macromol. Rapid Commun.* **2013**, *34*, 163–168.

109. Clement, B.; Trimaille, T.; Alluin, O.; Gigmes, D.; Mabrouk, K.; Feron, D.; Decherchi, P.; Marqueste, T.; Bertin, D. Convenient Access to Biocompatible Block Copolymers from SG1-Based Aliphatic Polyester Macro-Alkoxyamines. *Biomacromolecules* **2009**, *10*, 1436–1445.

110. Resendiz-Lara, D. A.; Wurm, F. R. Polyphosphonate-Based Macromolecular RAFT-CTA Enables the Synthesis of Well-Defined Block Copolymers Using Vinyl Monomers. *ACS Macro Lett.* **2021**, *10*, 1273–1279.

111. Liu, X.; Ni, P.; He, J.; Zhang, M. Synthesis and Micellization of pH/Temperature-Responsive Double-Hydrophilic Diblock Copolymers Polyphosphoester-block-poly[2-(dimethylamino)ethyl methacrylate] Prepared via ROP and ATRP. *Macromolecules* **2010**, *43*, 4771–4781.

112. Kang, H. U.; Yu, Y. C.; Shin, S. J.; Youk, J. H. One-Step Synthesis of Block Copolymers Using a Hydroxyl-Functionalized Trithiocarbonate RAFT Agent as a Dual Initiator for RAFT Polymerization and ROP. *J. Polym. Sci. A: Polym. Chem.* **2013**, *51*, 774–779.

113. Xia, Y.; Scheutz, G.; Easterling, C.; Zhao, J.; Sumerlin, B. S. Hybrid Block Copolymer Synthesis by Merging Photoiniferter and Organocatalytic Ring-Opening Polymerizations. *Angew. Chem. Int. Ed.* **2021**, *60*, 18537–18541.

114. Voit, B. I.; Lederer, A. Hyperbranched and Highly Branched Polymer Architectures—Synthetic Strategies and Major Characterization Aspects. *Chem. Rev.* **2009**, *109*, 5924–5973.

115. Zheng, Y.; Li, S.; Weng, Z.; Gao, C. Hyperbranched Polymers: Advances from Synthesis to Applications. *Chem. Soc. Rev.* **2015**, *44*, 4091–4130.

116. Jiang, W.; Zhou, Y.; Yan, D. Hyperbranched Polymer Vesicles: From Self-Assembly, Characterization, Mechanisms, and Properties to Applications. *Chem. Soc. Rev.* **2015**, *44*, 3874–3889.

117. Caminade, A.-M.; Yan, D.; Smith, D. K. Dendrimers and Hyperbranched Polymers. *Chem. Soc. Rev.* **2015**, *44*, 3870–3873.

118. Tsarevsky, N. V.; Huang, J.; Matyjaszewski, K. Synthesis of Hyperbranched Degradable Polymers by Atom Transfer Radical (Co)polymerization of Inimers with Ester or Disulfide Groups. *J. Polym. Sci. A: Polym. Chem.* **2009**, *47*, 6839–6851.

119. Mizutani, M.; Satoh, K.; Kamigaito, M. Metal-Catalyzed Radical Polyaddition for Aliphatic Polyesters via Evolution of Atom Transfer Radical Addition into Step-Growth Polymerization. *Macromolecules* **2009**, *42*, 472–480.

120. Graff, R. W.; Wang, X.; Gao, H. Exploring Self-Condensing Vinyl Polymerization of Inimers in Microemulsion To Regulate the Structures of Hyperbranched Polymers. *Macromolecules* **2015**, *48*, 2118–2126.

121. Sun, H.; Kabb, C. P.; Sumerlin, B. S. Thermally-Labile Segmented Hyperbranched Copolymers: Using Reversible-Covalent Chemistry to Investigate the Mechanism of Self-Condensing Vinyl Copolymerization. *Chem. Sci.* **2014**, *5*, 4646–4655.

122. Rosselgong, J.; Armes, S. P.; Barton, W.; Price, D. Synthesis of Highly Branched Methacrylic Copolymers: Observation of Near-Ideal Behavior Using RAFT Polymerization. *Macromolecules* **2009**, *42*, 5919–5924.

123. Vo, C. J.; Rosselgong, J.; Armes, S. P.; Billingham, N. C. RAFT Synthesis of Branched Acrylic Copolymers. *Macromolecules* **2007**, *40*, 7119–7125.

124. Wang, L.; Li, C.; Ryan, A. J.; Armes, S. P. Synthesis and Peptide-Induced Degradation of Biocompatible Fibers Based on Highly Branched Poly(2-hydroxyethyl methacrylate). *Adv. Mater.* **2006**, *18*, 1566–1570.

125. Oh, J. K.; Tang, C.; Gao, H.; Tsarevsky, N.; Matyjaszewski, K. Inverse Miniemulsion ATRP: A New Method for Synthesis and Functionalization of Well-Defined Water-Soluble/Cross-Linked Polymeric Particles. *J. Am. Chem. Soc.* **2006**, *128*, 5578–5584.

126. Oh, J. K.; Siegwart, D. J.; Matyjaszewski, K. Synthesis and Biodegradation of Nanogels as Delivery Carriers for Carbohydrate Drugs. *Biomacromolecules* **2007**, *8*, 3326–3331.

127. Oh, J. K.; Siegwart, D. J.; Lee, H.; Sherwood, G.; Peteau, L.; Hollinger, J. O.; Kataoka, K.; Matyjaszewski, K. Biodegradable Nanogels Prepared by Atom Transfer Radical Polymerization as Potential Drug Delivery Carriers: Synthesis, Biodegradation, in Vitro Release, and Bioconjugation. *J. Am. Chem. Soc.* **2007**, *129*, 5939–5945.

128. Sims, M. B.; Patel, K. Y.; Bhatta, M.; Mukherjee, S.; Sumerlin, B. S. Harnessing Imine Diversity to Tune Hyperbranched Polymer Degradation. *Macromolecules* **2018**, *51*, 356–363.

129. Levy, A.; Goldstein, H.; Brenman, D.; Diesendruck, C. E. Effect of Intramolecular Crosslinker Properties on the Mechanochemical Fragmentation of Covalently Folded Polymers. *J. Polym. Sci.* **2020**, *58*, 692–703.

130. Blencowe, A.; Tan, J. F.; Goh, T. K.; Qiao, G. G. Core Cross-Linked Star Polymers via Controlled Radical Polymerisation. *Polymer* **2009**, *50*, 5–32.

131. Ren, J. M.; McKenzie, T. G.; Fu, Q.; Wong, E. H. H.; Xu, J.; An, Z.; Shanmugam, S.; Davis, T. P.; Boyer, C.; Qiao, G. G. Star Polymers. *Chem. Rev.* **2016**, *116*, 6743–6836.

132. Gao, H.; Matyjaszewski, K. Synthesis of Functional Polymers with Controlled Architecture by CRP of Monomers in the Presence of Cross-Linkers: From Stars to Gels. *Prog. Polym. Sci.* **2009**, *34*, 317–350.

133. Goh, T. K.; Coventry, K. D.; Blencowe, A.; Qiao, G. G. Rheology of Core Cross-Linked Star Polymers. *Polymer* **2008**, *49*, 5095–5104.

134. Chmielarz, P. Synthesis of  $\alpha$ -D-Glucose-Based Star Polymers through Simplified Electrochemically Mediated ATRP. *Polymer* **2016**, *102*, 192–198.

135. Chmielarz, P.; Park, S.; Sobkowiak, A.; Matyjaszewski, K. Synthesis of  $\beta$ -Cyclodextrin-Based Star Polymers via a Simplified Electrochemically Mediated ATRP. *Polymer* **2016**, *88*, 36–42.

136. Zhu, W.; Nese, A.; Matyjaszewski, K. Thermoresponsive Star Triblock Copolymers by Combination of ROP and ATRP: From Micelles to Hydrogels. *J. Polym. Sci. A: Polym. Chem.* **2011**, *49*, 1942–1952.

137. Cuthbert, J.; Yerneni, S. S.; Sun, M.; Fu, T.; Matyjaszewski, K. Degradable Polymer Stars Based on Tannic Acid Cores by ATRP. *Polymers (Basel)* **2019**, *11*, 752.

138. Setijadi, E.; Tao, L.; Liu, J.; Jia, Z.; Boyer, C.; Davis, T. P. Biodegradable Star Polymers Functionalized with  $\beta$ -Cyclodextrin Inclusion Complexes. *Biomacromolecules* **2009**, *10*, 2699–2707.

139. Liu, J.; Liu, H.; Jia, Z.; Bulmus, V.; Davis, T. P. An Approach to Biodegradable Star Polymeric Architectures Using Disulfide Coupling. *Chem. Commun. (Camb.)* **2008**, *48*, 6582–6584.

140. Rosselgong, J.; Williams, E. G. L.; Le, T. P.; Grusche, F.; Hinton, T. M.; Tizard, M.; Gunatillake, P.; Thang, S. H. Core Degradable Star RAFT Polymers: Synthesis, Polymerization, and Degradation Studies. *Macromolecules* **2013**, *46*, 9181–9188.

141. Gao, H.; Tsarevsky, N. V.; Matyjaszewski, K. Synthesis of Degradable Miktoarm Star Copolymers via Atom Transfer Radical Polymerization. *Macromolecules* **2005**, *38*, 5995–6004.

142. Cho, H. Y.; Srinivasan, A.; Hong, J.; Hsu, E.; Liu, S.; Shrivats, A.; Kwak, D.; Bohaty, A. K.; Paik, H. J.; Hollinger, J. O.; Matyjaszewski, K. Synthesis of Biocompatible PEG-Based Star Polymers with Cationic and Degradable Core for siRNA Delivery. *Biomacromolecules* **2011**, *12*, 3478–3486.

143. Averick, S. E.; Paredes, E.; Irastorza, A.; Shrivats, A. R.; Srinivasan, A.; Siegwart, D. J.; Magenau, A. J.; Cho, H. Y.; Hsu, E.; Averick, A. A.; Kim, J.; Liu, S.; Hollinger, J. O.; Das, S. R.; Matyjaszewski, K. Preparation of Cationic Nanogels for Nucleic Acid Delivery. *Biomacromolecules* **2012**, *13*, 3445–3449.

144. Li, W.; Yoon, J. A.; Matyjaszewski, K. Dual-Reactive Surfactant Used for Synthesis of Functional Nanocapsules in Miniemulsion. *J. Am. Chem. Soc.* **2010**, *132*, 7823–7825.

145. Wiltshire, J. T.; Qiao, G. G. Selectively Degradable Core Cross-Linked Star Polymers. *Macromolecules* **2006**, *39*, 9018–9027.

146. Wiltshire, J. T.; Qiao, G. G. Synthesis of Core Cross-Linked Star Polymers with Adjustable Coronal Properties. *Macromolecules* **2008**, *41*, 623–631.

147. Dai, Y.; Sun, H.; Pal, S.; Zhang, Y.; Park, S.; Kabb, C. P.; Wei, W. D.; Sumerlin, B. S. Near-IR-Induced Dissociation of Thermally-Sensitive Star Polymers. *Chem. Sci.* **2017**, *8*, 1815–1821.

148. Bapat, A. P.; Ray, J. G.; Savin, D. A.; Hoff, E. A.; Patton, D. L.; Sumerlin, B. S. Dynamic-Covalent Nanostructures Prepared by Diels-Alder Reactions of Styrene-Maleic Anhydride-Derived Copolymers Obtained by One-Step Cascade Block Copolymerization. *Polym. Chem.* **2012**, *3*, 3112.

149. Amamoto, Y.; Kikuchi, M.; Otsuka, H.; Takahara, A. Arm-Replaceable Star-Like Nanogels: Arm Detachment and Arm Exchange Reactions by Dynamic Covalent Exchanges of Alkoxyamine Units. *Polym. J.* **2010**, *42*, 860–867.

150. Amamoto, Y.; Kikuchi, M.; Otsuka, H.; Takahara, A. Solvent-Controlled Formation of Star-like Nanogels via Dynamic Covalent Exchange of PSt-b-PMMA Diblock Copolymers with Alkoxyamine Units in the Side Chain. *Macromolecules* **2010**, *43*, 5470–5473.

151. Amamoto, Y.; Higaki, Y.; Matsuda, Y.; Otsuka, H.; Takahara, A. Programmed Thermodynamic Formation and Structure Analysis of Star-Like Nanogels with Core Cross-Linked by Thermally Exchangeable Dynamic Covalent Bonds. *J. Am. Chem. Soc.* **2007**, *129*, 13298–13304.

152. Xie, G.; Martinez, M. R.; Olszewski, M.; Sheiko, S. S.; Matyjaszewski, K. Molecular Bottlebrushes as Novel Materials. *Biomacromolecules* **2019**, *20*, 27–54.

153. Lee, H.-i.; Pietrasik, J.; Sheiko, S. S.; Matyjaszewski, K. Stimuli-Responsive Molecular Brushes. *Prog. Polym. Sci.* **2010**, *35*, 24–44.

154. Panyukov, S.; Zhulina, E. B.; Sheiko, S. S.; Randall, G. C.; Brock, J.; Rubinstein, M. Tension Amplification in Molecular Brushes in Solutions and on Substrates. *J. Phys. Chem. B* **2009**, *113*, 3750–3768.

155. Panyukov, S. V.; Sheiko, S. S.; Rubinstein, M. Amplification of Tension in Branched Macromolecules. *Phys. Rev. Lett.* **2009**, *102*, 148301.

156. Zheng, Z.; Müllner, M.; Ling, J.; Müller, A. H. E. Surface Interactions Surpass Carbon-Carbon Bond: Understanding and Control of the Scission Behavior of Core-Shell Polymer Brushes on Surfaces. *ACS Nano* **2013**, *7*, 2284-2291.

157. Sheiko, S. S.; Sun, F. C.; Randall, A.; Shirvanyants, D.; Rubinstein, M.; Lee, H. I.; Matyjaszewski, K. Adsorption-Induced Scission of Carbon-Carbon Bonds. *Nature* **2006**, *440*, 191-194.

158. Lebedeva, N. V.; Sun, F. C.; Lee, H.-i.; Matyjaszewski, K.; Sheiko, S. S. "Fatal Adsorption" of Brushlike Macromolecules: High Sensitivity of C-C Bond Cleavage Rates to Substrate Surface Energy. *J. Am. Chem. Soc.* **2008**, *130*, 4228-4229.

159. Park, I.; Shirvanyants, D.; Nese, A.; Matyjaszewski, K.; Rubinstein, M.; Sheiko, S. S. Spontaneous and Specific Activation of Chemical Bonds in Macromolecular Fluids. *J. Am. Chem. Soc.* **2010**, *132*, 12487-12491.

160. Lebedeva, N. V.; Nese, A.; Sun, F. C.; Matyjaszewski, K.; Sheiko, S. S. Anti-Arrhenius Cleavage of Covalent Bonds in Bottlebrush Macromolecules on Substrate. *Proc. Natl. Acad. Sci. U. S. A.* **2012**, *109*, 9276-9280.

161. Li, Y.; Nese, A.; Matyjaszewski, K.; Sheiko, S. S. Molecular Tensile Machines: Anti-Arrhenius Cleavage of Disulfide Bonds. *Macromolecules* **2013**, *46*, 7196-7201.

162. Park, I. S.; Nese, A.; Matyjaszewski, K. Molecular Tensile Testing Machines: Breaking a Specific Covalent Bond by Adsorption-Induced Tension in Brushlike Macromolecules. *Macromolecules* **2009**, *42*, 1805-1807.

163. Burdyńska, J.; Li, Y.; Aggarwal, A. V.; Höger, S.; Sheiko, S. S.; Matyjaszewski, K. Synthesis and Arm Dissociation in Molecular Stars with a Spoked Wheel Core and Bottlebrush Arms. *J. Am. Chem. Soc.* **2014**, *136*, 12762-12770.

164. Martinez, M. R.; Cong, Y.; Sheiko, S. S.; Matyjaszewski, K. A Thermodynamic Roadmap for the Grafting-through Polymerization of PDMS11MA. *ACS Macro Lett.* **2020**, *9*, 1303-1309.

165. Cho, H. Y.; Krys, P.; Szcześniak, K.; Schroeder, H.; Park, S.; Jurga, S.; Buback, M.; Matyjaszewski, K. Synthesis of Poly(OEOMA) Using Macromonomers via "Grafting-Through" ATRP. *Macromolecules* **2015**, *48*, 6385-6395.

166. Shinoda, H.; Miller, P. J.; Matyjaszewski, K. Improving the Structural Control of Graft Copolymers by Combining ATRP with the Macromonomer Method. *Macromolecules* **2001**, *34*, 3186-3194.

167. Raus, V.; Čadová, E.; Starovoytova, L.; Janata, M. ATRP of POSS Monomers Revisited: Toward High-Molecular-Weight Methacrylate-POSS (Co)Polymers. *Macromolecules* **2014**, *47*, 7311-7320.

168. Flanders, M. J.; Gramlich, W. M. Reversible-Addition Fragmentation Chain Transfer (RAFT) Mediated Depolymerization of Brush Polymers. *Polym. Chem.* **2018**, *9*, 2328-2335.

169. Martinez, M. R.; Dadashi-Silab, S.; Lorandi, F.; Zhao, Y.; Matyjaszewski, K. Depolymerization of P(PDMS11MA) Bottlebrushes via Atom Transfer Radical Polymerization with Activator Regeneration. *Macromolecules* **2021**, *54*, 5526-5538.

170. Beers, K. L.; Gaynor, S. G.; Matyjaszewski, K.; Sheiko, S. S.; Möller, M. The Synthesis of Densely Grafted Copolymers by Atom Transfer Radical Polymerization. *Macromolecules* **1998**, *31*, 9413-9415.

171. Xie, G.; Martinez, M. R.; Daniel, W. F. M.; Keith, A. N.; Ribelli, T. G.; Fantin, M.; Sheiko, S. S.; Matyjaszewski, K. Benefits of Catalyzed Radical Termination: High-Yield Synthesis of Polyacrylate Molecular Bottlebrushes without Gelation. *Macromolecules* **2018**, *51*, 6218-6225.

172. Martinez, M. R.; Sobieski, J.; Lorandi, F.; Fantin, M.; Dadashi-Silab, S.; Xie, G.; Olszewski, M.; Pan, X.; Ribelli, T. G.; Matyjaszewski, K. Understanding the Relationship between Catalytic Activity and Termination in photoATRP: Synthesis of Linear and Bottlebrush Polyacrylates. *Macromolecules* **2020**, *53*, 59-67.

173. Liu, Y.; Chen, P.; Li, Z. Molecular Bottlebrushes with Polypeptide Backbone Prepared via Ring-Opening Polymerization of NCA and ATRP. *Macromol. Rapid Commun.* **2012**, *33*, 287-295.

174. Olszewski, M.; Li, L.; Xie, G.; Keith, A.; Sheiko, S. S.; Matyjaszewski, K. Degradable Cellulose-Based Polymer Brushes with Controlled Grafting Densities. *J. Polym. Sci. A: Polym. Chem.* **2019**, *57*, 2426-2435.

175. Neugebauer, D.; Sumerlin, B. S.; Matyjaszewski, K.; Goodhart, B.; Sheiko, S. S. How Dense Are Cylindrical Brushes Grafted from a Multifunctional Macroinitiator? *Polymer* **2004**, *45*, 8173-8179.

176. Sumerlin, B. S.; Neugebauer, D.; Matyjaszewski, K. Initiation Efficiency in the Synthesis of Molecular Brushes by Grafting from via Atom Transfer Radical Polymerization. *Macromolecules* **2005**, *38*, 702-708.

177. Raj, W.; Jerczynski, K.; Rahimi, M.; Przekora, A.; Matyjaszewski, K.; Pietrasik, J. Molecular Bottlebrush with pH-Responsive Cleavable Bonds as a Unimolecular Vehicle for Anticancer Drug Delivery. *Mater. Sci. Eng. C* **2021**, *130*, 112439.

178. Gao, H.; Matyjaszewski, K. Synthesis of Molecular Brushes by "Grafting Onto" Method: Combination of ATRP and Click Reactions. *J. Am. Chem. Soc.* **2007**, *129*, 6633-6639.

179. Navarro, L. A.; Shah, T. P.; Zauscher, S. Grafting of Bottlebrush Polymers: Conformation and Kinetics. *Langmuir* **2020**, *36*, 4745-4756.

180. Zhu, W.; Zhang, L.; Chen, Y.; Zhang, K. A UV-Cleavable Bottlebrush Polymer with o-Nitrobenzyl-Linked Side Chains. *Macromol. Rapid Commun.* **2017**, *38*, 1700007.

181. Higaki, Y.; Otsuka, H.; Takahara, A. Dynamic Formation of Graft Polymers via Radical Crossover Reaction of Alkoxamines. *Macromolecules* **2004**, *37*, 1696-1701.

182. Cuthbert, J.; Wanasinghe, S. V.; Matyjaszewski, K.; Konkolewicz, D. Are RAFT and ATRP Universally Interchangeable Polymerization Methods in Network Formation? *Macromolecules* **2021**, *54*, 8331-8340.

183. Kamada, J.; Koynov, K.; Corten, C.; Juhari, A.; Yoon, J. A.; Urban, M. W.; Balazs, A. C.; Matyjaszewski, K. Redox Responsive Behavior of Thiol/Disulfide-Functionalized Star

Polymers Synthesized via Atom Transfer Radical Polymerization. *Macromolecules* **2010**, *43*, 4133–4139.

184. Tsarevsky, N. V.; Min, K.; Jahed, N. M.; Gao, H.; Matyjaszewski, K. Functional Degradable Polymeric Materials Prepared by Atom Transfer Radical Polymerization (ATRP). *ACS Symp. Ser.* **2006**, *939*, 184–200.

185. Lamson, M.; Epshteyn-Assor, Y.; Silverstein, M. S.; Matyjaszewski, K. Synthesis of Degradable polyHIPEs by AGET ATRP. *Polymer* **2013**, *54*, 4480–4485.

186. Dong, H.; Mantha, V.; Matyjaszewski, K. Thermally Responsive PM(EO)2MA Magnetic Microgels via Activators Generated by Electron Transfer Atom Transfer Radical Polymerization in Miniemulsion. *Chem. Mater.* **2009**, *21*, 3965–3972.

187. Johnson, J. A.; Finn, M. G.; Koberstein, J. T.; Turro, N. J. Synthesis of Photocleavable Linear Macromonomers by ATRP and Star Macromonomers by a Tandem ATRP-Click Reaction: Precursors to Photodegradable Model Networks. *Macromolecules* **2007**, *40*, 3589–3598.

188. Johnson, J. A.; Lewis, D. R.; Diaz, D. D.; Finn, M. G.; Koberstein, J. T.; Turro, N. J. Synthesis of Degradable Model Networks via ATRP and Click Chemistry. *J. Am. Chem. Soc.* **2006**, *128*, 6564–6565.

189. Johnson, J. A.; Baskin, J. M.; Bertozi, C. R.; Koberstein, J. T.; Turro, N. J. Copper-Free Click Chemistry for the In Situ Crosslinking of Photodegradable Star Polymers. *Chem. Commun. (Camb.)* **2008**, *26*, 3064–3066.

190. Amamoto, Y.; Kamada, J.; Otsuka, H.; Takahara, A.; Matyjaszewski, K. Repeatable Photoinduced Self-Healing of Covalently Cross-Linked Polymers through Reshuffling of Trithiocarbonate Units. *Angew. Chem. Int. Ed. Engl.* **2011**, *50*, 1660–1663.

191. Scheutz, G. M.; Lessard, J. J.; Sims, M. B.; Sumerlin, B. S. Adaptable Crosslinks in Polymeric Materials: Resolving the Intersection of Thermoplastics and Thermosets. *J. Am. Chem. Soc.* **2019**, *141*, 16181–16196.

192. Chen, M.; Gu, Y.; Singh, A.; Zhong, M.; Jordan, A. M.; Biswas, S.; Korley, L. T. J.; Balazs, A. C.; Johnson, J. A. Living Additive Manufacturing: Transformation of Parent Gels into Diversely Functionalized Daughter Gels Made Possible by Visible Light Photoredox Catalysis. *ACS Cent. Sci.* **2017**, *3*, 124–134.

193. Ida, S.; Kimura, R.; Tanimoto, S.; Hirokawa, Y. End-Crosslinking of Controlled Telechelic Poly(N-Isopropylacrylamide) toward a Homogeneous Gel Network with Photo-Induced Self-Healing. *Polym. J.* **2017**, *49*, 237–243.

194. Zhang, Z.; Corrigan, N.; Boyer, C. A Photoinduced Dual-Wavelength Approach for 3D Printing and Self-Healing of Thermosetting Materials. *Angew. Chem. Int. Ed.* **2022**, *61*, e202114111.

195. Li, L.; Chen, X.; Jin, K.; Rusayyis, M. B.; Torkelson, J. M. Arresting Elevated-Temperature Creep and Achieving Full Cross-Link Density Recovery in Reprocessable Polymer Networks and Network Composites via Nitroxide-Mediated Dynamic Chemistry. *Macromolecules* **2021**, *54*, 1452–1464.

196. Su, J.; Amamoto, Y.; Nishihara, M.; Takahara, A.; Otsuka, H. Reversible Cross-Linking of Hydrophilic Dynamic Covalent Polymers with Radically Exchangeable Alkoxyamines in Aqueous Media. *Polym. Chem.* **2011**, *2*, 2021–2026.

197. Martinez, M. R.; Zhuang, Z.; Treichel, M.; Cuthbert, J.; Sun, M.; Pietrasik, J.; Matyjaszewski, K. Thermally Degradable Poly(n-butyl acrylate) Model Networks Prepared by Photo-ATRP and Radical Trap-Assisted Atom Transfer Radical Coupling. *Polymers* **2022**, *14*, 713.

198. Pramanik, N. B.; Nando, G. B.; Singha, N. K. Self-Healing Polymeric Gel via RAFT Polymerization and Diels–Alder Click Chemistry. *Polymer* **2015**, *69*, 349–356.

199. Lessard, J. J.; Garcia, L. F.; Easterling, C. P.; Sims, M. B.; Bentz, K. C.; Arencibia, S.; Savin, D. A.; Sumerlin, B. S. Catalyst-Free Vitrimers from Vinyl Polymers. *Macromolecules* **2019**, *52*, 2105–2111.

200. Lessard, J. J.; Scheutz, G. M.; Sung, S. H.; Lantz, K. A.; Epps, T. H., 3rd; Sumerlin, B. S. Block Copolymer Vitrimers. *J. Am. Chem. Soc.* **2020**, *142*, 283–289.

201. Zaborniak, I.; Chmielarz, P.; Matyjaszewski, K. Modification of Wood-Based Materials by Atom Transfer Radical Polymerization Methods. *Eur. Polym. J.* **2019**, *120*, 109253.

202. Wang, J.; Zhang, D.; Chu, F. Wood-Derived Functional Polymeric Materials. *Adv. Mater.* **2021**, *33*, 2001135.

203. Kumar, M.; Gehlot, P. S.; Parihar, D.; Surolia, P. K.; Prasad, G. Promising Grafting Strategies on Cellulosic Backbone through Radical Polymerization Processes – A Review. *Eur. Polym. J.* **2021**, *152*, 110448.

204. Zhang, Z.; Sèbe, G.; Hou, Y.; Wang, J.; Huang, J.; Zhou, G. Grafting Polymers from Cellulose Nanocrystals via Surface-Initiated Atom Transfer Radical Polymerization. *J. Appl. Polym. Sci.* **2021**, *138*, 51458.

205. Wu, H.; Wu, L.; Lu, S.; Lin, X.; Xiao, H.; Ouyang, X.; Cao, S.; Chen, L.; Huang, L. Robust Superhydrophobic and Superoleophilic Filter Paper via Atom Transfer Radical Polymerization for Oil/Water Separation. *Carbohydr. Polym.* **2018**, *181*, 419–425.

206. Wang, L.; Wu, Y.; Men, Y.; Shen, J.; Liu, Z. Thermal-Sensitive Starch-g-PNIPAM Prepared by Cu (O) Catalyzed SET-LRP at Molecular Level. *RSC Adv.* **2015**, *5*, 70758–70765.

207. Yamamoto, K.; Yoshida, S.; Mine, S.; Kadokawa, J.-i. Synthesis of Chitin-Graft-Polystyrene via Atom Transfer Radical Polymerization Initiated from a Chitin Macroinitiator. *Polym. Chem.* **2013**, *4*, 3384–3389.

208. Pitarresi, G.; Fiorica, C.; Licciardi, M.; Palumbo, F. S.; Giammona, G. New Hyaluronic Acid Based Brush Copolymers Synthesized by Atom Transfer Radical Polymerization. *Carbohydr. Polym.* **2013**, *92*, 1054–1063.

209. Baker, S. L.; Kaupbayeva, B.; Lathwal, S.; Das, S. R.; Russell, A. J.; Matyjaszewski, K. Atom Transfer Radical Polymerization for Biorelated Hybrid Materials. *Biomacromolecules* **2019**, *20*, 4272–4298.

210. Gong, Y.; Leroux, J.-C.; Gauthier, M. A. Releasable Conjugation of Polymers to Proteins. *Bioconjugate Chem.* **2015**, *26*, 1172–1181.

211. Averick, S.; Mehl, R. A.; Das, S. R.; Matyjaszewski, K. Well-Defined Biohybrids Using Reversible-Deactivation Radical Polymerization Procedures. *J. Control. Release* **2015**, *205*, 45–57.

212. Messina, M. S.; Messina, K. M. M.; Bhattacharya, A.; Montgomery, H. R.; Maynard, H. D. Preparation of Biomolecule-Polymer Conjugates by Grafting-from Using ATRP, RAFT, or ROMP. *Prog. Polym. Sci.* **2020**, *100*, 101186.

213. Pelegri-O'Day, E. M.; Lin, E.-W.; Maynard, H. D. Therapeutic Protein-Polymer Conjugates: Advancing Beyond PEGylation. *J. Am. Chem. Soc.* **2014**, *136*, 14323-14332.

214. Carmali, S.; Murata, H.; Cummings, C.; Matyjaszewski, K.; Russell, A. J. Chapter Fifteen - Polymer-Based Protein Engineering: Synthesis and Characterization of Armored, High Graft Density Polymer-Protein Conjugates. *Methods Enzymol.* **2017**, *590*, 347-380.

215. De, P.; Li, M.; Gondi, S. R.; Sumerlin, B. S. Temperature-Regulated Activity of Responsive Polymer-Protein Conjugates Prepared by Grafting-from via RAFT Polymerization. *J. Am. Chem. Soc.* **2008**, *130*, 11288-11289.

216. Heredia, K. L.; Bontempo, D.; Ly, T.; Byers, J. T.; Halstenberg, S.; Maynard, H. D. In Situ Preparation of Protein-“Smart” Polymer Conjugates with Retention of Bioactivity. *J. Am. Chem. Soc.* **2005**, *127*, 16955-16960.

217. Fu, L.; Wang, Z.; Lathwal, S.; Enciso, A. E.; Simakova, A.; Das, S. R.; Russell, A. J.; Matyjaszewski, K. Synthesis of Polymer Bioconjugates via Photoinduced Atom Transfer Radical Polymerization under Blue Light Irradiation. *ACS Macro Lett.* **2018**, *7*, 1248-1253.

218. Tucker, B. S.; Coughlin, M. L.; Figg, C. A.; Sumerlin, B. S. Grafting-From Proteins Using Metal-Free PET-RAFT Polymerizations under Mild Visible-Light Irradiation. *ACS Macro Lett.* **2017**, *6*, 452-457.

219. Liu, J.; Bulmus, V.; Herlambang, D. L.; Barner-Kowollik, C.; Stenzel, M. H.; Davis, T. P. In Situ Formation of Protein-Polymer Conjugates through Reversible Addition Fragmentation Chain Transfer Polymerization. *Angew. Chem. Int. Ed.* **2007**, *46*, 3099-3103.

220. Averick, S.; Simakova, A.; Park, S.; Konkolewicz, D.; Magenau, A. J. D.; Mehl, R. A.; Matyjaszewski, K. ATRP under Biologically Relevant Conditions: Grafting from a Protein. *ACS Macro Lett.* **2012**, *1*, 6-10.

221. Lathwal, S.; Yerneni, S. S.; Boye, S.; Muza, U. L.; Takahashi, S.; Sugimoto, N.; Lederer, A.; Das, S. R.; Campbell, P. G.; Matyjaszewski, K. Engineering Exosome Polymer Hybrids by Atom Transfer Radical Polymerization. *Proc. Natl. Acad. Sci.* **2021**, *118*, e2020241118.

222. Murata, H.; Cummings, C. S.; Koepsel, R. R.; Russell, A. J. Polymer-Based Protein Engineering Can Rationally Tune Enzyme Activity, pH-Dependence, and Stability. *Biomacromolecules* **2013**, *14*, 1919-1926.

223. Kaupbayeva, B.; Murata, H.; Matyjaszewski, K.; Russell, A. J.; Boye, S.; Lederer, A. A Comprehensive Analysis in One Run-in-Depth Conformation Studies of Protein-Polymer Chimeras by Asymmetrical Flow Field-Flow Fractionation. *Chem. Sci.* **2021**, *12*, 13848-13856.

224. Baker, S. L.; Munasinghe, A.; Kaupbayeva, B.; Rebecca Kang, N.; Certiat, M.; Murata, H.; Matyjaszewski, K.; Lin, P.; Colina, C. M.; Russell, A. J. Transforming Protein-Polymer Conjugate Purification by Tuning Protein Solubility. *Nat. Commun.* **2019**, *10*, 4718.

225. Baker, S. L.; Murata, H.; Kaupbayeva, B.; Tasbolat, A.; Matyjaszewski, K.; Russell, A. J. Charge-Preserving Atom Transfer Radical Polymerization Initiator Rescues the Lost Function of Negatively Charged Protein-Polymer Conjugates. *Biomacromolecules* **2019**, *20*, 2392-2405.

226. Kaupbayeva, B.; Murata, H.; Lucas, A.; Matyjaszewski, K.; Minden, J. S.; Russell, A. J. Molecular Sieving on the Surface of a Nano-Armored Protein. *Biomacromolecules* **2019**, *20*, 1235-1245.

227. Murata, H.; Carmali, S.; Baker, S. L.; Matyjaszewski, K.; Russell, A. J. Solid-Phase Synthesis of Protein-Polymers on Reversible Immobilization Supports. *Nat. Commun.* **2018**, *9*, 845.

228. Heredia, K. L.; Nguyen, T. H.; Chang, C.-W.; Bulmus, V.; Davis, T. P.; Maynard, H. D. Reversible siRNA-Polymer Conjugates by RAFT Polymerization. *Chem. Commun.* **2008**, *28*, 3245-3247.

229. Bontempo, D.; Heredia, K. L.; Fish, B. A.; Maynard, H. D. Cysteine-Reactive Polymers Synthesized by Atom Transfer Radical Polymerization for Conjugation to Proteins. *J. Am. Chem. Soc.* **2004**, *126*, 15372-15373.

230. Vázquez-Dorbatt, V.; Tolstyka, Z. P.; Chang, C.-W.; Maynard, H. D. Synthesis of a Pyridyl Disulfide End-Functionalized Glycopolymers for Conjugation to Biomolecules and Patterning on Gold Surfaces. *Biomacromolecules* **2009**, *10*, 2207-2212.

231. Gunasekaran, K.; Nguyen, T. H.; Maynard, H. D.; Davis, T. P.; Bulmus, V. Conjugation of siRNA with Comb-Type PEG Enhances Serum Stability and Gene Silencing Efficiency. *Macromol. Rapid Commun.* **2011**, *32*, 654-659.

232. York, A. W.; Huang, F.; McCormick, C. L. Rational Design of Targeted Cancer Therapeutics through the Multiconjugation of Folate and Cleavable siRNA to RAFT-Synthesized (HPMA-s-APMA) Copolymers. *Biomacromolecules* **2010**, *11*, 505-514.

233. Averick, S.; Paredes, E.; Li, W.; Matyjaszewski, K.; Das, S. R. Direct DNA Conjugation to Star Polymers for Controlled Reversible Assemblies. *Bioconjugate Chem.* **2011**, *22*, 2030-2037.

234. Pyun, J.; Jia, S.; Kowalewski, T.; Patterson, G. D.; Matyjaszewski, K. Synthesis and Characterization of Organic/Inorganic Hybrid Nanoparticles: Kinetics of Surface-Initiated Atom Transfer Radical Polymerization and Morphology of Hybrid Nanoparticle Ultrathin Films. *Macromolecules* **2003**, *36*, 5094-5104.

235. von Werne, T.; Patten, T. E. Preparation of Structurally Well-Defined Polymer-Nanoparticle Hybrids with Controlled/Living Radical Polymerizations. *J. Am. Chem. Soc.* **1999**, *121*, 7409-7410.

236. Wang, Z.; Fantin, M.; Sobieski, J.; Wang, Z.; Yan, J.; Lee, J.; Liu, T.; Li, S.; Olszewski, M.; Bockstaller, M. R.; Matyjaszewski, K. Pushing the Limit: Synthesis of  $\text{SiO}_2$ -g-PMMA/PS Particle Brushes via ATRP with Very Low Concentration of Functionalized  $\text{SiO}_2$ -Br Nanoparticles. *Macromolecules* **2019**, *52*, 8713-8723.

237. Costanzo, P. J.; Beyer, F. L. Thermally Driven Assembly of Nanoparticles in Polymer Matrices. *Macromolecules* **2007**, *40*, 3996-4001.

238. Sato, T.; Ohishi, T.; Higaki, Y.; Takahara, A.; Otsuka, H. Radical Crossover Reactions of Alkoxyamine-Based Dynamic Covalent Polymer Brushes on Nanoparticles and the Effect on Their Dispersibility. *Polym. J.* **2016**, *48*, 147–155.

239. Sato, T.; Amamoto, Y.; Yamaguchi, H.; Ohishi, T.; Takahara, A.; Otsuka, H. Dynamic Covalent Polymer Brushes: Reversible Surface Modification of Reactive Polymer Brushes with Alkoxyamine-Based Dynamic Covalent Bonds. *Polym. Chem.* **2012**, *3*, 3077–3083.

240. Claus, T. K.; Telitel, S.; Welle, A.; Bastmeyer, M.; Vogt, A. P.; Delaittre, G.; Barner-Kowollik, C. Light-Driven Reversible Surface Functionalization with Anthracenes: Visible Light Writing and Mild UV Erasing. *Chem. Commun.* **2017**, *53*, 1599–1602.

241. Yardley, R. E.; Kenaree, A. R.; Gillies, E. R. Triggering Depolymerization: Progress and Opportunities for Self-Immulative Polymers. *Macromolecules* **2019**, *52*, 6342–6360.

242. Sagi, A.; Weinstain, R.; Karton, N.; Shabat, D. Self-Immulative Polymers. *J. Am. Chem. Soc.* **2008**, *130*, 5434–5435.

243. Sawada, H. Chapter 3. Thermodynamics of Radical Polymerization. *J. Macromol. Sci. C: Polym. Rev.* **1969**, *3*, 357–386.

244. Odian, G. *Principles of Polymerization*, 4th ed.; John Wiley & Sons, Inc.: Hoboken, NJ, **2004**.

245. Hutchinson, R. A.; Paquet, D. A.; Beuermann, S.; McMinn, J. H. Investigation of Methacrylate Free-Radical Depropagation Kinetics by Pulsed-Laser Polymerization. *Ind. Eng. Chem. Res.* **1998**, *37*, 3567–3574.

246. Wang, H. S.; Truong, N. P.; Pei, Z.; Coote, M. L.; Anastasaki, A. Reversing RAFT Polymerization: Near-Quantitative Monomer Generation Via a Catalyst-Free Depolymerization Approach. *J. Am. Chem. Soc.* **2022**, *144*, 4678–4684.

247. Xu, J.; He, J.; Fan, D.; Tang, W.; Yang, Y. Thermal Decomposition of Dithioesters and Its Effect on RAFT Polymerization. *Macromolecules* **2006**, *39*, 3753–3759.

248. Chong, B.; Moad, G.; Rizzardo, E.; Skidmore, M.; Thang, S. H. Thermolysis of RAFT-Synthesized Poly(methyl Methacrylate). *Aust. J. Chem.* **2006**, *59*, 755–762.

249. Sano, Y.; Konishi, T.; Sawamoto, M.; Ouchi, M. Controlled Radical Depolymerization of Chlorine-Capped PMMA via Reversible Activation of the Terminal Group by Ruthenium Catalyst. *Eur. Polym. J.* **2019**, *120*, 109181.

250. Martinez, M. R.; De Luca Bossa, F.; Olszewski, M.; Matyjaszewski, K. Copper(II) Chloride/Tris(2-pyridylmethyl)amine-Catalyzed Depolymerization of Poly(n-butyl methacrylate). *Macromolecules* **2022**, *55*, 78–87.

251. Jackson, A. T.; Bunn, A.; Priestnall, I. M.; Borman, C. D.; Irvine, D. J. Molecular Spectroscopic Characterisation of Poly(methyl Methacrylate) Generated by Means of Atom Transfer Radical Polymerisation (ATRP). *Polymer* **2006**, *47*, 1044–1054.

252. Bukanova, M. Z.; Neumolotov, N. K.; Jablanović, A. D.; Plutalova, A. V.; Chernikova, E. V.; Kudryavtsev, Y. V. Thermal Stability of RAFT-Based Poly(methyl Methacrylate): A Kinetic Study of the Dithiobenzoate and Trithiocarbonate End-Group Effect. *Polym. Degrad. Stab.* **2019**, *164*, 18–27.

253. Li, I.; Howell, B. A.; Matyjaszewski, K.; Shigemoto, T.; Smith, P. B.; Priddy, D. B. Kinetics of Decomposition of 2,2,6,6-Tetramethyl-1-(1-phenylethoxy)piperidine and Its Implications on Nitroxyl-Mediated Styrene Polymerization. *Macromolecules* **1995**, *28*, 6692–6693.

254. Garrison, J. B.; Hughes, R. W.; Sumerlin, B. S. Backbone Degradation of Polymethacrylates via Metal-Free Ambient-Temperature Photoinduced Single-Electron Transfer. *ACS Macro Lett.* **2022**, *11*, 441–446.

255. Pesenti, T.; Nicolas, J. 100th Anniversary of Macromolecular Science Viewpoint: Degradable Polymers from Radical Ring-Opening Polymerization: Latest Advances, New Directions, and Ongoing Challenges. *ACS Macro Lett.* **2020**, *9*, 1812–1835.